

PHYSICAL SEDIMENT MODELING OF THE MISSISSIPPI RIVER
ON A MICRO SCALE

by

ROBERT DALE DAVINROY JR., 1958-

A THESIS

Presented to the Faculty of the Graduate School of the

UNIVERSITY OF MISSOURI-ROLLA

In Partial Fulfillment of the Requirements for the Degree

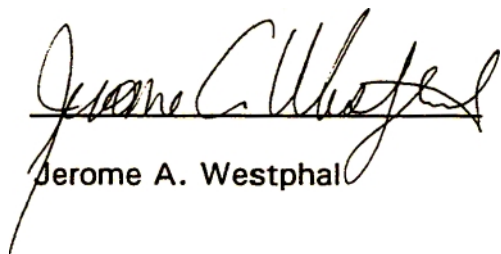
MASTER OF SCIENCE IN CIVIL ENGINEERING

1994

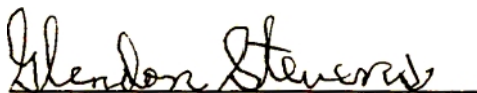
Approved by



Charles D. Morris (Advisor)



Jerome A. Westphal



Glendon T. Stevens



V. A. Samaranayake

ABSTRACT

The design, construction, operation, and testing methodology of an extremely small (horizontal scale: 1 inch = 15,000, vertical scale: 1 inch = 1200) physical sediment model (micro model) is presented for a reach of the Mississippi River. The utility of such a small model is demonstrated by a direct comparison to a larger model constructed at the United States Army Waterways Experiment Station and to the Mississippi River. Results from laboratory tests show that the micro model not only provides realistic simulation of sediment movement, but also generates usable velocity distribution data.

The model study was conducted in a table top size flume. Various operational devices were developed, including a sliding digital micrometer depth measurement system and a velocity measurement system using hot-film anemometry.

A new modeling methodology is presented that deviates considerably from past modeling procedures. The success of this methodology, as exemplified by the model survey results, and the potential use of this technology as a new engineering tool is discussed.

ACKNOWLEDGMENTS

The writing of this thesis was not possible without several important people. First of all, words cannot express the moral support I received from my dearest wife Mimi, who made it possible for me to endure many late nights and early mornings. Her warm smile and encouraging words helped me persevere, and to her I am forever grateful.

Appreciation goes out to my advisor, Dr. Charles Morris, and the other committee members, including Dr. Jerome Westphal, Dr. Jake Stevens, and Dr. V.A. Samaranayake. These men all helped me tremendously by sharing their knowledge and experience, and were always available to discuss the research and guide me no matter what time of day.

Additional people who contributed included: Messrs. Tom Bryson, Jim Morrison, Joe Wilson, Charles Patterson, James McCracken, Jeff Bradshaw, Steve Gabel, Bryan Parker, Teddy Martin, and Lloyd Coakley.

Finally, special thanks is extended to my superiors and colleagues at the Corps of Engineers, including Mr. Tom Lovelace, Mr. Claude Norman Strauser, and Mr. Steven L. Redington, who allowed me to return to school in the face of the Mississippi River flood of 1993. For them I am forever indebted, both in their knowledge and friendship they have given to me over the years.

TABLE OF CONTENTS

	Page
ABSTRACT	iii
ACKNOWLEDGEMENTS	iv
TABLE OF CONTENTS	v
LIST OF ILLUSTRATIONS	ix
LIST OF TABLES	xi
LIST OF MAPS	xii
SECTION	
I. INTRODUCTION	1
II. LITERATURE REVIEW	4
A. HISTORY OF PHYSICAL MODELS	4
B. SEDIMENT TRANSPORT AND THE NEED FOR COST EFFECTIVE PHYSICAL MODELING 12	
1. Sediment Transport Relationships	14
a. Einstein's Bed Load Equation	14
b. Toffaleti Procedure	15
c. Du Boys Formula	16
d. Ackers and White Equation	17
2. Structural Scour Equations	20
a. Laursen Pier Scour Equation	20
b. Inglis-Poona Equation	20
c. Liu Abutment Equation	21
3. Three-Dimensional Bend Flow Effects	21

	Page
4. Numerical Models	23
5. Physical Models	24
C. SIMILITUDE IN MODELING	25
1. Definition and Principles	26
2. Mathematical Similitude	30
3. Empirical Similitude	31
D. EMPIRICAL MOVABLE BED MODELING	33
1. Types of Movable Bed Models	34
2. Methodology	35
a. Distortion	35
b. Supplementary Slope	37
c. Discharge Scale	38
d. Time Scale	39
e. Bed Materials	39
f. General Design Considerations, Construction, and Model Operation	41
E. THE EXPERIMENTS OF OSBORNE REYNOLDS	43
III. PROCEDURE	49
A. MICRO MODEL THEORY	49
1. Geometric Scale Comparisons	49
a. Dogtooth Bend Model Scale	49
b. Micro Model Scale	55
2. State of Flow Computations	56

a. State of Flow in the Prototype	58
b. State of Flow in the Dogtooth Bend Model	58
c. State of Flow in the Micro Model	59
3. State of Sediment Transport	59
B. MODEL APPURTENANCES	63
1. Design, Materials, and Construction	63
a. Flume	63
b. Pump	63
c. Water Outlet Control	63
d. Alignment Insert	63
e. Sediment Input Bay	64
f. Tailbay	64
g. Drainage Reservoir and Pump Housing	64
2. Operation	65
a. Discharge and Stage	65
b. Bed Material Input	65
c. Slope	65
3. Data Collection and Output Scheme	65
C. CALIBRATION	68
1. Calibration Measurements	69
2. Geometric Scale Determination	69
3. Discharge Relation Curve	72

	Page
4. Slope	73
5. Average Annual Design Hydrograph	74
6. Time Scale and Sediment Input	75
7. Development of Starting Conditions	77
8. Base Condition	79
IV. RESULTS AND DISCUSSION	86
A. BASE CONDITION COMPARISONS	86
B. BENDWAY WEIR DESIGN TEST COMPARISONS	111
C. VELOCITY MEASUREMENTS	118
1 . Velocity Distribution Comparison With the Prototype	118
2. Plan View Isovels	123
D. STATISTICAL VARIANCE STUDY	126
V. CONCLUSIONS	136
APPENDICES	138
A. VELOCITY ISOVEL PROGRAM	138
B. STATISTICAL VARIANCE INPUT AND OUTPUT USING SAS	141
BIBLIOGRAPHY	150
VITA	153

LIST OF ILLUSTRATIONS

Figure		Page
1.	Model (Scale 1:200) of a Stretch of the Rhine River with the Groins as Actually Constructed in the Prototype	6
2.	Time Lapse Photography Study of Surface Currents, Model (Scale 1:200) of River Rhine at the Ryburg-Schworstadt Hydroelectric Plant	7
3.	Photograph Showing Bed Contours of the Previous Hydroelectric Model Study	7
4.	First Hydraulic Model at WES, Illinois River Model.....	9
5.	Model of the Yazoo Delta	10
6.	Comparison Between Computed and Measured Bed Material Discharges from the Niobrara River Near Cody, Nebraska	19
7.	Three-Dimensional Bend Flow Element	22
8.	Sand Bed Model at WES, Discharge Relation Curve	40
9.	Plan and Profile View of Typical Movable Bed Model	42
10.	Cross Section of a Movable Bed Model	43
11.	Map of Comparative Surveys in the Reynold's Experiment	45
12.	Micro Model of the Mississippi River	52
13.	Dogtooth Bend Model at WES	53
14.	Conceptual Volumetric Segment Comparisons of Prototype and the Two Models	54
15.	General Design Layout of Micro Model	64
16.	Sliding Micrometer System for the Collection of Depths	67
17.	Flow Chart of Survey Procedure	68
18.	Discharge Relation Curve, Model to Prototype	73

Figure	Page
19. Average Annual Design Hydrograph at Dogtooth Bend (Mile 23.3)	76
20. Calibration Runs at Control Section No. 2 (Mile 23.3)	78
21. Mississippi River Cross Sectional Comparisons at Control Section No. 1 (Mile 21.7)	82
22. Mississippi River Cross Sectional Comparisons at Control Section No. 2 (Mile 23.3)	83
23. Mississippi River Cross Sectional Comparisons at Control Section No. 3 (Mile 25.7)	84
24. Mississippi River Cross Sectional Comparisons at Control Section No. 4 (Mile 30.3)	85
25. Base Condition Comparison at Control Section No. 1 (Mile 21.7)	91
26. Base Condition Comparison at Control Section No. 2 (Mile 23.3)	92
27. Base Condition Comparison at Control Section No. 3 (Mile 25.7)	93
28. Base Condition Comparison at Control Section No. 4 (Mile 30.3)	94
29. Base Condition Comparison at Control Section No. 5 (Mile 32.8)	95
30. Anemometer System, Civil Engineering Department, UMR	120
31. Specifications for Hot-Film Anemometer Probe	121
32. Anemometer Probe and Sliding Micrometer Setup	121
33. Cross Sectional Velocity Isovels at Mile 34.3, Prototype	124
34. Cross Sectional Velocity Index Isovels at Mile 34.3, Micro Model	125

LIST OF TABLES

Table	Page
I. Flow Characteristics and Similitude Ratios	29

LIST OF MAPS

Map	Page
1. Location Map	50
2. Study Reach Map	51
3. Location of Control Sections	71
4. Micro Model Contour Map, Mile 29.3 to Mile 32.0	96
5. WES Model Contour Map, Mile 29.3 to Mile 32.0	97
6. Mississippi River Hydrographic Survey Map, Mile 29.3 to Mile 32.0	98
7. Micro Model Contour Map, Mile 26.5 to Mile 29.3	99
8. WES Model Contour Map, Mile 26.5 to Mile 29.3	100
9. Mississippi River Hydrographic Survey Map, Mile 26.5 to Mile 29.3	101
10. Micro Model Contour Map, Mile 24.2 to Mile 26.5	102
11. WES Model Contour Map, Mile 24.2 to Mile 26.5	103
12. Mississippi River Hydrographic Survey Map, Mile 24.2 to Mile 26.5	104
13. Micro Model Contour Map, Mile 22.1 to Mile 24.2	105
14. WES Model Contour Map, Mile 22.1 to Mile 24.2	106
15. Mississippi River Hydrographic Survey Map, Mile 22.1 to Mile 24.2	107
16. Micro Model Contour Map, Mile 18.9 to Mile 22.1	108
17. WES Model Contour Map, Mile 18.9 to Mile 22.1	109
18. Mississippi River Hydrographic Survey Map, Mile 18.9 to Mile 22.1	110

Map	Page
19. Micro Model Contour Map, Bendway Weir Test, Mile 29.3 to Mile 32.0	115
20. WES Model Contour Map, Bendway Weir Test, Mile 29.3 to Mile 32.0	116
21. Micro Model Contour Map, Bendway Weir Test, Mile 24.2 to Mile 26.5	117
22. WES Model Contour Map, Bendway Weir Test, Mile 24.2 to Mile 26.5	118
23. Velocity Index Isovels, Base Condition, Mile 29.3 to Mile 32.0	127
24. Velocity Index Isovels, Base Condition, Mile 22.1 to Mile 24.2	128
25. Velocity Index Isovels, Bendway Weir Test, Mile 29.3 to Mile 32.0	129
26. Velocity Index Isovels, Bendway Weir Test, Mile 22.1 to Mile 24.2	130

I. INTRODUCTION

Sedimentation is a major problem to mankind in the control and utilization of the water resources of the earth. Every flowing body of water, whether a large ocean or a small stream, contains some form of sedimentation, the degree of which depends on the magnitude of the physical forces and the quantity and type of available geological materials.

Sedimentation is encountered in many aspects of civil engineering. The design of irrigation and drainage canals, the channel improvement and stabilization of rivers for navigation and flood control, the design of reservoirs, the design of coastal and inland ports, the purification of public water supply, and the management of soil erosion within watersheds are just a few of the areas directly related to sedimentation.

The process and control of sedimentation is complex. Many notable scholars, including Reynolds, Froude, and Einstein have studied sedimentation and its effects. A multitude of different engineering approaches have been developed in the treatment of sedimentation, from the simplest of empirical equations, to the most complex of numerical models. As a result, discrepancies and conflicts have been common. Probably no other branch of engineering contains such great disparity among theory, technique, and practice.

The engineer often realizes that in order to solve a particular sediment problem, the chosen design approach may depend largely on budget and time constraints. For example;

1.) Use of a simple equation could supply a swift and inexpensive answer, but this attempt may not adequately describe the processes at hand.

2.) Application of a numerical model may be a possibility, but unless the engineer is highly trained and thoroughly familiar with the operation and limitations of the model, the quality and dependability of the solutions could be unsatisfactory.

3.) Employment of a physical model may be another option, but the time and cost required for the model study could make this impractical.

4.) An in-situ study could be considered, but again, as with the physical model, the time and cost issue could still be a major concern.

The above dilemmas provide inspiration for developing some other approach or alternative for the study of sedimentation problems. This is the driving force for the research and technology presented in this thesis.

The technology presented is called "micro modeling" which refers to the physical modeling of sediment transport on a micro scale. The technology is relatively inexpensive, supplies quick and qualitative answers, and can be used by most engineers trained in the area of hydraulics. Therefore, micro modeling has the potential to become an important sedimentation analysis tool in the future.

This thesis concentrates on both past and present approaches to the analysis of sedimentation problems. This focus establishes the framework for the micro modeling concept. Because the concept incorporates the use

of a physical model, attention is directed toward physical modeling and, more specifically, toward movable bed modeling.

Methodologies and analysis of the micro model conducted in the laboratory are presented and discussed. Data in the form of cross sections and contour maps are generated and compared to both a large physical model and the Mississippi River. Conclusions about the overall performance of the model and future considerations are discussed.

II. LITERATURE REVIEW

A. HISTORY OF PHYSICAL MODELS

The idea of using physical models to analyze problems in hydraulics dates back to the 17th century when Sir Isaac Newton, in 1686, made the observation that "the particles of similar systems will continue to move among themselves with like motions and in proportional times" (1).

Studies were made with scale models in 1787 by Dubuat (2), and by Froude, a naval engineer who used toy-sized boats in a tank (3). In 1875, Fargue of France made a study of the Garonne River in Bordeaux using a hydraulic model. Yet probably the most intensive model study was first carried out by Osborne Reynolds. In 1887, Reynolds submitted a report to the British Association entitled "On Certain Laws Relating to the Regime of Rivers and Estuaries, and on the Possibility of Experiments on a Small Scale" (4). In this report, Professor Reynolds, who already was an acclaimed scholar in hydraulics, described an experiment by which he constructed a small scale physical model of the estuary of the Mersey River in England.

Reynold's model was approximately 6.56 ft in length, was built to a horizontal scale of 1:30,000, and was composed of a zinc-lined flume covered with sand. Reynolds was able to show that in such a model the hydraulic characteristics of the real estuary could be made to reproduce themselves. This experiment is described in detail in a following section of this thesis.

Shortly after Reynold's experiments and near the turn of the century, the idea of using physical models started to gain widespread attention throughout Europe. In 1900, the German professor Herbert Engles of the Technical College at Dresden visited a laboratory at the University of Michigan. Engles observed a Michigan instructor using a glass sided flume to demonstrate flow over a weir. Engles returned to Germany and built a small laboratory in the basement of the college. This was the start of the so called hydraulic laboratory boom in Germany.

From approximately 1900 to the start of World War I, ten major laboratories were established throughout Germany. These laboratories studied a multitude of hydraulic engineering problems using both fixed bed and movable bed models. The most noteworthy facilities in both scope and magnitude were the River-Hydraulic Laboratory of the Technical University at Brunswick and the Hydraulic Laboratory at the Technical University of Dresden (5). Many experiments directly related to the study of rivers were carried out in these two laboratories including: the movement of sedimentary material and its disturbance at river diversions, the movement of sedimentary material in river bends, the effect of spur dikes on sandy river beds, the formation of shifting sand bars in river beds, and an investigation of groins on the River Rhine (Figure 1), to name a few. These early German studies were in far advance of other river studies conducted throughout the world and set a precedence for physical river modeling.

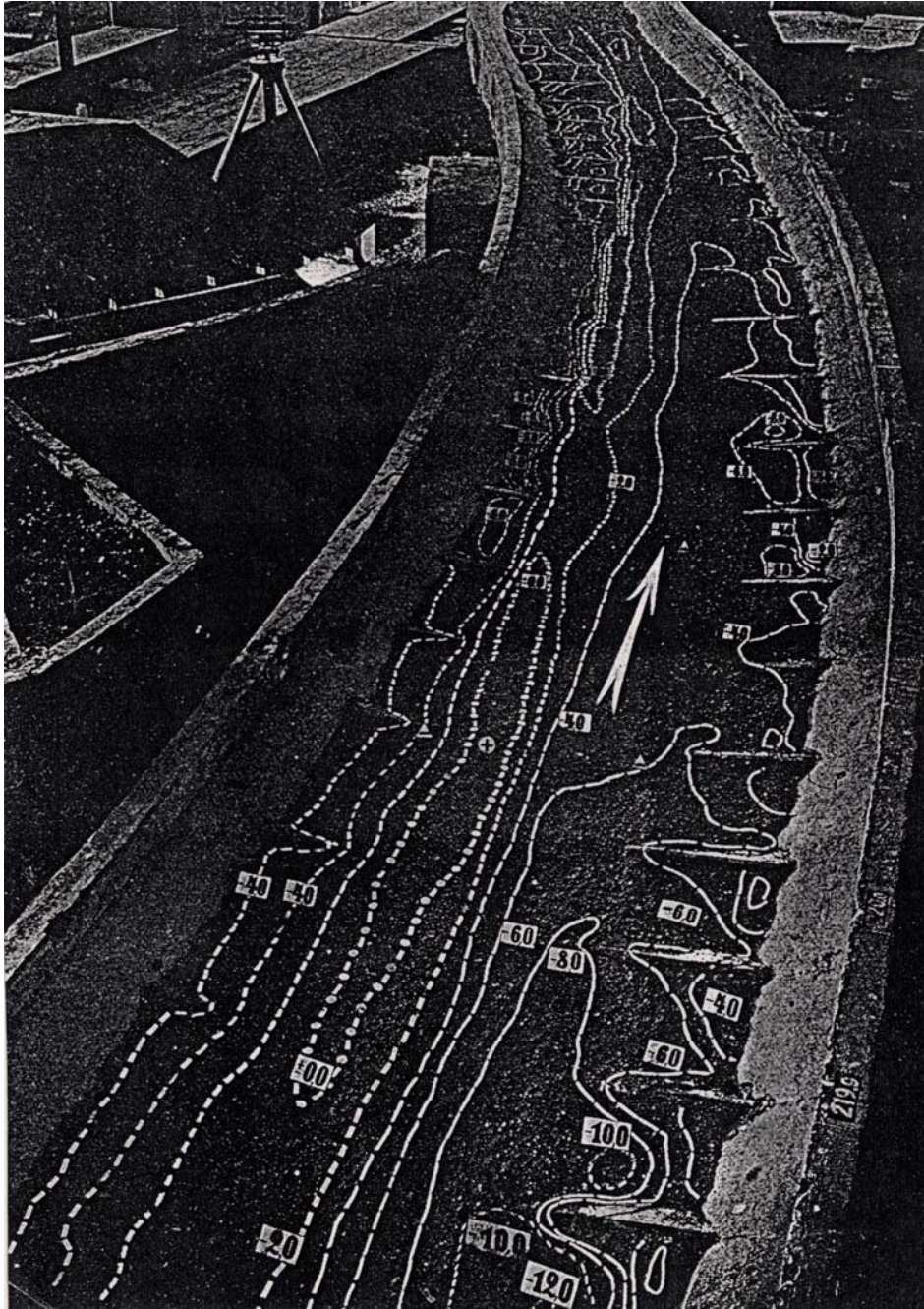


Figure 1. Model (Scale 1:200) of a Stretch of the Rhine River with the Groins as Actually Constructed in the Prototype (from "Hydraulic Laboratory Practice", 1929)

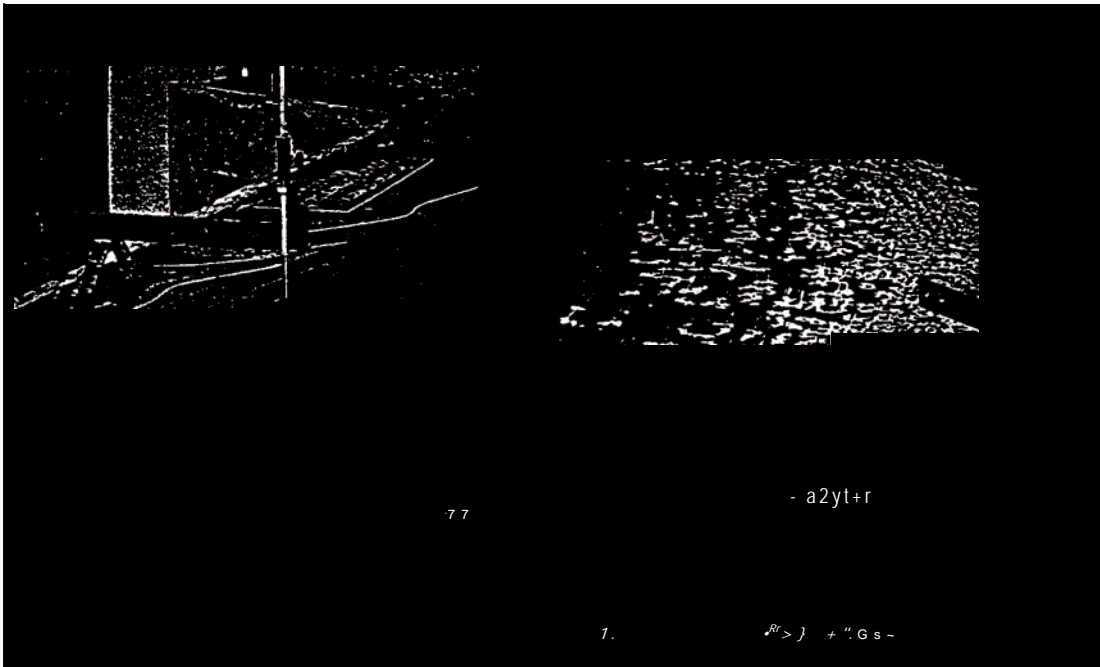


Figure 2. Time Lapse Photography Study of Surface Currents, Model (Scale 1:200) of the River Rhine at the Ryburg-Schworstadt Hydroelectric Plant (from "Hydraulic Laboratory Practice", 1929)

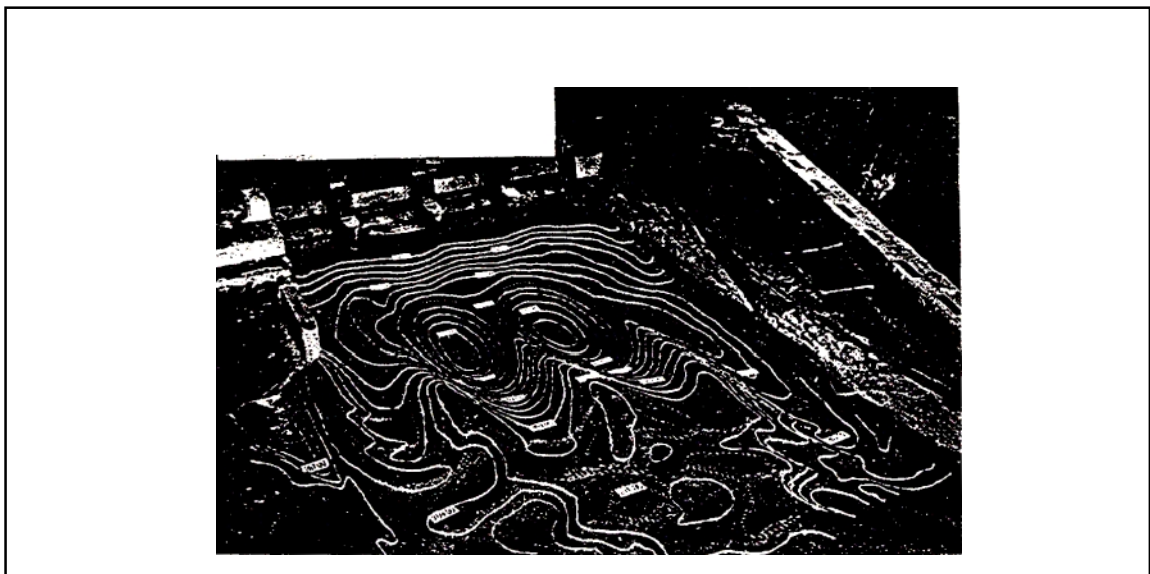


Figure 3. Photograph Showing Bed Contours of the Previous Hydroelectric Model Study (from "Hydraulic Laboratory Practice", 1929)

The early German models ranged in scale from 1:10 to 1:200 horizontal, and the testing medium was that of water and pumice sand having a specific gravity of 1.7. As illustrated in Figures 1, 2, and 3, the Germans paid extreme attention to detail, and were firm believers in time lapse photography of water flow and detailed contour mapping of the model bed.

Other laboratories in Europe were soon established. About the same time that Engles started his laboratory in Germany, Dr. J. Thijsse constructed a lab at Delft in Holland where he was professor of hydraulics. In the next few years, hydraulics laboratories were established in France, Italy, and Czechoslovakia (6).

The European laboratories and model experiments created interest among some American scientists, including John R. Freeman, who visited the Dresden laboratory on the eve of World War I. Freeman revisited the laboratory after the war, where he discovered that the laboratory had been completely rebuilt. There was also a new lab rebuilt at Delft. As Freeman observed the rapid extension and detail of the laboratories of Europe, he began campaigning for the construction of a major laboratory in the United States. After many hearings and debates by Congress and others, in 1928, the construction of a federal hydraulics laboratory was authorized. In 1930, construction of the laboratory started in Vicksburg, Mississippi. This was the birth of the Waterways Experiment Station (WES) (7).

The first model constructed at WES was a large outdoor model of the Illinois River. The model was made by directly excavating the local

Mississippi loess soils (figure 4), and was used to develop flood profiles.

Engineers at WES gained confidence by the success of this model, spawning the next, more involved study of the Lower Mississippi River. This study involved determining the backwater limits in the Yazoo Delta.



Figure 4. First Hydraulic Model at WES, Illinois River Model
(from "History of WES")

In 1927, a devastating flood washed away many of the levees constructed to protect cities and farmland in the Yazoo Basin. A much larger model representing 100 miles or so of the Mississippi River was needed. The expedient of building on bare ground could not be used as it had been in

the Illinois River model because the model would be used over and over again. Thus, the model was constructed completely out of concrete (Figure 5). As with the first study, this model also was used for the determination of flood profiles.

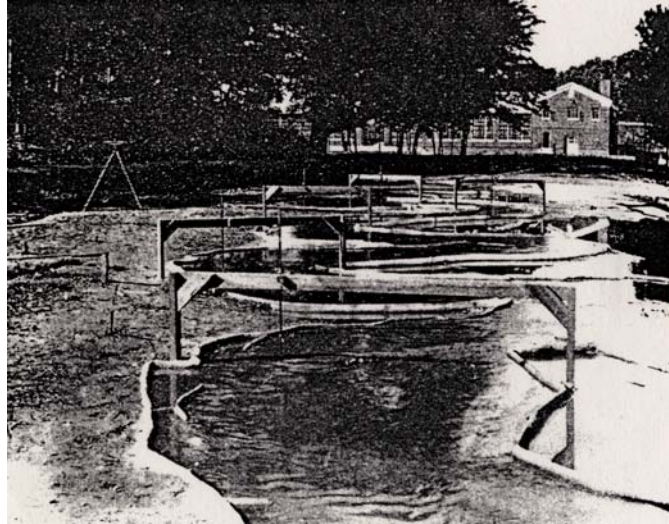


Figure 5. Model of the Yazoo Delta

horizontal scale of 1:2400 was chosen. This caused doubts and fears in many. "From the beginning, American engineers had realized that the European ideas would not always apply to American problems" (7). The

A horizontal scaled of 1:2400 was chosen. This caused doubts and fears in many. "From the beginning, American engineers had realized that the European ideas would not always apply to American problems" European laboratories believed that models with a scale less than 1:300 were too small and gave unreliable results. Nonetheless, the American engineers continued with the construction. A model with a 20:1 distortion (the horizontal to vertical scale ratio) was eventually used.

Extreme distortion of models was also not accepted in Europe, but the Americans believed that depths could be determined more precisely by using a larger distorted scale. Also, to develop proper flow characteristics, the larger vertical scale enabled engineers to apply roughness to the model in the form of "roughness bolts".

A total of 210 recording gages were contained in the model. Completed in 1935, the model reproduced 600 miles of river in 1000 feet, and the full size of the floodplain, some 16,000 square miles, was reduced to approximately 2 acres. A crew of 18 men was needed to operate the model. The time scale was approximately 1 day = 5 1/2 minutes, and the 1927 flood, which lasted about 4 months, was simulated in the model in about 14 hours (7).

Since the historical advent of the first model study at WES, hundreds of studies have since taken place, employing both fixed bed and movable bed models. These models have been used to analyze a multitude of design problems including flood control, urban hydraulics, lock and dam design, navigation channel design, harbor design, tidal studies, hydropower, and dredging.

The trend for using physical models was paralleled by other federal agencies including the Bureau of Reclamation, the Mead Laboratory, and the Navy. In addition, both private and university laboratories were established throughout the country. The Corps of Engineers focused on problems of the Inland Waterways System, the Bureau studied the rivers and streams of the West, the Mead Laboratory concentrated on the Missouri River, and the Navy studied ship design. The private and university laboratories concentrated their efforts on smaller water resource related problems.

Physical models are still in use throughout the world, however their use is declining. The main reasons for this rest on the fact that physical models are expensive and generally take considerable time, sometimes years, before results become available. The recent introduction of numerical models are being used more frequently as a cheaper alternative for the study of sedimentation. Unfortunately, numerical modeling is mainly dependent on empirical transport relationships developed in the laboratory, and requires an operator who is highly trained in the operational intricacies of the model.

B. SEDIMENT TRANSPORT AND THE NEED FOR COST EFFECTIVE

PHYSICAL MODELING

The transport or movement of sediment in alluvial streams and rivers is a very complex process. The term "sediment transport" can be described as the process by which the applied shear stress on the bed of an alluvial

channel exceeds the threshold value for the given bed material, resulting in the downstream movement of particles on the bed (10).

Sediment transport in alluvial rivers and streams is a complex phenomenon that might never be completely reduced to a rational solution. It represents the most extreme degree of unsteady, non-uniform flow, because both the bed and the water surface may undergo continual, simultaneous change. Some have referred to the phenomenon as loose boundary hydraulics (10). Many have developed various sediment transport relationships, but the practicality and confidence of applying these relationships to specific sedimentation analysis often does not meet the needs and expectations of the engineer.

For example, consider a river engineer who intends to analyze a series of dikes to be constructed in a reach of river. The engineer wishes to analyze the effects of proposed dikes on the navigation channel as well as defining intricate details of scour and deposition surrounding each dike. To carry out this analysis, the engineer would need to calculate the total sediment transport rate and define the sediment distribution both laterally at each cross section and longitudinally along the total river reach. Furthermore, if the river contains bends, centrifugal force effects would also have to be accounted for in the sediment distribution issue. The total number of calculations for even the shortest of study reaches would become quite tedious, requiring the solution of many interdependent parameters.

To address these complications, this section is classified into five major parts; sediment transport relationships, structural scour and deposition equations, three-dimensional bend flow effects, numerical modeling, and physical modeling. To conclude this section, an argument is made for the need for cost effective and time responsive physical modeling.

1. Sediment Transport Relationships. In reference to the previous problem scenario, the calculation of a sediment transport rate depends on choosing one of the many transport relationships that exist, and then measuring or estimating the required variables. These relationships or equations vary in both form and complexity. Also, the answers obtained from each often vary considerably.

To gain an understanding of this dilemma, four of the more popular sediment transport relationships used today are presented here and briefly discussed. It is not the intent of this thesis to investigate these equations in detail, rather, the goal is to illustrate the wide variability in both the input requirements and resulting answers obtained from each approach. All of these relationships, as diverse as they are, attempt to describe the same basic process.

a. Einstein's Bed Load Equation. From laboratory flume experiments, Einstein (8) developed a dimensionless function based upon the probability of movement of any one sediment particle expressed in terms of weight rate of sediment transport as:

$$\phi = \frac{q_B}{\gamma_s} \left[\frac{\rho}{\rho_s - \rho} \frac{1}{gd^3} \right]^{\frac{1}{2}} \quad (1)$$

where:

q_B = weight of sediment load per unit time per unit width of channel

γ_s = specific weight of the sediment

ρ = specific gravity of the fluid

ρ_s = specific gravity of the sediment

g = acceleration of gravity

d = sediment particle size

In this equation, the transport rate, q_B , is solved by obtaining an experimental value of the probability function, Φ , from a curve developed by Einstein from his flume experiments.

b. Toffaleti Procedure. Toffaleti (9) developed a procedure to calculate the total sediment load utilizing data taken from seven major rivers within the United States and the results of flume studies conducted in the laboratory. In this procedure, the stream is divided into four major zones, each zone being evaluated by individual empirical equations. The computation is tedious because each zone has to be evaluated for different grain size fractions. Thirteen equations are used in the total transport calculation, expressed as tons/day/ft. Total sediment load is then determined by summing the individual transport rates of the fraction/zone matrix. The equations require the following known or estimated parameters;

average vertical velocity profile, hydraulic radius, water temperature, water surface width, bed slope, and grain size distribution of the sediment.

c. Du Boys Formula. Du Boys conceived a method based upon mobilization of bed sediment in layers within which a linear velocity profile is assumed (10). The tractive force of flow or shear stress balances the resistance between layers, expressed as:

$$\tau_o = C_f n \varepsilon (\gamma_s - \gamma) \quad (2)$$

where τ_o = bed shear stress

C_f = the coefficient of friction between layers

ε = the thickness of each layer

γ_s = specific weight of the sediment

γ = specific weight of the fluid

The total transport equation is written as:

$$g_s = \Psi_D \tau_o (\tau_o - \tau_c) \quad (3)$$

where: g_s = sediment discharge

Ψ_D = coefficient

τ_o = bed shear stress

τ_c = critical bed shear stress at which sediment movement begins

The critical condition for sediment movement is given by $n = 1$, thus:

$$\tau_c = C_f \varepsilon (\gamma_s - \gamma) \quad (4)$$

then for $n \geq 1$,

$$\tau_o = n\tau_c \quad (5)$$

d. Ackers and White Equation. Ackers and White (11) developed a total sediment load equation based upon the collection of more than one thousand sets of data points. This relationship is probably the most widely used by engineers today. The equation takes the basic form:

$$\left[\frac{U_*}{U} \right]^{C_1} \frac{\gamma_f C D}{\gamma_s d} = C_2 \left[\frac{F_1}{C_b} - 1 \right]^{C_4} \quad (6)$$

where,

$$F_1 = \left[\frac{U}{\sqrt{32} \log(10D/d)} \right]^{1-C_1} \frac{U_*^{C_1}}{[(\Delta\gamma_s/\rho_f)d]^{\frac{1}{2}}} \quad (7)$$

in which the values of the coefficients C_1 , C_2 , C_3 , and C_4 are given as a function of d_* by:

$$d_* = \left(\frac{\Delta\gamma_s}{\rho_f v^2} \right)^{\frac{1}{3}} d \quad (8)$$

For $1.0 < d_* \leq 60.0$

$$C_1 = 1.0 - 0.56 \log d_* \quad (9)$$

$$C_2 = 10 [2.86 \log d_* - (\log d_*)^2 - 3.53] \quad (10)$$

$$C_3 = \frac{0.23}{d_*^{0.5}} + 0.14 \quad (11)$$

$$C_4 = \frac{9.66}{d_*} + 1.34 \quad (12)$$

for $d_* > 60.0$

$$C_1 = 0, C_2 = 0.025, C_3 = 0.17, C_4 = 1.50$$

The parameters in the relationship are:

C = bed load concentration by weight

U = mean flow velocity

U_* = shear velocity

D = depth of stream

d = grain diameter

d_* = average particle size

γ_s = specific weight of sediment

γ_f = specific weight of fluid

ρ_f = specific gravity of fluid

$$\Delta \gamma_s = \gamma_s - \gamma_f$$

In using these transport relationships, one has to keep in mind that most of the equations have only been tested and developed for sand-bed flumes and channels. Simons states: "During experimentation, in general, the range of sediment sizes was small, the discharge was small, the slope varied over

a significant range, and the flow conditions were usually steady and uniform" (12).

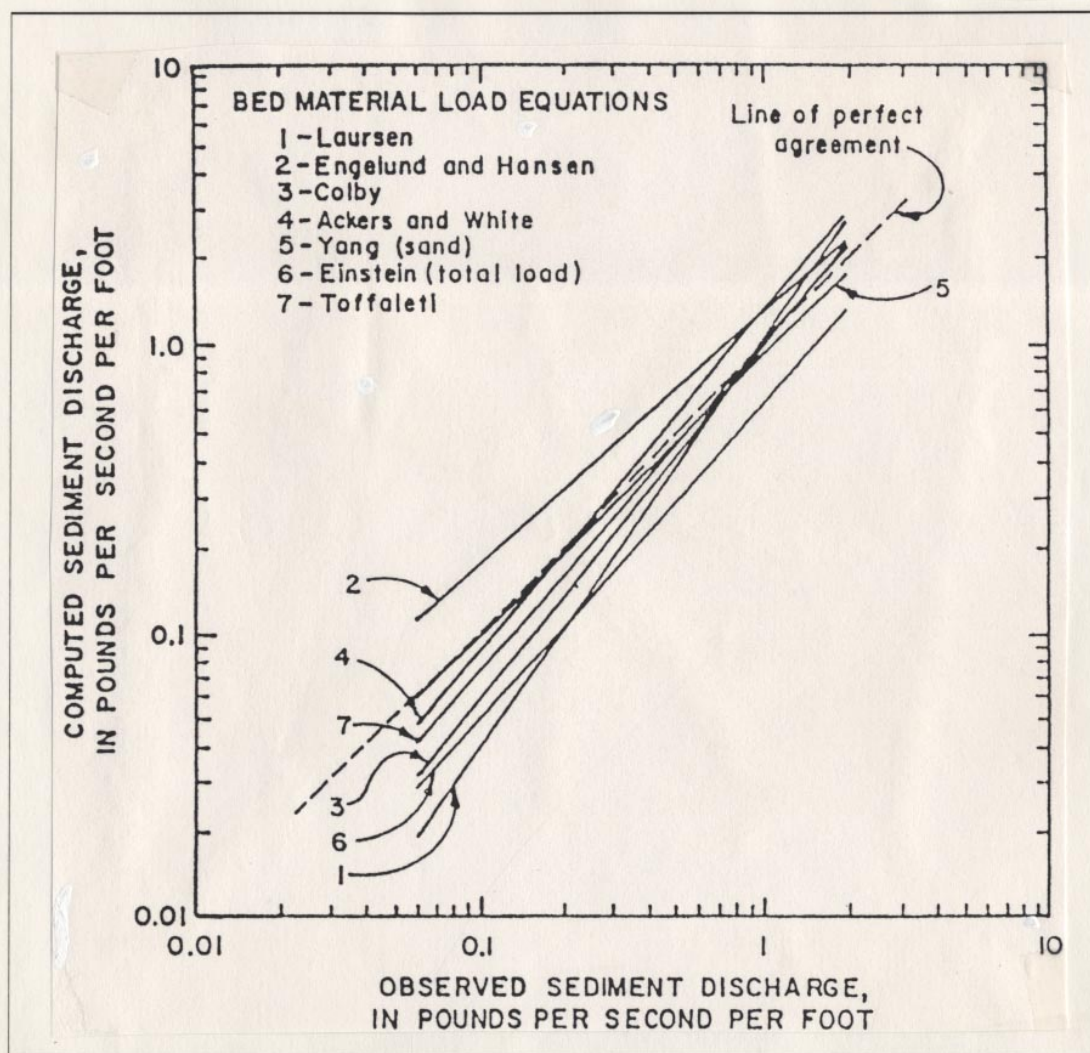


Figure 6. Comparison Between Computed and Measured Bed Material Discharges from the Niobrara River Near Cody, Nebraska

Furthermore, the transport methods discussed previously are based upon varying theoretical considerations, statistical interpretations of basic data, and limited verification of the relations with field data (12). Stevens and Yang (12) developed several comparative plots utilizing seven different transport relations applied at specific sites, illustrating the wide range of answers (Figure 6). The deviation in the values obtained between each of the methods can be observed in the graph.

2. Structural Scour Equations. Many problems encountered in rivers and streams involve local scour around various structures including bridge piers, bridge abutments, dikes, revetments, etc. A multitude of relatively simple empirical equations have been developed to calculate the expected scour at these structures. Most of these equations are based on results of laboratory experiments and, in a few cases, upon collected field data. A few of the more popular formulas include:

a. Laursen Pier Scour Equation. For a square-nosed pier aligned with the flow (13),

$$D = 1.5b^{0.7} h^{0.3} \quad (13)$$

where: D = scour depth measured from mean bed elevation in feet

b = width of the pier in feet

H = flow depth

b. Inglis-Poona Equation (14). For computation of a square nosed pier aligned with the flow:

$$\frac{D^*_{\max}}{b} = 1.7(q^{0.67}b)^{0.78} \quad (14)$$

where:

D^* = maximum scour depth measured from the water surface in feet

q = unit discharge in ft^2 per second

b = square nosed pier width

c. Liu (1961) Abutment Scour Equation (14). On the basis of dimensional analysis and laboratory tests, to evaluate scour from abutments which encroach into the main channel:

$$\frac{d_s}{y_o} = 2.15 \left[\frac{L}{y_o} \right]^{0.4} Fr^{0.33} \quad (15)$$

where: d_s = depth of scour in feet

y_o = depth between top of abutment and floodplain in feet

L = length of structure

Fr = Froude number

The answers obtained from the above equations vary with one another considerably (Westphal 1993). Also, these equations merely address the total amount of expected scour, and do not indicate the actual shape of the scour hole. The deposition of material removed from the scour hole and its location are not addressed.

3. Three-Dimensional Bend Flow Effects. Whether the transport relations or the scour equations are used, it must be kept in mind that these relationships are estimations based on two-dimensional flow and do not address three-dimensional flow effects encountered in bends.

Figure 7 depicts a three-dimensional bend flow element. Besides the normal and lateral velocity, transverse velocity components occur as well.

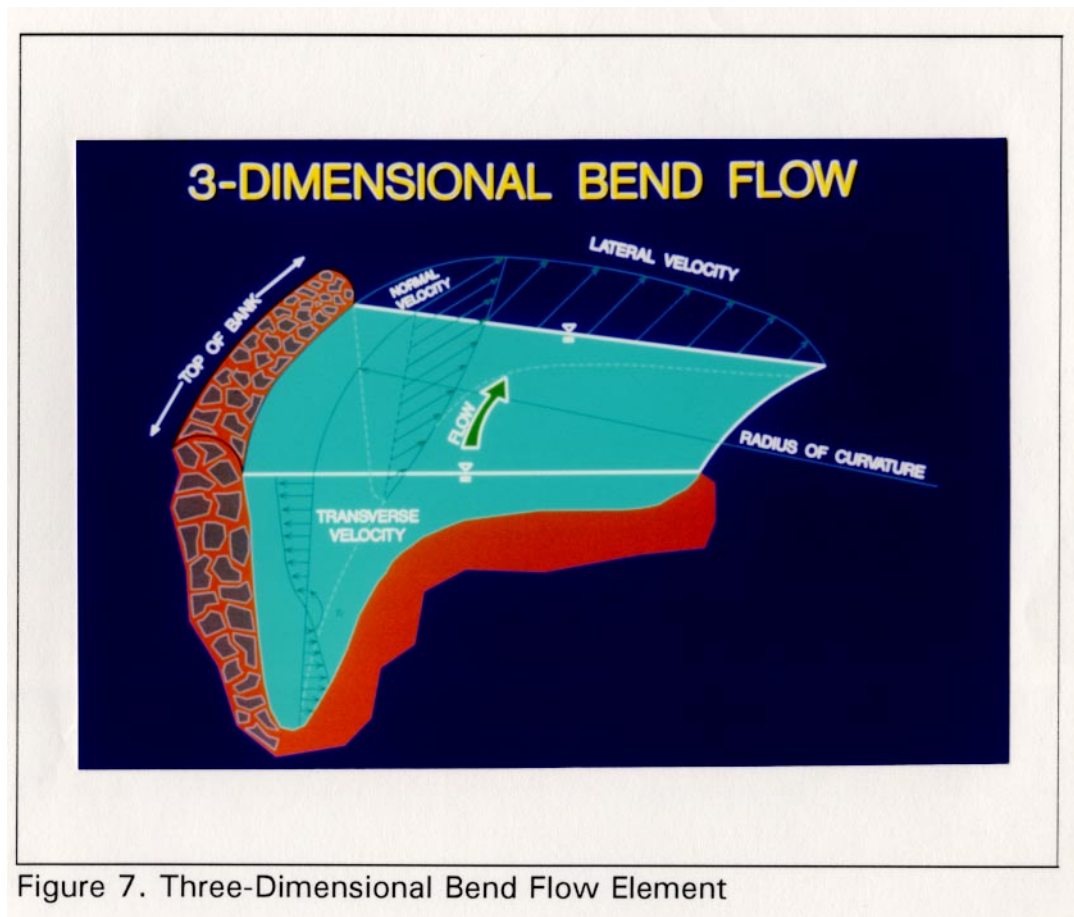


Figure 7. Three-Dimensional Bend Flow Element

This transverse velocity, or secondary current, spirals about the channel cross-sectional axis. This spiralling effect is a direct result of the torque established from the centrifugal force action of the water flowing around the curve of the bend (15).

Secondary currents have been measured in both bends and straight reaches, although in bends the phenomena becomes much more pronounced.

The cells in bends are so predominant that they play a major role in the total sediment transport scheme, and have a profound effect on the scour and depositional patterns of the bed (16).

The mechanics of bend flow are often ignored. Many engineers have designed and constructed structures in bends based upon straight reach mechanics, only to discover later that the structures in the prototype behave much differently than expected. This is likely a direct result of the presence of secondary currents, which cannot be overlooked without serious consequences.

4. Numerical Models. Several numerical/mathematical sediment models have been developed recently, incorporating the simplest to the most complex transport relationships. These generally fall under two categories, one-dimensional and two dimensional models.

HEC-6 (17) is a one-dimensional, fixed bed sediment transport model widely used by the Corps of Engineers and others. This model routes flow through the system by using a standard step procedure. The user selects one of the transport functions to be used in the evaluation of total sediment load at each cross section. Sediment data from the field is required for input, including sediment load curves and bed material gradation. The output is limited to predicting only average bed conditions within a cross section. Dynamic changes in the bed of a cross section due to scour or deposition and the resulting bed configuration are not simulated. This program is

appropriately used for the general long term simulation of stream bed profile behavior, ie. aggradation and degradation.

TABS-2 is a two-dimensional sediment, movable bed transport model used by the Corps of Engineers (18). This model employs the two dimensional depth averaged hydrodynamic model, RMA-2V, as input to the two-dimensional fine grained sediment model, STUDH. The Ackers-White equation is used as the transport function. Both flow and sediment are modeled using finite element analysis. As with HEC-6, sediment field data are required.

The numerical models are only as reliable as the transport relationship they use, and do not address the bend flow issue. Although answers can be achieved from these models in a relatively short time, a typical study can be expensive.

5. Physical Models. Historically, the use of physical models as a means of analyzing sediment phenomena have been the tool of choice by most engineers. In physical models, the overall sediment transport phenomena, including both the three-dimensional mechanics and the resulting sediment distribution, are all inherently addressed in the operational dynamics of the model itself. Scour holes and point bars form easily, and secondary currents have been measured in these model and displayed through flow visualization techniques. Comparative surveys with the prototype verify the high degree of confidence by which these models can be used.

Unfortunately, even though a high level of confidence can be obtained by use of a physical model, time and cost have always been the limiting factors for more widespread use and application. Unless a large amount of space, resources, and money is available, the use of physical models is impractical for most engineers.

The need exists for a cost effective and time responsive physical modeling alternative. If micro models could somehow be constructed and operated to behave as the large models that have been used throughout history, then a new realm of physical modeling could be established. This is the basis and motivation for the research described in this thesis.

C. SIMILITUDE IN MODELING

In order to properly design and operate a physical hydraulic model, a thorough understanding of the basic principles of similitude is a requirement. The laws of similitude serve as a foundation by which indications and results of models may be used to predict prototype behavior.

Fixed bed and movable bed physical hydraulic models are the two types used in the analysis of alluvial systems. The practical application of using either type model depends on the fact that no complete similitude exists. Thus, the modeler must decide if the deviations in similitude are acceptable for the particular parameters under study. As such, variable similitude criteria have been established through trial and error and experience by experimenters over the years.

1. Definition and Principles. Similitude can be defined as a known and usually limited correspondence between the behavior of a model and that of its prototype, with or without geometric similarity (19). The term similarity serves as a broad based definition. A model may be exactly similar in one regard but fall short in another. Complete similitude requires that the systems in question be geometrically, kinematically, and dynamically similar. In theory, a dynamically similar model predicts any hydraulic property of the phenomena under investigation. This is attained by multiplying the model value by an appropriate factor. Unfortunately, it is impossible to develop such a model with the constraint that water must be used as the model fluid.

The three classes of similitude are:

- 1). Geometric Similarity. The ratios of all linear dimensions between model and prototype are equal. This relationship is independent of forces or motion.
- 2). Kinematic Similarity. This refers to similarity of motion. The ratios of the components of velocity at all common points in two geometrically similar systems are equal. This will result in the two states of motion in each system to be kinematically similar. The corresponding paths of the common point particles will also then be geometrically similar.
- 3). Dynamic Similarity. If the systems are geometrically and kinematically similar, and if the ratio of all common point forces are equal, then the systems are dynamically similar.

The above conditions of complete similitude can be developed from Newton's second law of motion:

$$Ma = F_t = F_p + F_g + F_v + F_t + F_e \quad (14)$$

where:

F_t = total force

F_p = pressure force

F_g = force due to gravitational effects

F_v = viscous force

F_t = force due to surface tension

F_e = force due to elastic compression

The term Ma is the inertial force, which represents the mass reaction to all of the acting forces. Complete dynamic similitude, as stated previously, requires that:

$$\frac{M_m a_m}{M_p a_p} = \frac{(F_p)_m}{(F_p)_p} = \frac{(F_g)_m}{(F_g)_p} = \frac{(F_v)_m}{(F_v)_p} = \frac{(F_t)_m}{(F_t)_p} = \frac{(F_e)_m}{(F_e)_p} \quad (15)$$

On the other hand, for overall similarity, the ratio of the inertial forces must equal the ratio of the vector sums of the active forces:

$$\frac{M_m a_m}{M_p a_p} = \frac{(F_p + F_g + F_v + F_t + F_e)_m}{(F_p + F_g + F_v + F_t + F_e)_p} \quad (16)$$

In most open channel systems, the gravitational effects predominate. In this case, a similitude criteria can be established by equating the ratio of inertial force to gravity force and neglecting all other forces.

The mass density, ρ , is defined as the mass per unit volume. Hence:

$$M = \rho Vol \quad (17)$$

Volume has the dimensions L^3 , thus:

$$M = \rho L^3 \quad (18)$$

Acceleration, a , has the dimensions L / T^2 . Representing the inertial force by Ma ,

$$Ma = \rho L^3 \frac{L}{T^2} = \rho L^2 V^2 \quad (19)$$

Also, the gravitational force per unit volume of fluid, defined as the specific weight, γ , yields:

$$F_g = \gamma Vol = \gamma L^3 \quad (20)$$

The ratio of inertial to gravitational forces gives:

$$\frac{Ma}{F_g} = \frac{\rho L^2 V^2}{\gamma L^3} = \frac{V^2}{gL} \quad (21)$$

The resulting ratio, V^2/gL , is known as the kinetic flow factor (25).

Reducing V to a single power, and expressing the ratio as a variable, the dimensionless quantity is called the Froude number F ,

$$F = \frac{V}{\sqrt{gL}} \quad (22)$$

Thus, a pertinent similitude criterion has been established which states that the Froude number (or kinetic flow factor) must be the same in both the model and the prototype. A number of scale relationships (19) can be obtained by this criterion and are listed below in Table I.

Table I. Flow Characteristics and Similitude Ratios
(from "Engineering Hydraulics", 1949)

Characteristic	Dimension	Scale ratios for the laws of	
		Froude	Reynolds
<i>Geometric</i>			
Length	L	L_r	L_r
Area	L^2	L_r^2	L_r^2
Volume	L^3	L_r^3	L_r^3
<i>Kinematic</i>			
Time	T	$\left(\frac{L\rho}{\gamma}\right)_r^{1/2}$	$\left(\frac{L^2\rho}{\mu}\right)_r$
Velocity	LT^{-1}	$\left(\frac{L\gamma}{\rho}\right)_r^{1/2}$	$\left(\frac{\mu}{L\rho}\right)_r$
Acceleration	LT^{-2}	$\left(\frac{\gamma}{\rho}\right)_r$	$\left(\frac{\mu^2}{\rho^2 L^3}\right)_r$
Discharge	$L^3 T^{-1}$	$\left[L^{3/2}\left(\frac{\gamma}{\rho}\right)^{1/2}\right]_r$	$\left(\frac{L\mu}{\rho}\right)_r$
<i>Dynamic</i>			
Mass	M	$(L^3\rho)_r$	$(L^3\rho)_r$
Force	MLT^{-2}	$(L^3\gamma)_r$	$\left(\frac{\mu^2}{\rho}\right)_r$
Pressure intensity	$ML^{-1}T^{-2}$	$(L\gamma)_r$	$\left(\frac{\mu^2}{L^2\rho}\right)_r$
Impulse and momentum	MLT^{-1}	$[L^{3/2}(\rho\gamma)^{1/2}]_r$	$(L^2\mu)_r$
Energy and work	ML^2T^{-2}	$(L^4\gamma)_r$	$\left(\frac{L\mu^2}{\rho}\right)_r$
Power	ML^2T^{-3}	$\left(\frac{L^{7/2}\gamma^{3/2}}{\rho^{1/2}}\right)_r$	$\left(\frac{\mu^3}{L\rho^2}\right)_r$

Note: When g is the same for model and prototype, $(\gamma/\rho)_r = 1$.

As will be addressed under a subsequent section on empirical similitude, the conditions under which the Froude Law applies might be compromised. Yalin (21) questions: "Knowing that the realization of the dynamically similar behavior of all properties is impossible, how to ensure the dynamical similarity of at least those properties which will be measured and/or observed?"

Yalin's question is the premise for all models, whether they are numerical or physical. We cannot model every phenomenon that exists. However, we can focus on those characteristics that are measurable. This is the basis of physical hydraulic modelling in the broadest sense. For further investigation, similitude is classified into two categories; mathematical similitude and empirical similitude.

2. Mathematical Similitude. The previous derivations fall under the category of mathematical similitude. A scaled down model of the prototype may be designed by following the rational relationships just discussed. This approach has proven to be viable for the design of dams, spillways, canals, and other hydraulic structures. However, it must be kept in mind that even these type of models are imperfect, especially considering that water is predominately used as the model fluid. Care must be taken to focus on those investigations that can be addressed by deviating from certain requirements or variables in complete dynamic similitude.

Physical models containing fixed beds have been used in canal and river water surface profile studies. These models follow mathematical similitude

to some degree, although a distortion of slope and an exaggeration of roughness is often necessary. Hence, they are typically referred to as "modified Froude models". They are "roughness" models because the application of roughness throughout the model is a major factor in the model performance and prototype verification. The roughness is adjusted until proper water surface profiles can be reproduced. The Corps of Engineers has experienced much success with these type of models in the study of floods on the Mississippi River (7).

To a limited degree, investigations involving sedimentation have been conducted with models using Froude scaling. Because the Reynolds number is generally too small in these models to achieve complete dynamic similarity, modifications to simulate proper sediment transport have been attempted using dimensionless unit sediment discharge curves (20).

3. Empirical Similitude. The other type of similitude is empirical similitude. Although this type of similitude is often disregarded in text books, it applies directly to sediment models. As emphasized by Reynolds (4), Warnock (19), Yalin (21), and others, empirical similitude deviates from the rational similitude analysis that can be applied to models involving hydraulic structures or other fixed boundary studies.

Yalin (1971) states:

If the model operates with the prototype fluid (water), then the dynamically similar reproduction of sediment transport in a small scale model is a theoretically predictable impossibility. At the same time, it also follows that all the well-known difficulties in reproducing sediment transport in a small scale model occur not because we do not know

what the criteria of similarity are, but because we cannot apply them under existing technical and economical restrictions, which compel us to use water in the model.

On the other hand, a visual demonstration of the possibility of dynamically similar reproduction of sediment transport in a small scale model, irrespective of whether such a model can or cannot be used in practice, is undoubtedly desirable. There is no alternative therefore to seeking special solutions where the identity of some of the variable can be relaxed, and so make small-scale models a practical possibility (21).

Yalin's logic transcends the modeling approach to most sediment models. Instead of arranging the various hydraulic forces involved to meet definite requirements of similitude, the successful prosecution of a sediment model study requires that the combined action of the hydraulic forces bring about similitude with respect to the all important phenomenon of bed movement, which is the essence of this type of model study.

As applied specifically to river models, Franco (22) gives another description of the empirical similitude approach:

In actuality, models of rivers are small rivers patterned after larger rivers and adjusted to reproduce the characteristics of the larger rivers.

Reynolds (4) observed that a highly distorted, extremely small scale model of the Mercy Estuary produced extraordinary similarity in bed configuration as compared to the prototype (Section F). Reynolds "relaxed" the laws of similitude, and was surprised to learn how well his model imitated the movement of sediment as compared to the prototype.

D. EMPIRICAL MOVABLE BED MODELING

Physical models that contain a particular bed material and are designed to simulate the movement of bed sediment only, while not including suspended sediment, are commonly categorized and referred to as "movable bed" models. Typical movable bed modeling does not follow the complete laws of similitude and is considered to be an empirical approach to the modeling of sediment transport.

Therefore, adjustments (model calibrations) are made through a trial and error procedure until similarity is achieved between the resulting bed configuration of the model and that of the prototype. After this is accomplished, impacts of various structural alternatives, such as dikes, weirs, revetments, and realignments might then be investigated.

The primary step in the development of a movable bed model involves the selection of suitable scales and bed material which will result in two-phase flow similar to the prototype. To accomplish this, a thorough knowledge of the characteristics of the prototype based upon the collection and study of hydraulic and hydrographic data is required. In addition, experience in the field of river mechanics and movable-bed hydraulic models is needed for proper model operation (19).

In concise terms, the forces needed to reproduce the required bed movement and resultant bed configuration are obtained by distorting the linear scales, changing the slope and discharge, or both. The choice of a suitable bed material must also be made. A few of the materials that have

been used in movable bed models include sand, crushed coal, gilsonite, walnut shell?) and pumice. Others materials have been used with varying degrees of success.

1. Types of Movable Bed Models. The Corps of Engineers has used movable bed models extensively for the study of navigation channel development of the inland waterway system of the United States. This includes river, estuary, and ocean studies. These models employ an empirical similitude approach. One particular model of this type is discussed in more detail in Section III. A.

The Bureau of Reclamation has conducted movable bed studies using a rational methodology that incorporates modified Froude and Reynolds modeling principles. These type of sediment models have been used for the study of various control structures and diversions for rivers and streams in the western part of the United States (20).

Dominant discharge is a method used by many universities and private laboratories. This method subjects the model to a single peak discharge. This type of modelling is used for the study of localized effects in small rivers and streams including bridge pier scour, low water dams, stabilization, channelization works, and soil conservation.

Movable bed models, although small in comparison to the prototype, are usually quite large and expensive to construct, operate, and maintain. With a few exceptions, the facilities that house the flumes, pumps, reservoirs, and various controllers are expansive, usually requiring from one half to as much

as two acres of space. The construction costs are often hundreds of thousands of dollars. A complete model study may take from one to three years to complete, and it is not uncommon for the cost of an entire model study to approach one million dollars.

However, the expense of these models has been justified because the benefits usually far outweigh the costs. Prototype construction is costly, and mistakes in design add to these costs. Model studies have supplied the most practical, economical design solution for many sedimentation problems.

The results from the Corps of Engineers Dogtooth Bend Model Study (Section M. A) enabled engineers to solve a complex navigation problem in bends of the Mississippi River. The most efficient design of underwater rock structures, called Bendway Weirs, was achievable only after the results of many tests in this model. The model tests supplied answers to important design details such as height, spacing, and alignment of structures. Information like this cannot be obtained from empirical equations or from numerical models.

2. Methodology. A basic understanding of the methodology of empirical movable bed modeling is required for the prosecution of the modeling technique presented in this thesis. Therefore, basic considerations usually included in this type of modeling are discussed as follows:

a. Distortion. If exact geometric similitude were taken into account with the dimensions of a particular large watercourse like the Mississippi River, the resultant dimensions of the model would cause a great reduction

in the hydraulic forces. These reduced forces would no longer be sufficient to move the bed material. This is why Reynolds, in his experiment of 1887, distorted the linear scale ratio of his model. Distortion of the linear scale ratio can be defined simply as the deviation between the vertical and horizontal scale. The result is an exaggeration in all vertical dimensions and slopes of the model.

In nature, when comparing small streams with large rivers, we find natural distortion. The width-depth ratio of a small stream is much less than that of a major river. The forces necessary to move sediment in natural watercourses are generated by the geometric configuration of the channel. As Franco (22) states "...in natural streams, the size of bed material does not vary in direct proportion to the size of the river and tends to be larger in the smaller streams".

Nature compensates for size by "distorting" or creating a smaller width-depth ratio in the stream channel in order that sufficient hydraulic forces are generated to move the bed material. This is why one notices great similarity in the smallest of streams as compared to the largest of rivers, regardless of the size of bed materials. This principle is of paramount importance to the theory of movable-bed models and the findings of this thesis.

There are limitations and effects of distortion that should be noted. First, the exaggeration of the vertical scale may increase the height of the channel banks of the model well beyond the natural angle of repose and cause the banks to slough off or cave into the channel. This problem is

eliminated if working with a totally reveted river, or with the assumption of permanent banks and the principal interest is the movement of material within the channel.

Another adverse effect of distortion is the increase of the longitudinal slope of the stream. The flow regimen is disturbed to a point where artificial model roughness is required. However, because roughness is a function of the bed material, the possibility of adding artificial roughness to the bed does not exist. A distortion in the discharge and velocity scales will automatically result. This is acceptable because the model is not designed to reproduce water surface profiles.

A final point to consider with respect to distortion is the lateral distribution of velocity. Many critics of distorted models argue that the velocity distribution of the model will not be the same as in the prototype. The more geometrically distorted the model is, the more distorted the velocity distribution is. However, just as the resultant, distorted bed configuration is used for design analysis, so too may the velocity distribution which produced this bed configuration be used. By making a direct comparison to available prototype data, measured velocity distributions in the model should be similar to the prototype, and this is investigated further in a subsequent section.

b. Supplementary Slope. In addition to the slope that results from the distortion of the vertical scale, specified areas along the channel reach usually require an additional slope adjustment to develop the forces that are

necessary for adequate movement of the bed material. This may be an increase or decrease in slope. WES has labeled this slope as supplementary slope (22).

Movable bed models do not offer the luxury of adding or removing roughness to the channel because the model employs moving bed material. In fixed bed models, roughness can be employed directly to the model in the form of roughness bolts, or roughness can be reduced by smoothing the channel. In movable bed models, the roughness of the bed cannot be controlled. Therefore, the slope of the channel bottom is locally increased or decreased as required.

Supplementary slope is slope applied at specific reaches throughout the model. The supplementary slope is applied by adjusting, at various locations, the height of a metal railing that parallels the longitudinal alignment of the model. Modeling templates (Figure 10) are then adjusted and used either at a higher or lower reference elevation (depending on the slope required). The end result is a model that contains varying slope within the model flume (33).

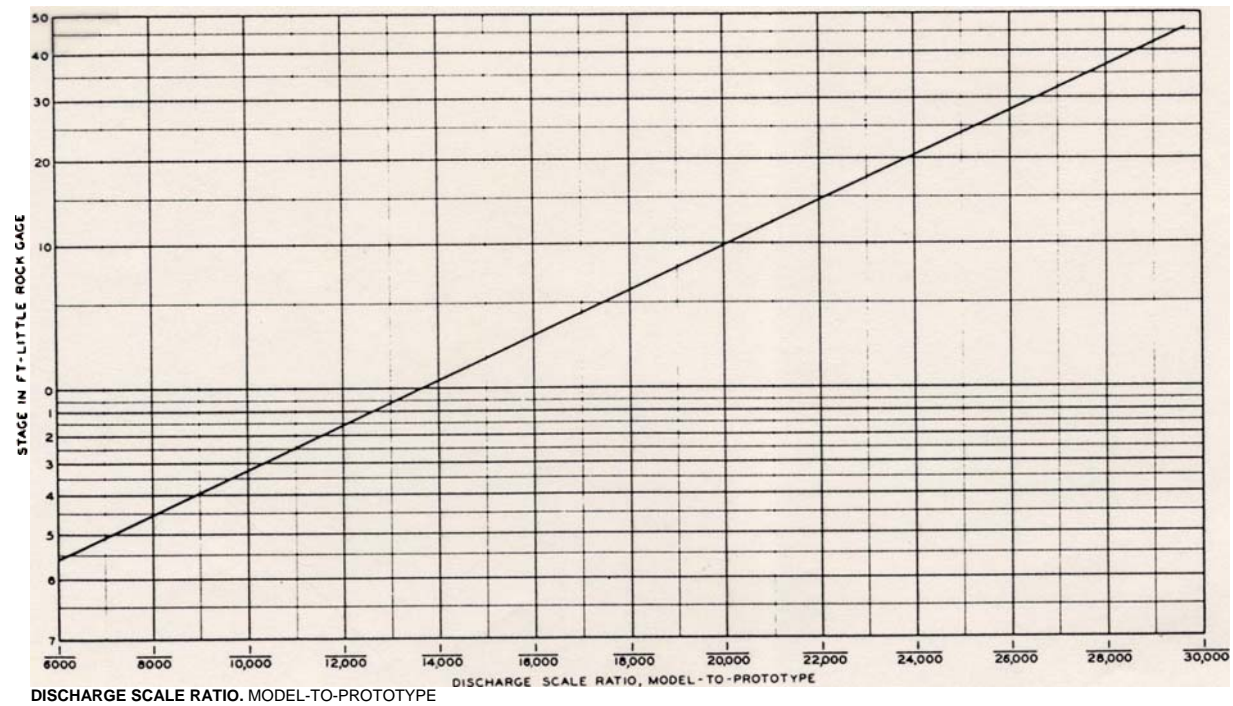
c. Discharge Scale. Because of the linear scale distortion, the discharge scale is distorted. The model discharge scale that is required to maintain the correct depths for the various stages of flow must be determined experimentally through operation of the model. The discharge relation is dependent on the model linear scales and on the bed material type (22). Because the small size of the model provides force limitations as discussed in

the previous section, additional forces are generated by an increase in the discharge scale, model to prototype, than the theoretical scale based upon the model dimension scales. Various discharge relation curves have been developed at WES, including the one shown in Figure 8. A direct discharge curve with the prototype under study may be required when large variations between stage and discharge occur in the prototype (22).

The adjustment of the discharge scale is based upon intuition. The modeler observes the movement of sediment in the model at all stages and compares this to the prototype, if possible. Too little or too much sediment movement might require the adjustment of the discharge scale.

d. Time Scale. Because these models are not Froude models (discussed in Section C), the time scale has been developed empirically through trial and error. Generally, most movable bed studies at WES use a time scale of approximately 5 to 8 minutes per prototype day, or between 30 and 50 hours per prototype year.

e. Bed Materials. Many different materials have been used historically for model bed material including sand (s.g. 2.65), crushed coal (s.g. 1.3), gilsonite (s.g. 1.06), and walnut shell (s.g. 1.3) to name a few. The choice of material will not only influence the magnitude of the distortion required for sufficient bed movement, but also governs the relative time scale used in the model.



Sand-bed model, discharge relation curve,
scale 1:250-1:36

Figure 8. Sand Bed Model at WES, Discharge Relation Curve (Franco 1978)

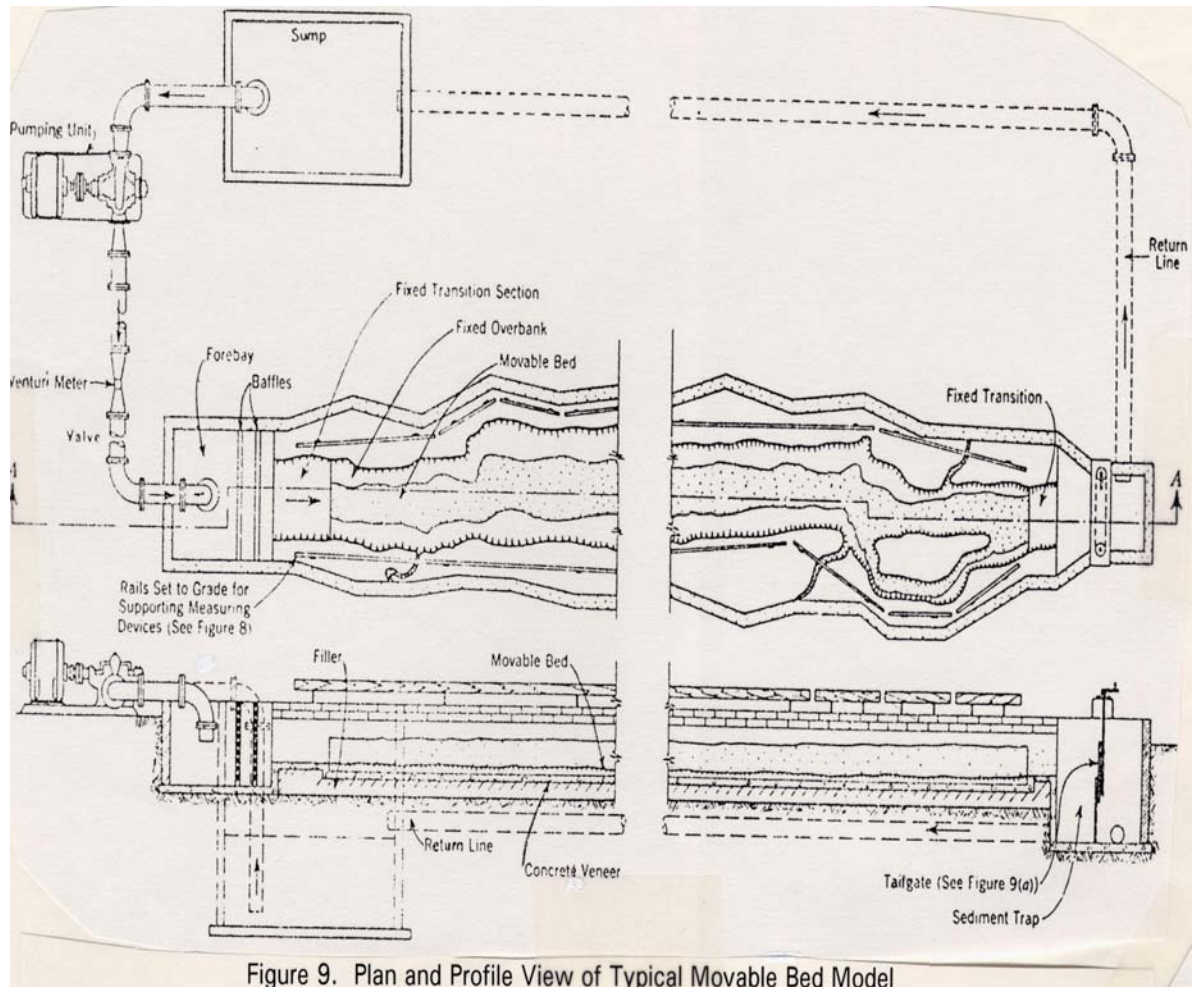
European models typically employ sand, while WES has had success using crushed coal. A few laboratories in Canada have used gilsonite to simulate both bed movement and suspended sediment movement.

f. General Design Considerations, Construction, and Model Operation.

Figure 9 illustrates a typical plan and profile section of a movable bed model. In simple terms, the first step in the design of a typical movable bed model involves construction of a flume. The material of choice is usually concrete. Special appurtenances of the model include a forebay, baffles, upstream and downstream transition sections, a tailgate, a sediment trap, a return line, a sump, a pumping unit, water surface gages, and a discharge control valve. Railings are constructed above the model for creating longitudinal slope. The whole system is usually operated in three ways; manually, electronically, or by computer.

A plan view of the river or stream segment under study is laid out within the concrete flume. Filler material is placed on either side of the channel banks and is capped with additional concrete. The resulting rectangular void serves as a flume within a flume (Figure 10), simulating a scaled down version of the prototype.

The chosen model bed material is filled within the created flume. The next step involves the placement of male templates on top of the river alignment to form the bed topography. The templates are fabricated out of sheet metal based upon cross sectional survey data. The templates are placed in position on the railing, and the model bed material is molded to the



configuration of the template. Between templates, the sediment is molded by hand and by eye.

The actual model study might then proceed. A hydrograph is simulated by use of the discharge control device and tailbay. After a test is run, the model bed is surveyed using a level and rod. Results are then presented in the form of contours and/or cross sections.

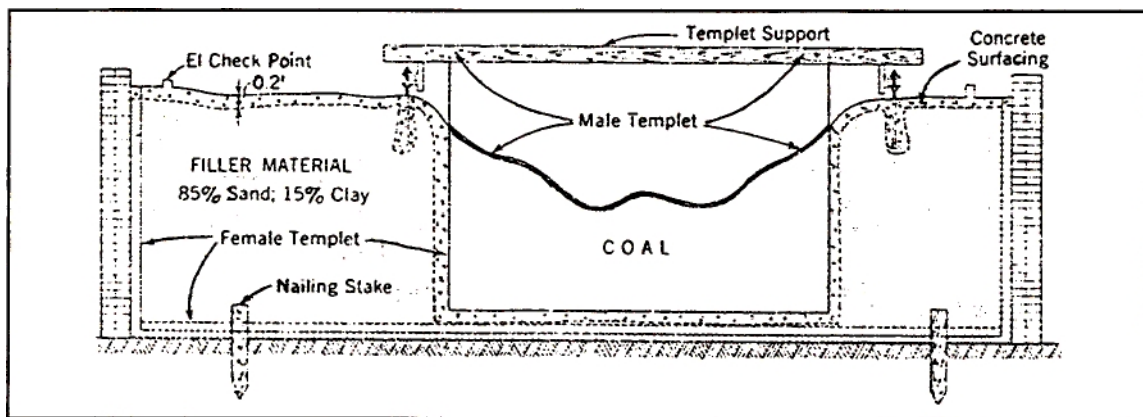


Figure 10. Cross Section of a Movable Bed Model, Obtained from WES

E. THE EXPERIMENTS OF OSBORNE REYNOLDS

Although they took place in the previous century, the experiments of Osborne Reynolds are of paramount importance to movable bed modeling and thus serve as a historical reference for the work conducted in this research.

The following are excerpts taken from Reynold's observations and conclusions during his first model study in 1887 of the estuary of the River Mersey (4):

The horizontal scale was two inches to a mile (1:31,800), and the vertical scale was one inch to eighty feet (1:960). Sand was the bed medium. A vessel was constructed having a flat bottom and a vertical boundary of the same shape as the high tide outline of the inner estuary. A shallow tin pan was hinged on to the otherwise open channel at the end, by raising and lowering which, when full of water, the motion of the tide could be produced throughout the model through the narrows.

In the first instance the tide pan was raised and lowered by hand, but as at the first trial it became evident that the model was not only going to show the expected circulation, but was also capable of showing, by the change in the position of the sand, the effect of this circulation on the configuration of the estuary and other important effects,...

Professor Reynolds eventually developed a time scale scheme based on the theory of wave motions, since the velocities *vary* as the square roots of wave heights. The velocities in his model corresponded to the velocities in the channel as the square roots of the vertical scales, about 1/31, and the ratio of the periods was the ratio of horizontal scales divided by the ratio of velocities, or $31/31800 = 1/1026$. The total prototype tidal period was approximately 40,700 seconds, thus, the tidal period of the model was $40,700/1026 = 40$ seconds. After developing an automated, continual tide generator and running numerous tests, Professor Reynolds made the following conclusions:

On one occasion the model was kept going for 6,000 tides, and a survey was then made of the state of the sand. And this will be seen to present a remarkable resemblance in the general features to the charts of the Mersey, of which three, 1861, 1871, 1881-are shown: in fact, the survey from the model presents a great resemblance to any one of these as they do to each other.

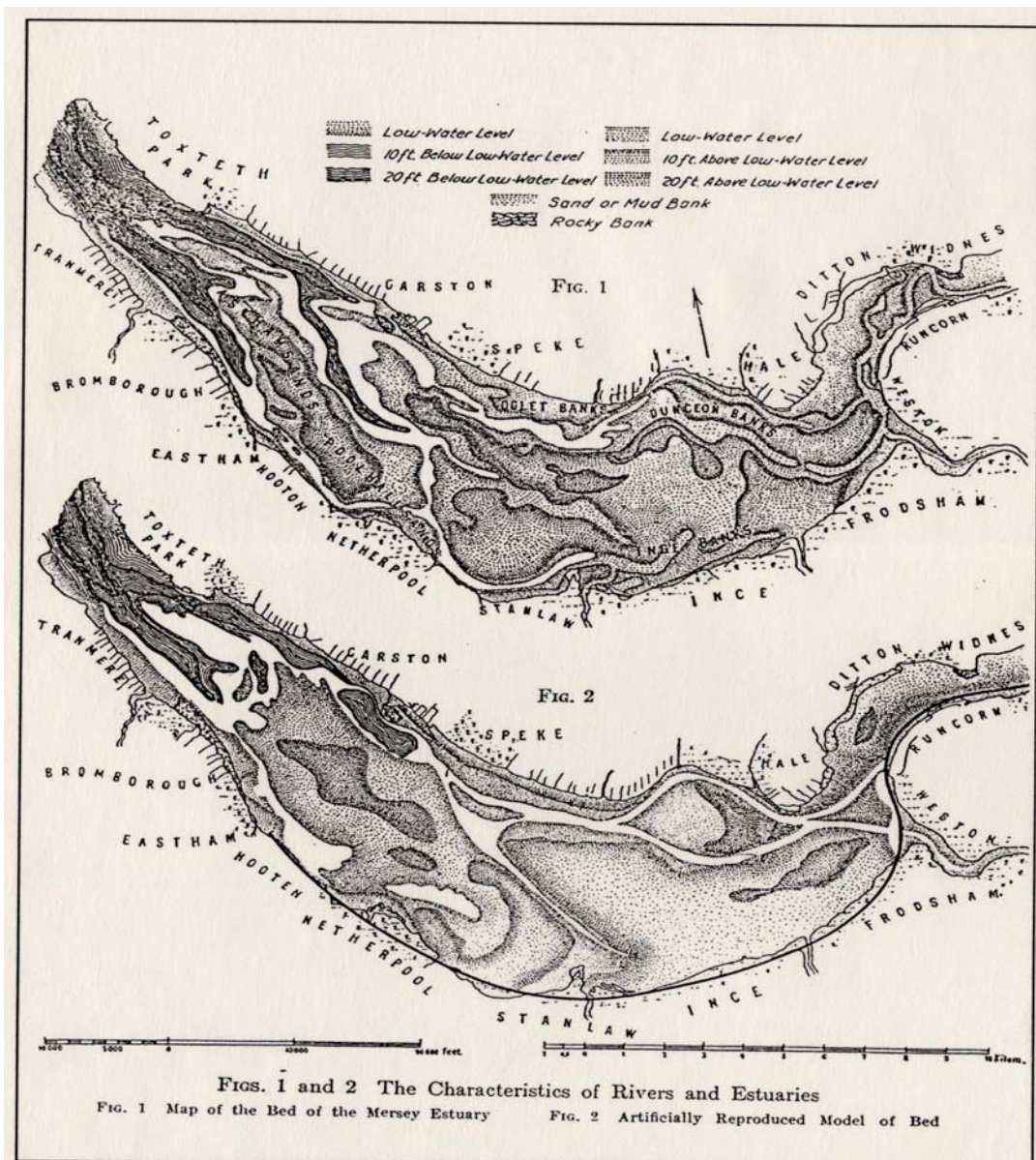


Figure 11. Map of Comparative Surveys in the Reynold's Experiment, from "Hydraulic Laboratory Practice"

In one respect the great difference between the model and the estuary calls for remark: this is the much greater depth of the model as compared with its length and breadth. The vertical scale being 33 feet to an inch, and the horizontal scale 880 feet to an inch, so that the vertical heights are nearly twenty-seven times greater than the horizontal distances, such a difference is necessary to get any results at all with such small scale models; and it is only natural to suppose that it would materially affect the action. As a matter of fact, however, it does not seem to do so. And, further, it would seem that, notwithstanding the general resemblance on the regime of the beds of large and small streams running over sand, there is in these a similar difference in vertical scale, the smaller streams not only have a greater slope, but also have greater depth as compared with their breadth and steeper banks.

So far as the theory of hydrodynamics will apply, it seems that in the model the effects of momentum of the water would be greater as compared to the bottom resistances than in the estuary, and I think that they are. In the model it certainly seems that the general regime is determined by the momentum effects, and from the almost exact resemblance which this regime bears to that of the estuary, it would seem that, although the momentum effects may be diminished by the greater resistance on the bottom, they are still the prevailing influence in determining the configuration of the banks.

In the meantime I have called attention to these results because this method of experimenting seems to afford a ready means of investigating and determining beforehand the effects of any proposed estuary or harbor works; a means which, after what I have seen, should feel it madness to neglect before entering upon any costly undertaking.

Reynold's research into small scale physical modeling continued with the submittal of three consecutive reports to the British Association in 1889, 1890, and 1891. These reports were an extension of Reynold's original experiments on the estuary of Mercy. Reynolds advanced the detail of the original model by developing an automated tidal model.

Reynolds stated that one of the largest difficulties of the modeling process was being able to readily obtain detailed survey information of the bed. The nature of the model enabled Reynolds to develop a simple survey system. After each test, the model was flooded in small, equal depth increments. At each increment, the water's edge was delineated by a piece of cotton string. A light was mounted within the model, and a glass cover was then placed on top of the flume. The string was traced on a gridded map to produce referenced contours. The total time to conduct one survey in this manner was 5 hours.

Reynolds noted particular problems with the fowling of the sand. The fines apparently created adverse effects to some of his experiments, making it difficult to see the actions of the water during extreme fowling cases. However, Reynolds concluded that similarity was remarkably true, even though the model scales were drastically distorted and the model was extremely small.

The practical application of Reynold's model operation showed that proposed training works in the upper reaches of the River Mersey would have adverse impacts to the navigation channel, and as a result, all future construction plans in the upper Mersey were rejected.

In spite of Reynold's experiments, published results of other model studies with similar scales are non-existent. Although the concept of movable bed modelling was used extensively thereafter in the laboratories of Europe, the physical scale predominately used for river studies varied

between 1:10 and 1:300 horizontal and contained little or no distortion. The Europeans were convinced that any distortion in scale would generate improper influence of flow around structures, thereby rendering the results unreliable.

Fortunately, the rivers under study in Europe were much smaller in size than those of the United States. Scales could be made large while still providing a manageable model size. Studies were limited to comparatively short reaches to further minimize costs.

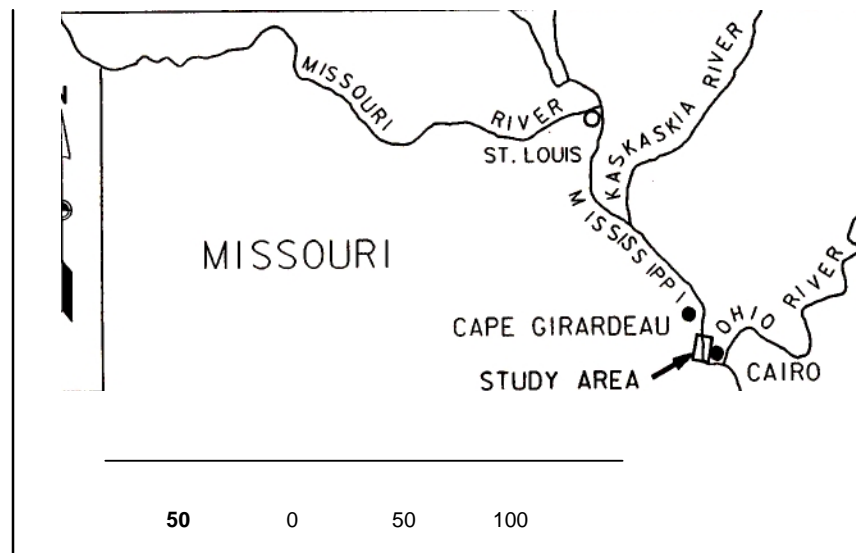
III. PROCEDURE

A. MICRO MODEL THEORY

Because small streams display similar tendencies of sediment transport as compared to larger rivers, there exists the possibility that extremely small movable bed models with scales approximately 1:15,000 horizontal and 1:1200 vertical can be designed to simulate the tendencies of the prototype. This is the hypothesis of this thesis. Reynolds proved that this hypothesis was valid as applied to the modeling of estuaries. To explore the validity of this reasoning as applied to rivers, a model roughly the size of a table top with the scales discussed above was designed by the author (hereafter called "micro model"). The bed material used was ground plastic with a specific gravity of 1.23. The micro model represented approximately 20 miles of the Mississippi River, although only 15 of these miles were actually calibrated and studied in this research. Maps 1 and 2 are location and study reach maps of the area under analysis. Figure 12 is a photograph illustrating the representative layout of the micro model.

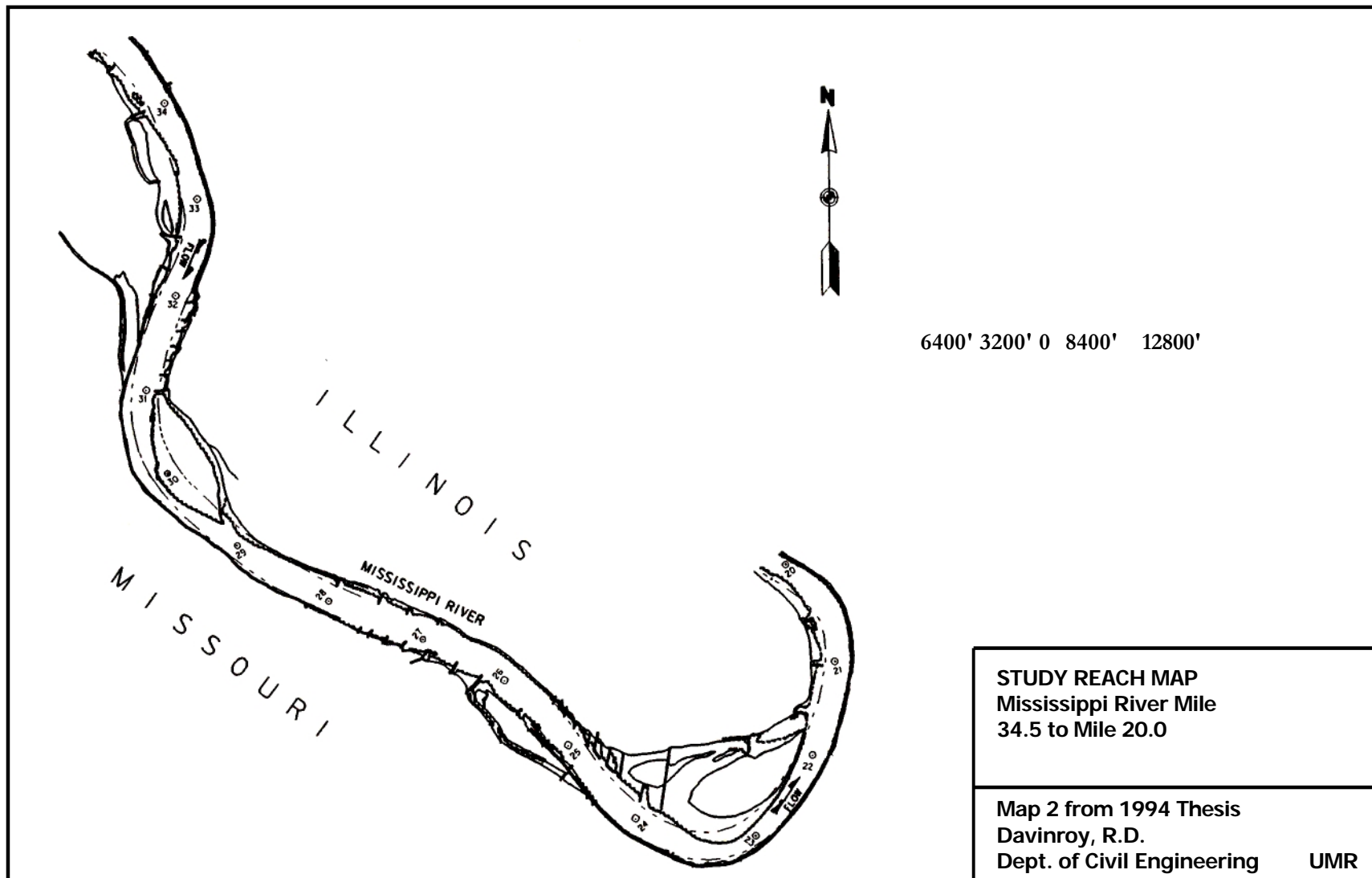
1. Geometric Scale Comparisons. Before describing the details of design, construction, and operation of the micro model, a discussion of the comparison of scales between the micro model, a larger movable bed model of the Mississippi River previously constructed, and the prototype is warranted.

a. Dogtooth Bend Model Scale. A movable bed model developed for the St. Louis District Corps of Engineers was constructed at the Waterways



LOCATION MAP
Mississippi River

Map 1 from 1994 Thesis
Davinroy, R.D.
Dept. of Civil Engineering UMR



Map 2. Study Reach Map



Figure 12. Micro Model of the Mississippi River

Experiment Station (WES) in Vicksburg, Mississippi (Figure 13). This model represented the same 20 mile prototype study reach of the Mississippi River as that modeled by the micro model. The WES model was successfully used for the design of channel improvement works, namely the design of Bendway Weirs (discussed in a proceeding section). Because the model studied navigation problems in bends, and in particular, problems at a major bend at Mile 22.0 to 24.0 (Dogtooth Bend), the model has been referred to as the Dogtooth Bend model (24).



Figure 13. Dogtooth Bend Model at WES

The Dogtooth Bend used a horizontal scale of 1:400 and a vertical scale of 1:100. For the 20 mile reach of the prototype, the physical dimensions of the model were approximately 5 feet in average width, 0.5 feet in average depth, and 265 feet in length (88 yards). The scale of the model is typical for most Mississippi River navigation studies conducted at WES. Scales of past studies have generally ranged between 1:250 and 1:540 (22).

To show how the two models compare to the prototype, volumes rather than areas were used because it was felt this comparison gives a more dramatic description of the relative differences in geometric scales between the two models and the prototype.

Consider the representative volumetric segment of the prototype and the Dogtooth Bend model in Figure 14. The volumetric segment of the model,

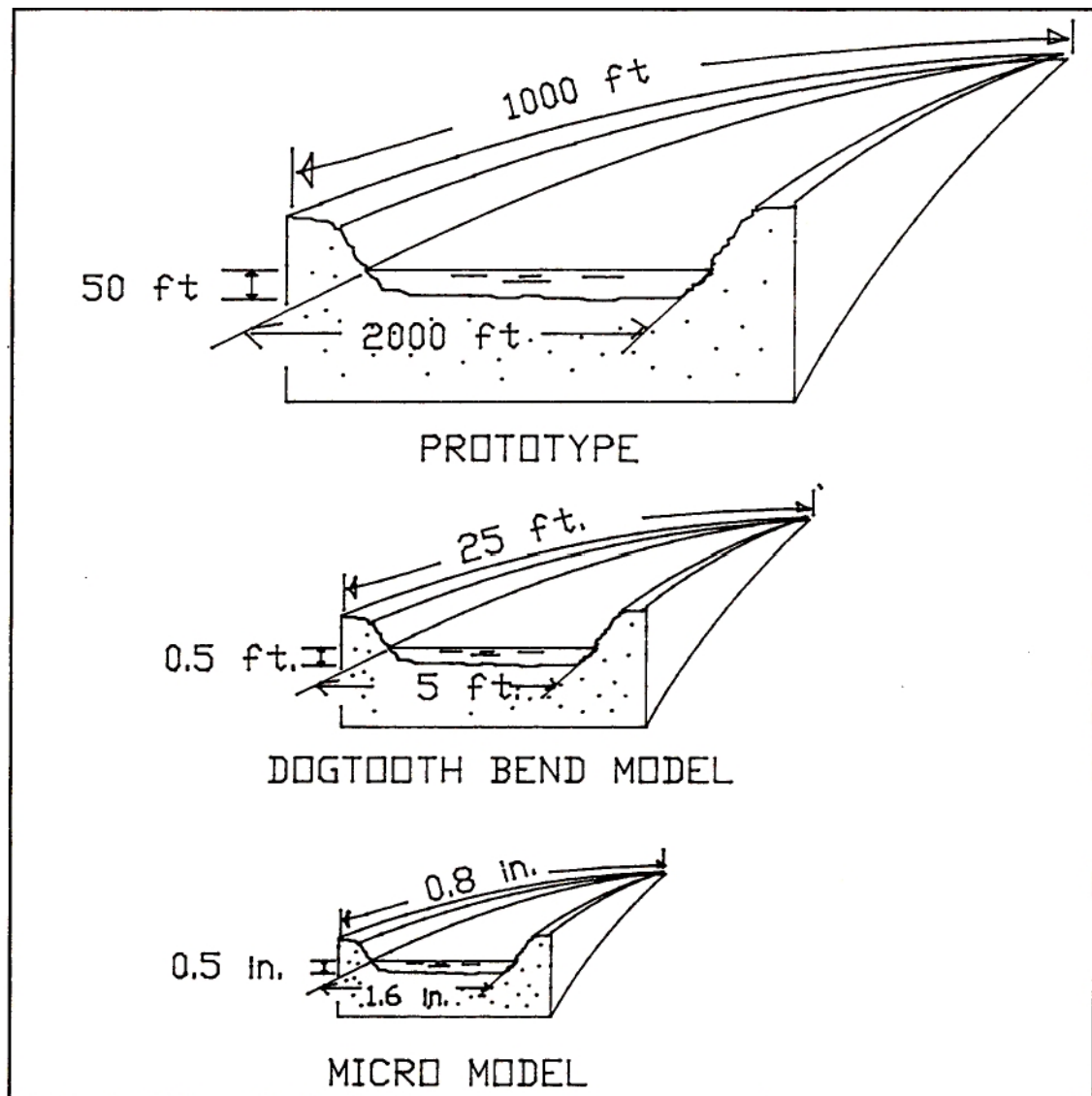


Figure 14. Conceptual Volumetric Comparisons of Prototype and the Two Models

V_m , is computed as 6.25 ft^3 . The volumetric segment of the prototype, V_p , is computed as $100,000,000 \text{ ft}^3$. The volumetric ratio of the prototype to the model, V_p / V_m , is thus 16,000,000. The WES model is approximately

16,000,000 times smaller than the prototype, or built to a 1/16 millionth scale.

Ironically, even though the actual physical dimensions of the model are quite large, the relative scale of the model as compared to the prototype is small. If a model that is 16 million times smaller than the prototype, as is the case with the Dogtooth Bend Model, can be made to produce a bed configuration that is similar to that of the prototype, then what is the lower size limit on a movable bed model that can achieve this same similarity?

Intuitively, the physical limitation of the size of the model relies on a variety of factors. Probably the two most important factors are the practicality of measurement and the effects of the physical forces.

b. Micro Model Scale. If a model is too small, it would become impossible to make measurements that could be projected to the prototype. One of the goals of this thesis and micro model theory in general was to design, construct, and operate a model that was small yet sufficiently large to make useful measurements of bed topography and velocities. A size with a horizontal scale of 1:15,000 and a vertical scale of an inch for each 100 ft. (1:1200) was chosen as a starting point. This gives a distortion 12.5. The horizontal scale is the same scale as some of the aerial photography of the Mississippi River used by the Corps of Engineers. The measurement of model depths to the thousands of an inch was made with a digital micrometer.

For the 20 mile prototype reach, the average physical dimensions of the micro model were 1.6 inches in width, 0.5 inches in depth, and 84 inches in length (7 feet). Referring again to Figure 14, the volumetric segment of the micro model, V_{mm} , is computed as 0.0003704 ft^3 . The prototype to model ratio, V_p / V_{mm} , is computed as 270,000,000,000.

Thus, the micro model is approximately 270,000,000 times smaller than the prototype, or built to a $1/270$ millionth scale. This extremely small scale model would suggest upon first consideration a tool of limited value or use. However, remember that the Dogtooth Bend model is approximately 16 million times smaller than the prototype. In relative terms, how much smaller is the micro model than the large model to the prototype?

The ratio, V_m / V_{mm} , is computed as 16,875. The question becomes, how small is permissible without adversely effecting the sediment response of the model?

2. State of Flow Computations. As previously discussed, movable bed model theory employs an empirical approach to similitude. The laws of similitude are relaxed or deviated from, and a process called adjustment/calibration has been developed whereby parameters of the physical model are adjusted until characteristics of the prototype are sufficiently represented. However, in order to apply this concept, a basic understanding of the various states of flow experienced in the prototype and the two models is necessary.

Gravitational and viscous effects must be considered when describing the various states of flow. Each effect is evaluated by the Froude and Reynold's laws, respectively. For gravitational effects, the ratio of inertial forces to gravity forces, known as the Froude number (equation 18, Section IC) is used. When F is equal to 1, then the flow is considered to be in the critical state. If F is less than 1, then the flow is subcritical. Here the gravity forces have a large influence and the velocities are thus small. This state of flow is often described as tranquil and streaming. If F is greater than 1, then the flow is supercritical. In this condition the inertial forces are dominant, so the velocity is large and the flow is described as rapid, shooting, and torrential (25).

The effect of viscosity upon flow is expressed as the ratio of inertial forces to viscous forces, known as the Reynolds number, defined as,

$$R = \frac{VL}{\nu} \quad (23)$$

where:

V = the velocity of flow in feet per second

L = characteristic length defined as the hydraulic radius
(area / wetted perimeter)

ν = the kinematic viscosity of water in ft^2/sec .

If R is less than or equal to 500, then the flow is often assumed to be laminar. In laminar flow the viscous forces dominate, and the fluid particles move along definite, smooth paths in a coherent pattern. If R is equal to or greater than 12,500, then the flow is considered turbulent. In turbulent flow,

the inertial forces are so large compared to the viscous forces that the fluid particles move in an incoherent or random fashion. If R is between the range of 500 to 12,500, then the flow is considered transitional. In this condition the flow is neither laminar or turbulent. This condition has been described also as the mixed state (26).

a. State of Flow in the Prototype. Much has been written about the state of flow conditions experienced in the prototype, or Mississippi River. Based on data collected from numerous studies conducted on the Middle Mississippi River by the Corps of Engineers, the average velocity for a typical straight reach section of the river flowing at midbank stage is approximately three feet per second. Using the typical dimensions illustrated in Figure 14, under midbank conditions, and defining the hydraulic depth, D , as equal to the average depth, the hydraulic depth is 25 ft. The Froude number is computed as 0.1057. Therefore, the flow is subcritical as a result of the low velocity and the relatively large section.

The hydraulic radius, L , under conditions depicted in Figure 14, is 24.39 ft. The Reynolds number is thus computed as 6.775×10^6 , and the flow is considered to be turbulent. Obviously, these numbers will vary over any given time period because the velocity and section areas change with varying discharge and stage.

b. State of Flow in the Dogtooth Bend Model. Dimensions of a typical straight reach section of the Dogtooth Bend model at midbank conditions are shown in Figure 14. The average velocity during this condition was

approximately one foot per second, based on model study information from the Corps of Engineers. The Froude number is 0.3524, so the flow is subcritical. The Reynolds number is 21,000, so the flow is turbulent.

c. State of Flow in Micro Model. Floats were used to determine the magnitude of the velocity in the micro model at midbank conditions. Results showed that the velocity was 0.6 ft./sec. Referring again to the dimensions of Figure 14, the Froude number is 0.6221, so the flow is subcritical. The Reynolds number is 1100, so the flow is transitional, or in the mixed state.

What conclusions can be made from these comparisons? It can be observed by these calculations that the state of flow conditions, i.e., the Reynolds and Froude numbers, are significantly different in the prototype and the two models. However, as will be illustrated in the comparative model surveys of Section IIC, both models exhibit the ability to replicate a similar bed configuration as compared to the prototype. How can this be possible if the state of flow conditions are so drastically different between model and prototype? The answer lies not in the relative state of flow, but the relative state of the sediment transport, which is discussed in the following section.

3. State of Sediment Transport. In examining differences in the sediment transport characteristics of the prototype and the two models, a variety of variables must be taken into consideration, including: drag force, shear stress, density, particle size, viscosity, etc. The intent of this section is to explain why the sediment transport characteristics between the models

and the prototype are similar, as verified by the bed configuration surveys in Section IIC.

Intuitively, the answer at first would seem to lie in the relative specific densities of the material being used in the models. For the Dogtooth Bend model, the material was crush coal with a specific gravity of 1.3, and the micro model, plastic, with a specific gravity of 1.23. These materials are approximately 5.5 to 6 times lighter than sand (specific gravity 2.65) when submerged in water (22). This would attribute to the relative ease of transport as visualized in the model. However, Reynolds showed that even a material as dense as sand could be used in a model that was almost as small as the micro model.

The main difference between the Reynolds model and the micro model was the time scale used. In the Reynolds model, the simulation of a tidal year required approximately 8 hours. In the micro model, the simulation of a yearly hydrograph required 2 minutes.

To investigate the influence of material density, tests were conducted in the micro model using sand. The transport tendencies were similar as with the plastic, but it took a longer period of time for the development of the bed configuration. The model was run for two hours at peak flow to examine the formation of the point bars at the two main bends at mile 30 and mile 23. At the end of two hours, the bars were approximately 10 percent formed. This verifies the results of the Reynolds model. This same test, using plastic, required only 50 seconds to fully develop the point bars and

obtain sediment transport equilibrium (sediment input equalling sediment output). Deductively then, any material density within reason could be used in the micro model. The main difference would lie in the relative time scale required for sediment transport.

Physical scale is an important factor in this process as well. In the larger WES model, the density of the material (1.3) was nearly the same as the plastic used in the micro model (1.23). Yet, in the WES model, a much longer time scale was required for the simulation of the yearly hydrograph (approximately 40 hours vs. 2 minutes). The difference was not in the relative ease of transport, since the densities were nearly the same, but in the total volume of material being moved in any given location.

Concerning particle size of the bed material, a rationalization might be made that since the relative scale of particle size is so drastically different between the models and the prototype, then the practicality of similar transport would be out of the question. However, as Franco (22) states:

In natural streams, the size of bed material does not vary in direct proportion to the size of the river and tends to be larger in the smaller streams. Since the same general laws apply to rivers whether large or small and whether moving in sand, gravel, or clay, the size of the material forming the channel should not in itself affect channel development.

This quote is verified by the observation of the sediment transport in the models and the resultant bed configurations. Regardless of relative particle size, model to prototype, similar sediment transport was observed in both models.

One final point needs to be made on sediment transport similarity. This concerns the erosional and depositional criteria of the prototype as compared to the model. Most model bed materials are non-cohesive. Thus, the two phase flow in the model is such that the sediment transport process is totally bed-load. The rate of transport is proportional to the excess shear stress (excess shear stress over the critical value for initiation of motion). In contrast, the prototype contains non-cohesive and cohesive sediments in which the cohesive particles, once eroded, are transported at a rate dependent only on their concentration and the velocity of flow until they approach the bed and the bed shear force permits redeposition. In short, the task of the modeler is to achieve correspondence between the ability of the model to transport and deposit available non-cohesive sediment and the ability of the prototype to transport and deposit both non-cohesive and cohesive sediment.

Literature has been written on this difference in transport scheme of model and prototype. MacAnally (18) hypothesized that under certain conditions, suspended sediments resulting from the cohesive transport scheme of the prototype may contribute significant material deposition upstream of dams, lock chambers, and other backwater inducing structures.

In summary, the physical scales and associated forces of the two models are significantly different than the prototype. However, by combining bed materials of low density, large relative particle size, and appropriate time scales, and, by skillfully employing the calibration variables of slope,

discharge, and sediment input, the models can both be made to transport sediment in a similar fashion as the prototype. Caution must be taken, however, to consider those instances where suspended sediment contribution may be great enough to have significant effects.

B. MODEL APPURTENANCES

1. Design, Materials, and Construction. Figure 15 is an illustration of the general design layout of the micro model. A descriptive checklist included:

a. Flume. The flume was constructed out of lightweight wood with a fiberglass coating. The dimensions were 5 feet by 2 feet by 0.5 feet. The flume was elevated 4 feet off the ground on a custom built stand. The stand contained bottom screws for the adjustment of model slope.

b. Pump. A 12 volt, submersible centrifugal pump rated at 300 gph was used. Voltage was supplied by a D.C. power supply.

c. Water Outlet Control. Water flow was manually controlled by the installation of a series of ball valves at the entrance to the model.

d. Alignment Insert. A rectangular insert was prepared containing an exact scaled "plan view" alignment of the Mississippi River. The channel of the alignment was precision formed out of laminated corkboard strips to a depth of 3 inches. The insert was fit within the rectangular flume, and could be replaced with other inserts if desired.

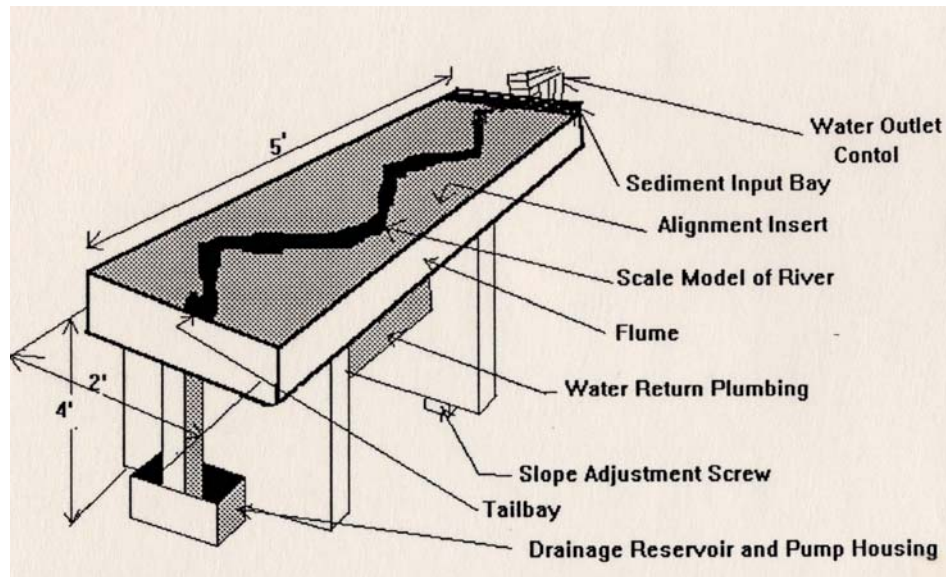


Figure 15. General Design Layout of Micro Model

e. Sediment Input Bay. At the upper end of the flume, an input bay was constructed for the introduction and storage of sediment.

f. Tailbay. A tailbay was constructed out of corkboard and placed at the end of the alignment insert. This was used for additional slope adjustment during the operation of the model.

g. Drainage Reservoir and Pump Housing. A plastic drainage reservoir which contained a catch basin for the sediment and housing for the pump was located at the lower end of the flume.

2. Operation. The extreme smallness of scale of the micro model yielded tremendous advantages in operation. The entire model was run manually by one person in the following manner:

a. Discharge and Stage. The discharge and stage was simulated in the micro model by controlling the ball valve at the control outlet and simultaneously reading 2 staff gages marked on the sides of the model banks. A stopwatch was used to produce the desired time increments of the design hydrograph.

b. Bed Material Input. A lump sum quantity of bed material (plastic) was introduced into the upper end of the study reach before each run by use of a calibrated measuring cup. This quantity was determined experimentally through trial and error. The idea was to place enough material so that the model could feed itself, exhausting the entire amount just at the end of the simulated design hydrograph.

c. Slope. Slope was supplied by the combined use of the slope adjustment screws and the tailbay.

3. Data Collection and Output Scheme. One of the most critical considerations in this research was the development of method to accurately and efficiently define the topography of the resultant bed configuration after each design hydrograph. This was achieved by use of a survey system developed by the author. The system involved the following procedure:

1). Eighty cross section locations perpendicular to the flow were marked in plan view on top of the alignment insert. The alignment of the

channel and the cross section locations were then traced to a plan view map.

2). The traced map was digitized into the computer using AUTOCAD (26).

3). The plan view alignment boundary of the river and all cross section locations were translated into an x and y coordinate system by use of the AUTOLISP program SHCROSS1(27).

4). A digital micrometer was mounted on a sliding ruler and placed at each cross section location (Figure 16). Depths were read to the nearest hundredth of an inch along even increments of the channel and recorded into the computer.

5). After all the points were collected and recorded (approximately 350 points), the data was entered into the computer as a comma delimited file.

6). The data file was read by again using SHCROSS1. All points were automatically translated onto the original digitized map of the river in x, y, and z coordinates. SHCROSS1 then created two output files, RIVER.BLN and RIVER.XYZ. The first file contained all points of the river alignment in x and y coordinates. The second file contained all collected depth points in x, y, and z coordinates. Both files were in comma delimited format.

7). The two files were then read by SURFER (28). A 150 by 150 grid file (RIVER.GRD) was created. A contour map of the bed configuration within the channel was produced from the grid file and output as the plot file

RIVER.PLT. One complete survey required about 2 hours to complete.

Figure 17 is a flow chart of the survey system procedure. Purchase or development of an automated, three-dimensional digitizing system could not only improve accuracy in the survey measurements, but could also save costs in the future. Such a system would improve the modeler's ability to run many more model tests and analyze the surveys in an even shorter period of time.

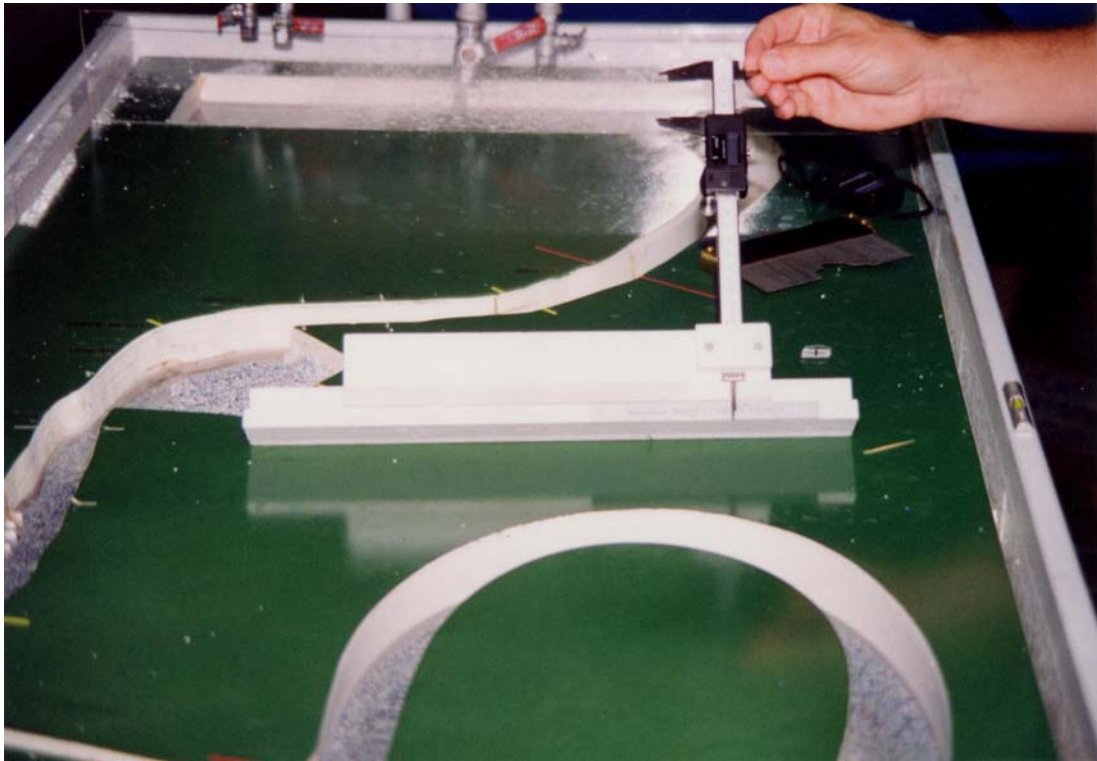


Figure 16. Sliding Micrometer System for the Collection of Depths

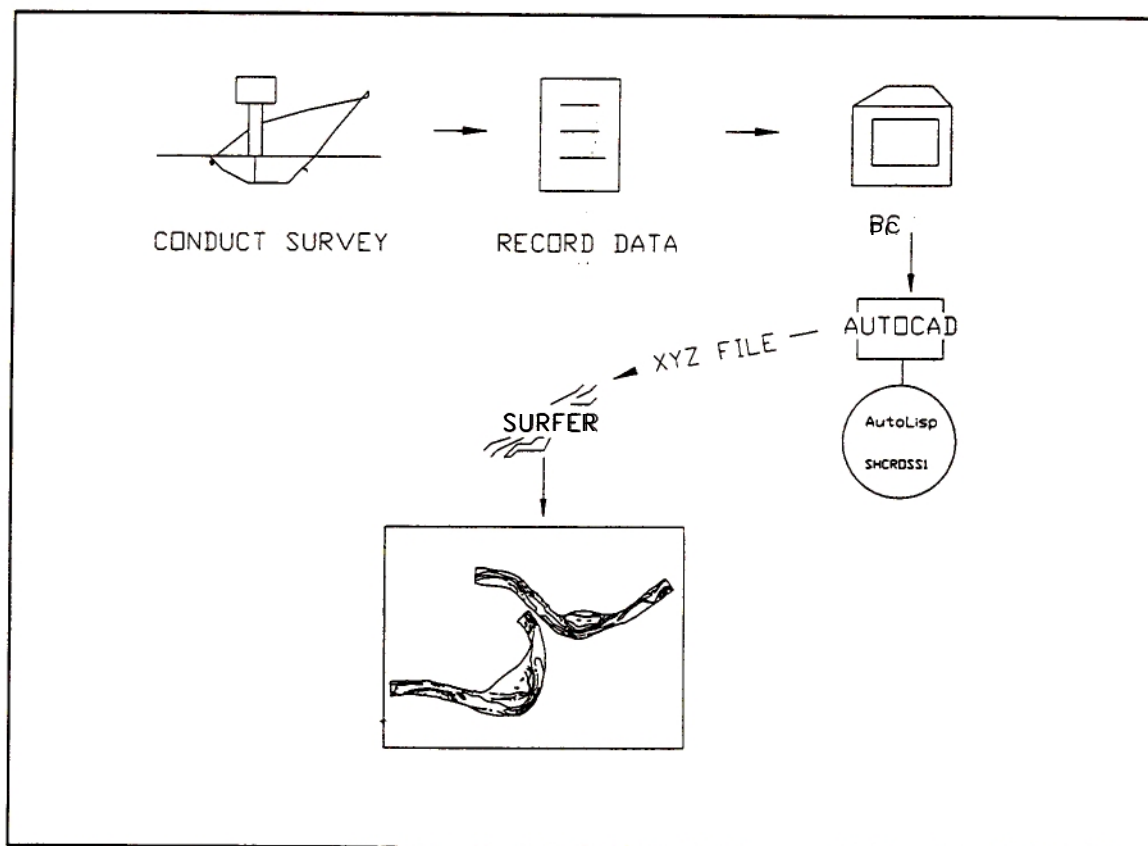


Figure 17. Flow Chart of Survey Procedure.

C. CALIBRATION

As with the use of any hydraulic model, whether it be physical or mathematical, the calibration of the model is the most critical step in obtaining a useable tool by which to investigate future design impacts. Calibration may be complex or simple. A model that contains a multitude of variables to adjust during the calibration phase does not necessarily suggest that the particular model is more reliable or accurate in its predictive abilities. Only after the evaluation of actual events can the model be rated in its performance on replicating the conditions of the prototype.

In perspective, the calibration process of the micro model combines existing movable modeling procedures with new procedures never before proposed. The micro model calibration process is outlined in this section, and when deviations from standard procedures occur, some discussion will follow.

1. Calibration Measurements. The three main calibration factors, discharge, slope, and sediment were measured in the model as follows:

1). Discharge was measured by the simple use of a calibrated cup and stopwatch. A total of 10 discharge measurements were made for individual stages of 0,15,20,25, and 30 feet above LWRP. LWRP is the acronym used by the Corps of Engineers for the Low Water Reference Plane, a design datum plane established on the Mississippi River based on a discharge of 54,000 cfs.

2). Slope was measured with a level in terms of the water surface as related to LWRP.

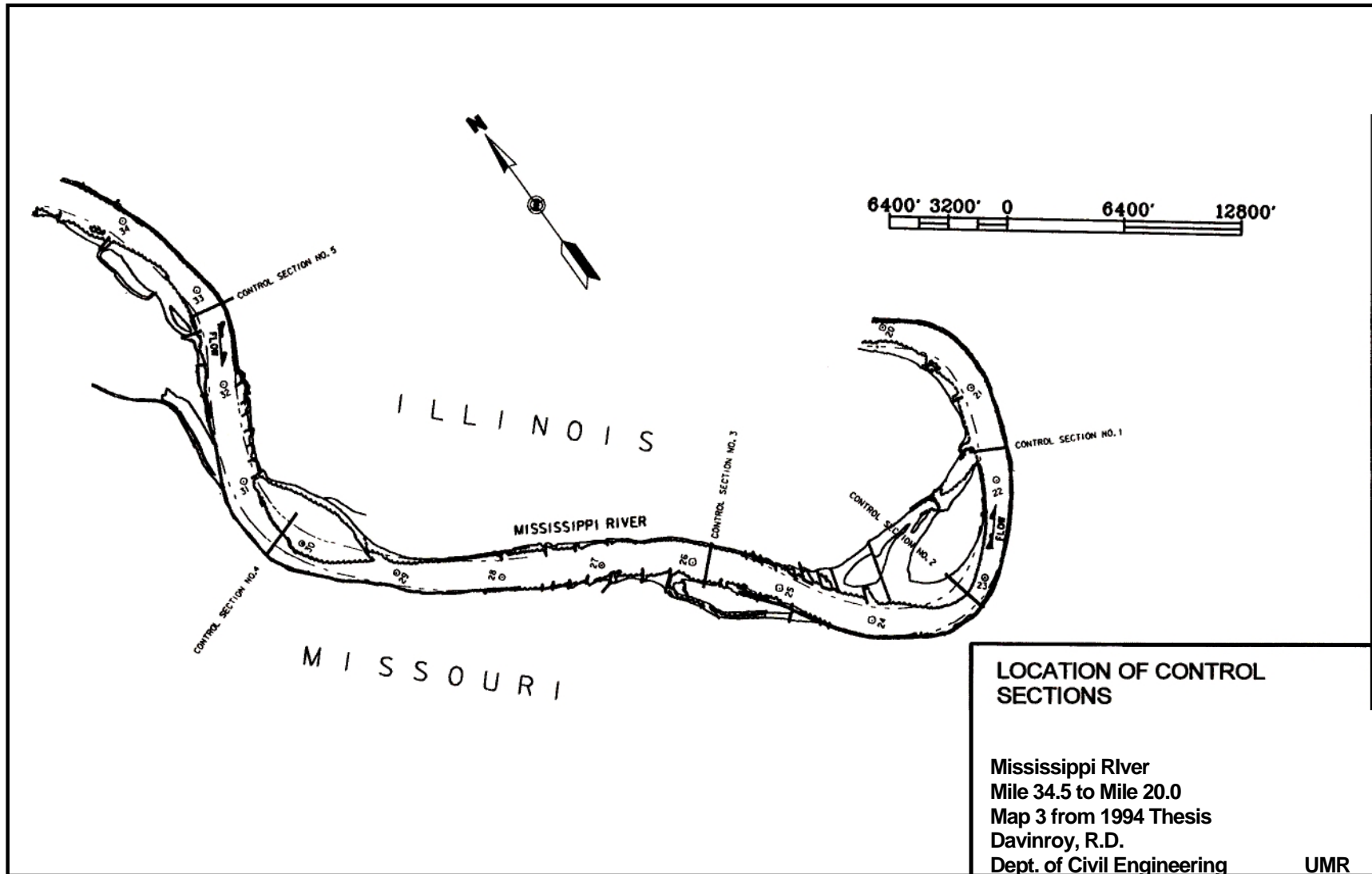
3). Sediment was measured as a volume by use of a calibration cup.

2. Geometric Scale Determination. In movable bed modeling, suitable scales are selected by the modeler before construction. Templates are made according to this scale from a prototype survey or surveys, and the banks and bed of the model are formed or molded. Then, during the calibration phase, variables of the model such as slope, discharge, etc. are adjusted until satisfactory similarity with the prototype is achieved.

A different approach was taken in this research. First, the plan view alignment and corresponding banks of the prototype were constructed in the micro model to a predetermined horizontal scale. Second, however, instead of preparing templates and forcing the micro model to respond to a fixed vertical scale, the channel flume was homogeneously filled with sediment to approximately fifty percent of the total depth (approximately 1 inch in depth from the top bank). A number of different steady state discharges of 10 minutes each were then simulated in the model. After each run, the bed of the model was compared to the prototype at five strategically placed control sections along the study reach (Map 3).

This procedure was an important step because it enabled the modeler to determine the vertical scale according to the already preset horizontal scale. The goal was to close in on a scale that generated satisfactory bed movement while at the same time allowing for direct measurements and conversion to the prototype. Theoretically, for a preset horizontal scale, there is an optimum vertical scale that will most effectively replicate the sediment transport tendencies of the prototype.

In this particular case, with a chosen horizontal scale of 1:1250, the best vertical scale seemed to be in the order of 1 inch = 80 feet, or 1:960. However, to eliminate the application of a scale factor to the readings from the micrometer, a scale of 1 inch = 100 feet (1:1200) was chosen. Additional flow simulation and surveys collected at the 5 control sections indicated that this slight deviance did not significantly change the response



Map 3. Location of Control Sections

of the model. In the future, use of a three-dimensional digitizer would enable a direct vertical scale measurement.

For the above scales, the distortion was thus 12.5. Reynolds, in his River Mersey model, used a distortion of 33. Literature recommends that models have a distortion of no greater than five (22). However, this applies to much larger models in which the above experimental procedure would be economically impractical.

3. Discharge Relation Curve. Once the vertical scale was established, a discharge relation curve of the model vs. the prototype was developed. Using Mississippi River flow data obtained from the St. Louis District Corps of Engineers and the computed average values of the model measurements, the discharge relation curve of figure 18 was developed. This curve can be compared to the curve of Figure 8 to illustrate the difference in discharge between the micro model and larger models at WES.

The discharge relation curve might be used as a measure of the expected discharge response relationship between the micro model and the prototype. However, only after a number of micro model studies can a more accurate measurement of this relationship be known. Theoretically, the procedure would be to plot a multitude of points from many studies and draw a best fit line. Another approach would be to develop an envelop of curves. This information could then be used to "zero in" on the discharge scale the modeler would need to use for a given scale, slope, etc.

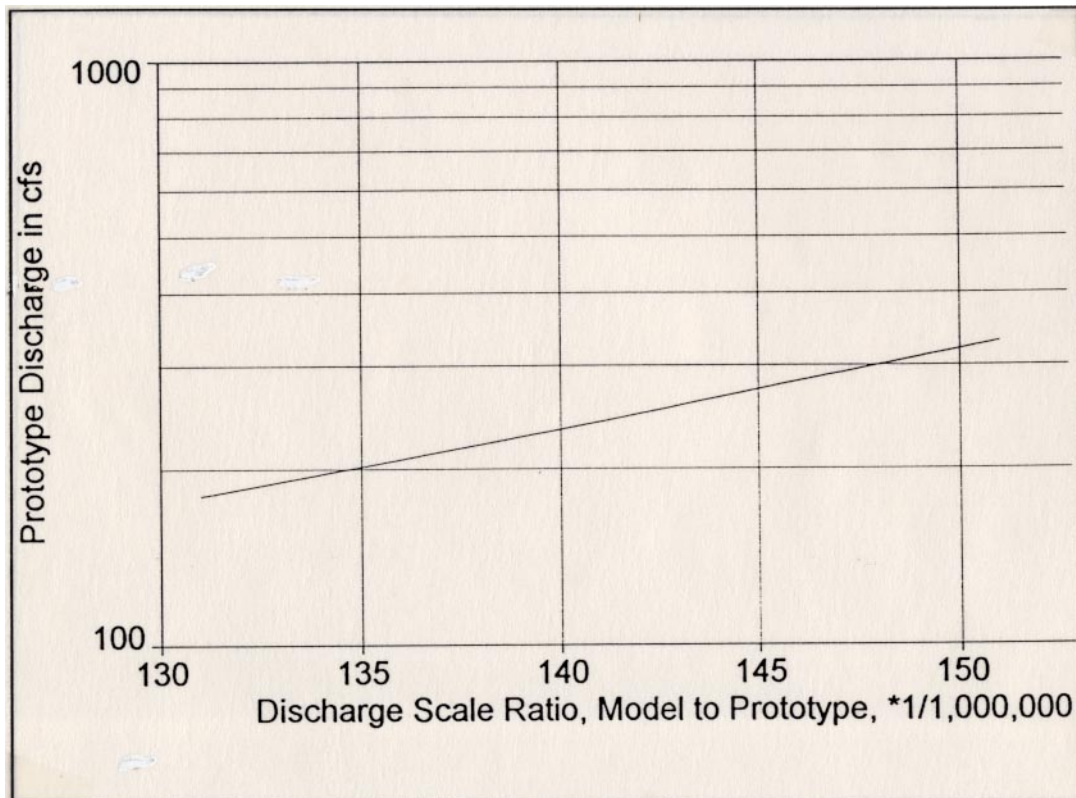


Figure 18. Discharge Relation Curve, Model to Prototype

4. Slope. Once the geometric scales were determined, the model slope was adjusted until satisfactory bed development was observed in the model. This was a trial and error process that involved many hours of adjustment. The slope that provided satisfactory bed movement and channel shaping throughout most of the model study reach for the vertical scale of 1:1200 was a slope of 0.02067.

This slope was measured relative to LWRP, and all referenced stages were assumed parallel to this plane in the model. The actual slope of LWRP on the Mississippi River between Mile 40.0 and Mile 20.0 is 0.65 feet per mile, or 0.0000947. Thus, the micro model slope was approximately 218 times greater than the prototype slope.

In model scale terms, the slope of 0.02067 represented a prototype slope of 8.73 ft per mile, or roughly 17 times the slope of the prototype. This is 1.36 times greater than the vertical distortion. These ratios may be used as a guide for future micro model studies, although only by conducting a number of studies will more exact model to prototype slope relationships and model slope to model distortion relationships be more fully known.

The extreme differences in slope are acceptable as long as one realizes that water surface profiles are not being modeled. The large slope is a necessity for a model of this small a scale because adequate forces are required to move the bed material of the model.

No additional supplementary slope (Section IE) was used because of the nature of the micro model. Supplementary slope could not be applied because the modelling process did not employ the use of templates. Also, because the movement of material in this model was so dynamic over such a short time period, even if supplementary slope could have been applied, the effects would have been quickly eliminated.

5. Average Annual Design Hydrograph. To calibrate the micro model and predict future responses, an average annual design hydrograph was developed. This hydrograph was formulated by the author during the Dogtooth Bend Model Study (16). The hydrograph was based upon 10 years of record (1973 to 1983). Volumetric flow data for gaging stations located in the proximity of the study reach (Mile 40 to Mile 20) were obtained from the United States Geological Survey. The data was averaged for each month

over the ten year period. These values were then converted to average monthly discharges and input into the computer program HEC-2 (29). Water surface profiles were computed for the study reach. The resulting model stage/discharge hydrograph (stair-stepped for model operation) at control section 23.3 is shown in Figure 19.

All stages and bed elevations on the model were measured in relation to LWRP, as discussed previously. LWRP is a datum used for dike construction, dredging, and development of the 9 foot navigation channel on the Mississippi River.

6. Time Scale and Sediment Input. A micro model time scale was developed based upon experimentation. Representative yearly durations were simulated in the model, ranging from 20 minutes to 1 minute. Tests revealed that adequate sediment movement could occur within a minimum duration of 2 minutes. Thus, one prototype day equaled 10 seconds on the model.

For the simulation of one design hydrograph in the model, the addition of 10 ounces of sediment was required. The material was introduced at the upper end of the model. This same amount was consistently added before the start of each test. This quantity was established through trial and error, as discussed previously.

It should be noted that because the time scale is determined empirically in movable bed modelling, the time is not interpreted in any way as being related to the actual time required to accomplish the measured bed changes.

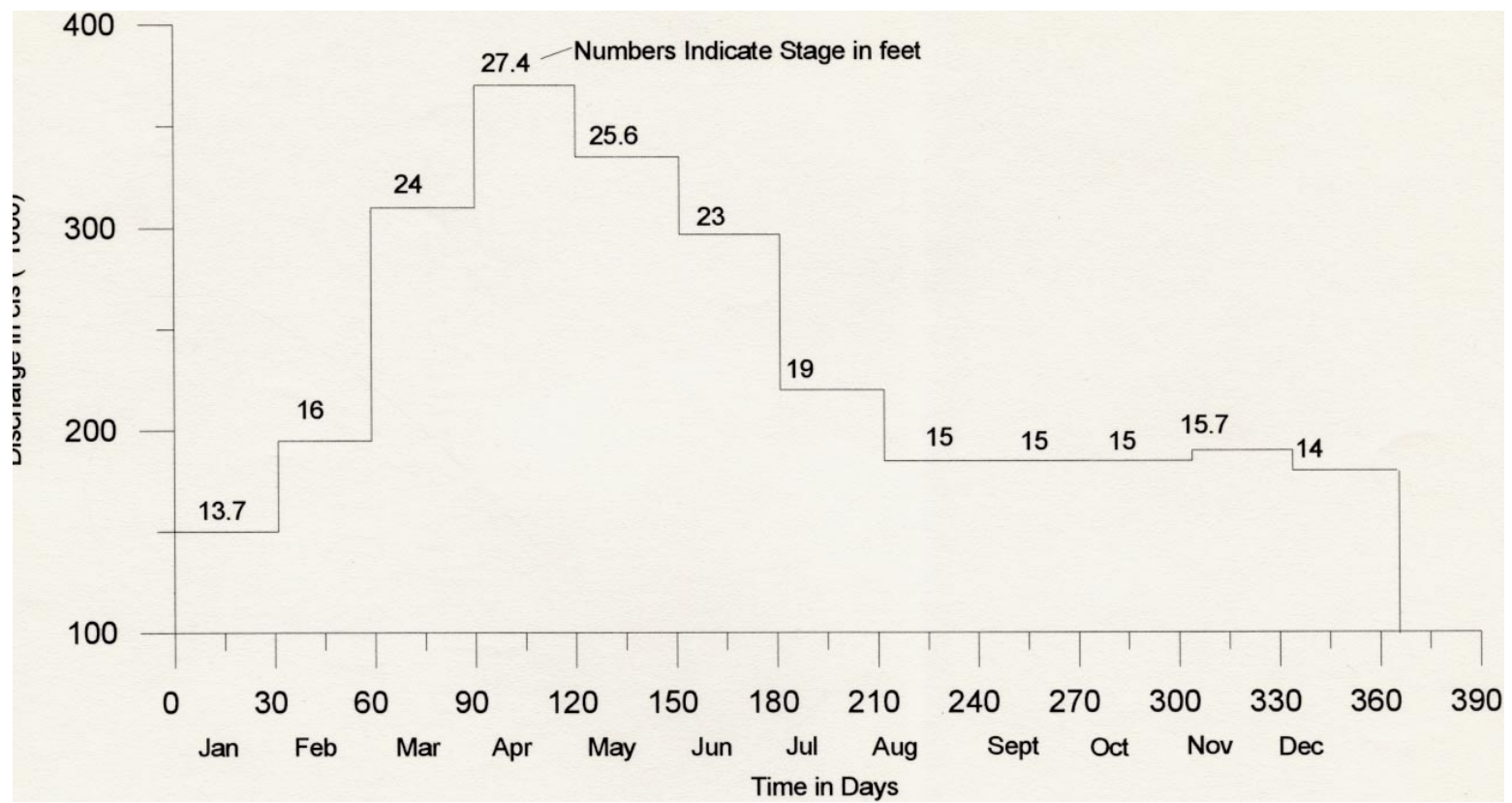


Figure 19. Average Annual Design Hydrograph at Dogtooth Bend, Mile 23.3

However, by studying the prototype and conducting surveys over the course of a yearly hydrograph, one might be able to establish some sort of time correlation of sediment movement between the model and the prototype. This is additional research that may further benefit the use of the micro model.

7. Development of Starting Conditions. Once the vertical scale was chosen, the bed was again homogeneously filled to approximately fifty percent of the capacity of the channel. The next step paralleled the approach developed in the model scale selection. Instead of molding a starting bed configuration from templates based upon prototype surveys, the bed configuration was formed naturally from the physical alignment of the river.

To fully develop the configuration of the point bars of the bends, consecutive design hydrographs were run. Full bed development occurred after 5 runs.

The resulting cross section was then compared to the prototype at the five control sections. If deviations were apparent, then an adjustment in the slope and discharge scale was made, and the procedure repeated. Figure 20 shows a comparison of the calibration runs vs. the 1983 prototype survey.

This method directly deviates from movable bed model procedures used today and in the past because it does not force the river model to start at a predetermined bed configuration. It eliminates the need for the use of templates. Instead, the method uses the scaled horizontal alignment

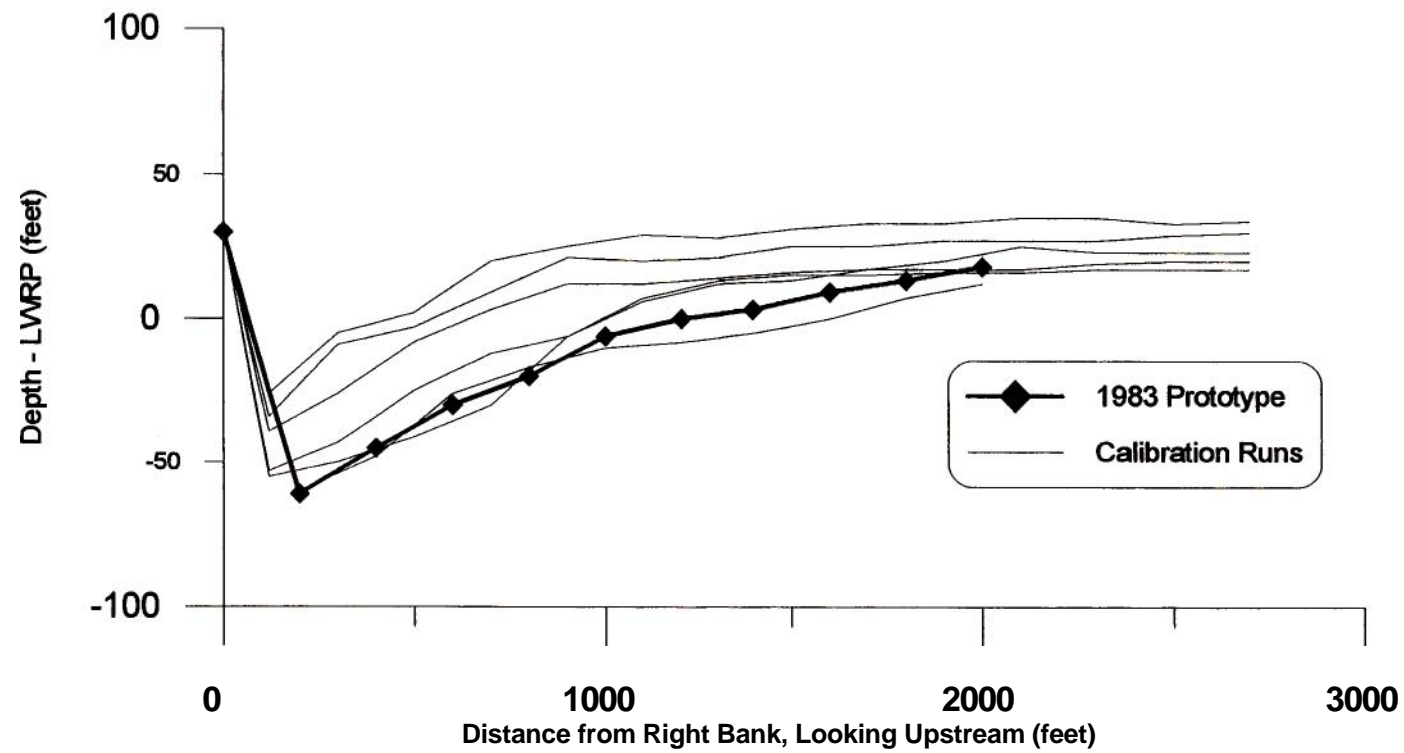


Figure 20. Calibration Runs at Control Section No. 2 (Mile 23.3)

constructed in the model to determine the bed configuration. The captured channel alignment in the prototype is undoubtedly the single, most dominating factor in the development of the bed configuration. The more accurate the model plan view alignment is constructed, the more accurate the simulation of sediment transport of the model vs. the prototype.

8. Base Condition. Once a satisfactory bed configuration was achieved as compared to the prototype, a base condition was established. The base condition essentially serves as the comparison survey for all future tests. The base condition represents expected conditions in the prototype with no additional structural measures added to the river.

Again using the average annual design hydrograph, seven individual runs were made in the micro model. After each run, cross sectional point data was collected and recorded. A computer data file with the averaged point values was then created, and a resultant contour map was generated using the survey procedure discussed in Section IIB.

The base condition determination of the micro model also deviates from standard procedures used today. For example, in the Dogtooth Bend Model Study at WES, the bed of the model was initially molded using templates based on the 1983 prototype survey. Individual base test runs were then made with the average annual design hydrograph. Surveys were conducted after each run, and the response of each test was rated by the stability of the model, measured in terms of the bed material input/output balance (Derrick 1994). A total of 12 runs were made in this manner until

satisfactory stability was achieved. The bed survey from the final run was then chosen as the comparative base condition for all future design improvements, while the other surveys were ignored.

It should be noted that the base condition itself, for all practicality, served as the verification of the model when compared to prototype data later than 1983. This can be explained by the following hypothesis:

There is a natural, cyclic repeatability in the bed configuration of the Mississippi River, as verified by the 1983, 1986, and 1987 prototype comparison plots (Figures 21 through 24). These surveys were low water surveys. For most alluvial rivers, where meandering is almost totally eliminated by reveted banks, the bed is contained within a captured alignment or a captured rivercourse. The lateral erosion factor is almost non-existent. Thus, the river may produce variability in the movement of sediment throughout the course of the hydrograph, but as the recession occurs, the bed will generally tend to develop into its original low water configuration.

This hypothesis originates from the comparison of the surveys (Figures 21 through 24). Analysis shows that over a 5 year period, limited variance between cross sections occurred. Surveys from years prior to 1983 were not made available. However, the author has studied many surveys of the Mississippi River and can attest to the fact that this hypothesis seems valid.

The above discussion on variance of the bed configuration is the rationale behind averaging a number of runs on the micro model and using

the average point values as a representation of the expected bed configuration of the prototype. This may be expressed in another way as the ultimate sediment response of the river averaged over a given period of time. This expected bed configuration response, when compared to the 1986 and 1987 surveys of the prototype, serves as verification of the model.

Aside from lateral channel meandering, another possible way this cyclic tendency for channel reshaping might not occur is if there were aggradation or degradation of the channel, creating a relative deepening or swallowing of the bed. This could occur on a large river, but generally only over a very long period of time. Caution should be taken on smaller streams where changed basin land use practices or gravel mining operations could have a more sudden impact on aggradation/degradation of the channels.

If aggradation/degradation were to take place, the cross sections would reflect either a deepening or shallowing of the channel near the thalweg. However, the general distribution of sediments and the resultant bed configuration in the channel should still be somewhat similar from year to year.

The variance or lack thereof of the bed configuration of the prototype can be analyzed by statistical means. This warrants investigation into future research, which could be used to further describe the processes of the prototype.

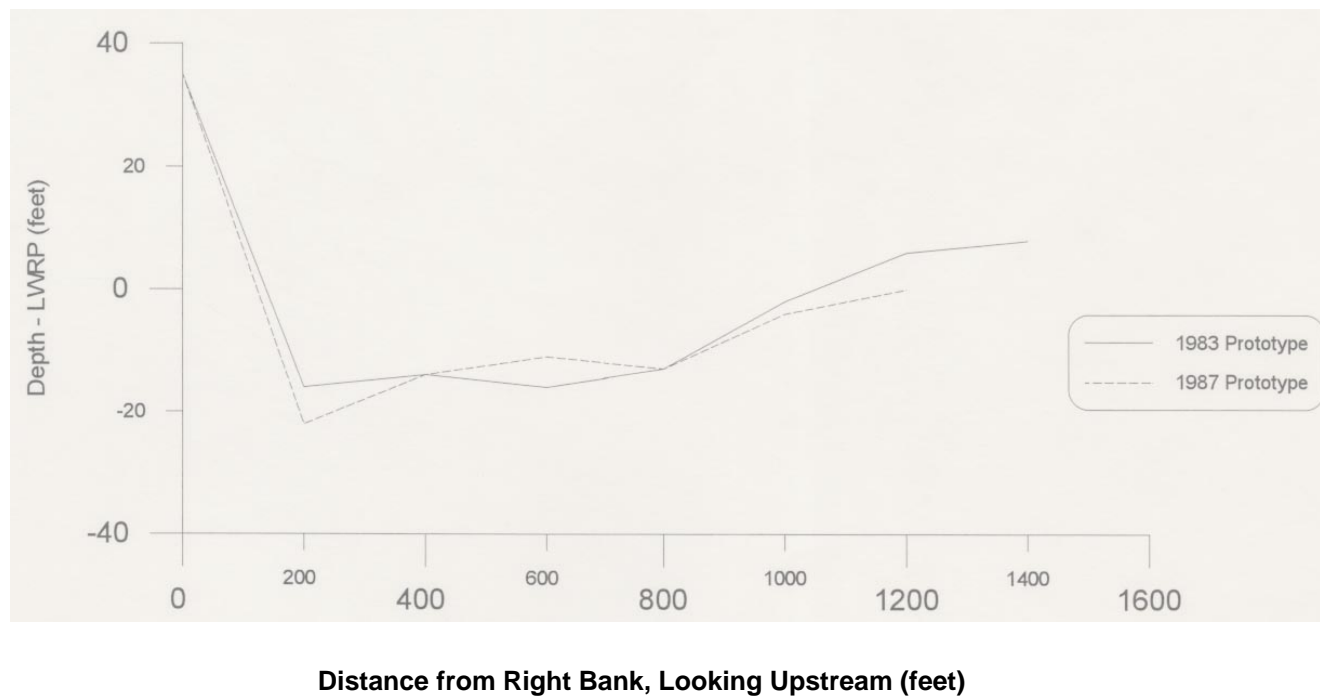
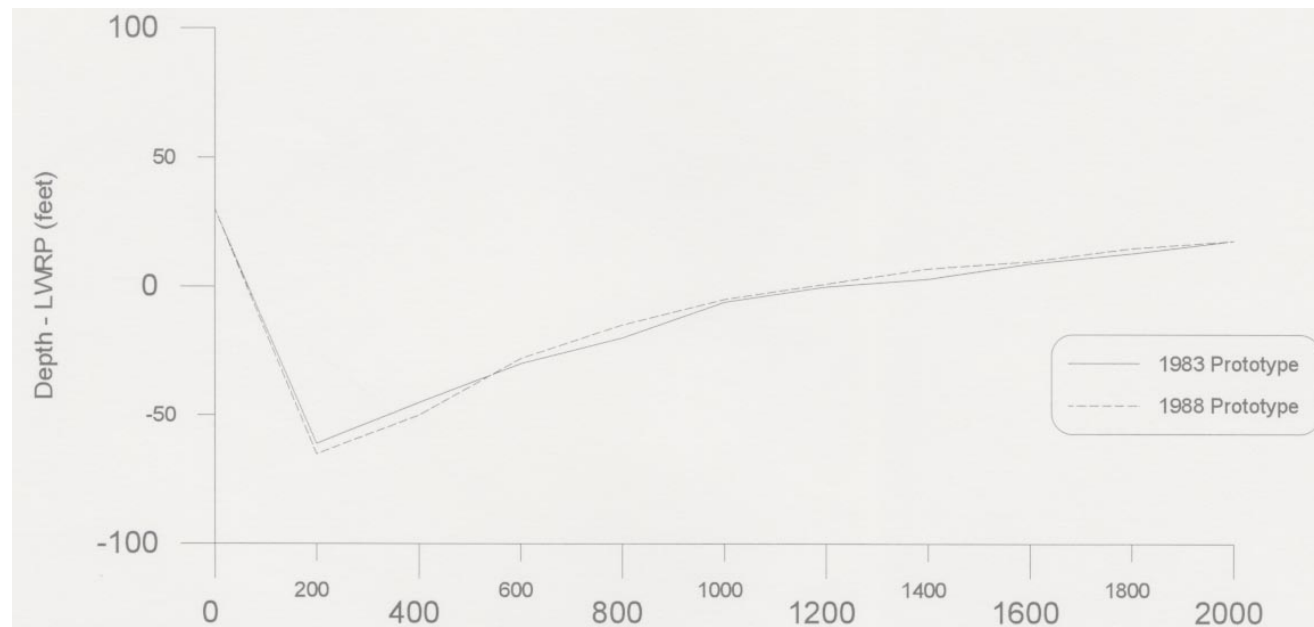


Figure 21. Mississippi River Cross Sectional Comparisons at Control Section No. 1 (Mile 21.7)



Distance from Right Bank, Looking Downstream (feet)

Figure 22. Mississippi River Cross Sectional Comparisons at Control Section No. 2 (Mile 23.3)

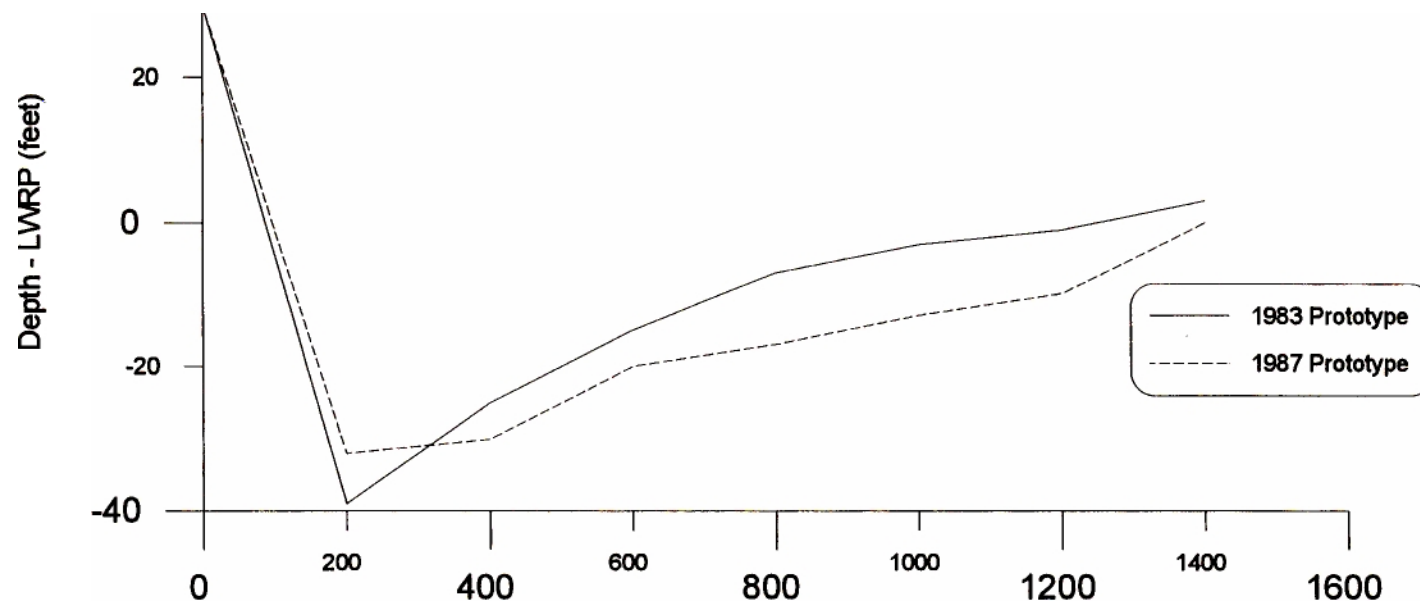


Figure 23. Mississippi River Cross Sectional Comparisons at Control Section No. 3 (Mile 25.7)

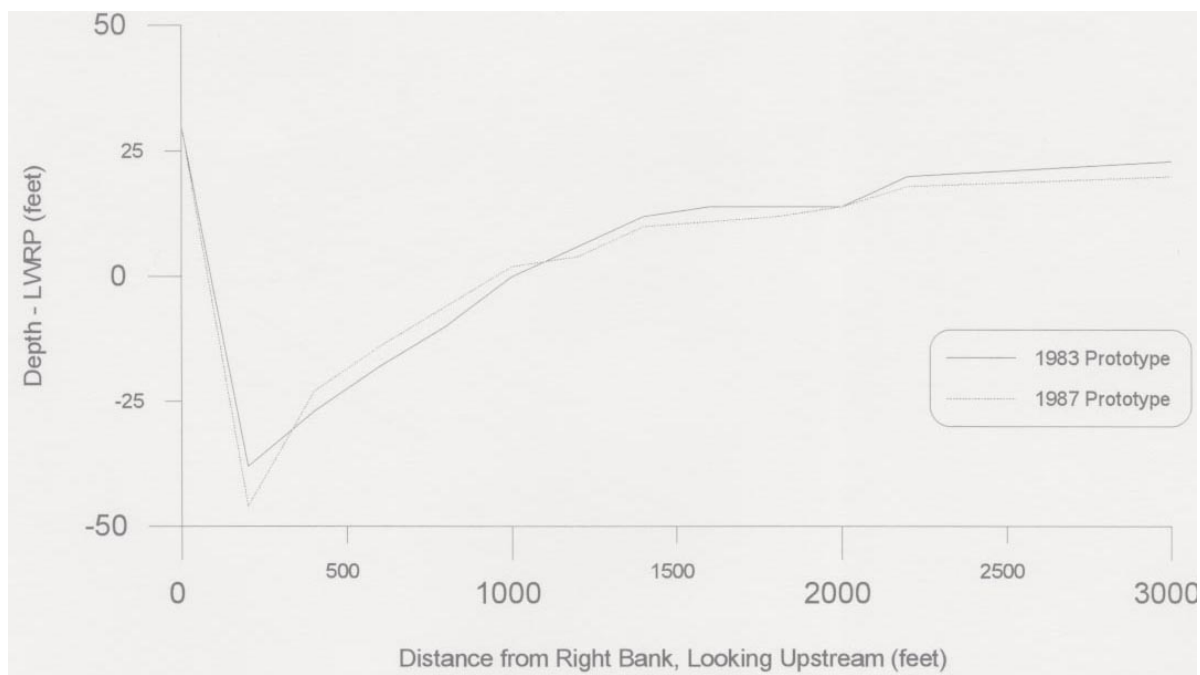


Figure 24. Mississippi River Cross Sectional Comparisons at Control Section No. 4 (Mile 30.3)

IV. RESULTS AND DISCUSSION

A. BASE CONDITION COMPARISONS

Cross sectional comparison plots of the base condition at the five control sections were generated between the models and both the 1983 and 1986-87 Mississippi River prototype survey. These are contained in the next five figures. Comparisons of these plots revealed the following:

At Control Section No. 1 (Figure 25), the micro model was approximately 10 feet deeper than the prototype, while the WES model was approximately 5 feet deeper. This deepening was not a problem in either case because the section was at the lower end of the two models and well downstream of the areas under direct study. Overall, both models showed good sediment distribution qualities, as verified by the shapes of the cross sections.

Control Section No. 2 (Figure 26) was located in the middle of Dogtooth Bend, Mile 23.3. The micro model displayed excellent correlation with the prototype. The WES model showed good correlation, but was approximately 20 feet deeper in the navigation channel. Overall, both models exhibited outstanding sediment distribution as compared with the Mississippi River hydrographic survey.

At Control Section No. 3 (Figure 27), both models displayed good correlation with the prototype. Note the variance in the prototype data.

Control Section No. 4 (Figure 28) was located in the middle of Prices Bend, Mile 30.3. Both models were approximately 20 feet deeper than the

prototype in the main channel. The WES model was approximately 400 feet wider between depths 0 to -10 LWRP. Both models again showed bed configurations similar to the prototype.

Control Section No. 5 (Figure 29) was located at Mile 32.8. The micro model exhibited excellent correlation with the prototype, while the WES model was slightly deeper toward the sand bar side of the channel. Bed configuration similarity was again achieved with both models.

Base condition contour maps were also prepared for the micro model between Mile 32.0 and Mile 20.0. These were compared to maps of the Dogtooth Bend Model Study obtained from WES and the 1986-87 prototype survey (maps 4 through 18). Before inspection of the maps, the following comments are in order:

- 1). The contours of the micro model study were generated numerically by use of the computer, while the contours of both the WES model and the prototype were drawn by hand. Therefore, the general look of the contours was different in each case. Contours on the micro model maps tended to be more rounded and were not closed at the boundary. Contours on the maps of the WES model and the Mississippi River tended to be more elliptical in shape and were closed at the boundary.

- 2). All three sets of maps contained approximately the same amount of cross sectional survey data. More data could have better defined the topography in all three cases and given more precise comparisons.

However, for the purposes of this analysis, the contouring was adequate enough for the analysis of general trends.

3). In the future, the contours of the micro model could be improved by the use of a three-dimensional digitizer. Many more points could be collected in this manner, supplying a more accurate representation of the final model survey. In the prototype, new hydrographic survey technology has recently been applied to collect a much greater amount of survey data (16). This data will be made available for the entire Middle Mississippi River in the next few years.

Upon inspection of the maps, the following general tendencies were observed: Starting upstream at mile 32.0, both models exhibited a scour hole formation in the dike field on the left descending bank. This hole was deeper and wider than in the prototype, but the important point to be made is that the hole occurred in the same general location. A bar formation was located directly across the river channel in all three cases.

Between Mile 31.0 and 29.0, the major point bar formation of the prototype at Prices Bend was displayed in both models. The side channel formation was not displayed in the micro model. This was due to a modeling error. The upstream alignment of the model insert at mile 31.1(L) was different than the prototype. In the micro model, the left bank was constructed too far inward toward the main channel at 31.1 L, and this undoubtedly blocked out approach flow to the side channel.

In the WES model, the side channel was molded into the bed. The observed flow through the channel at the higher stages was minimal, and the tendency for left bank erosion, as found in the prototype, was not apparent in the model (33).

At mile 27.6, a scour hole was observed on both models and the prototype at two dikes on the right descending bank, Dike 27.6 R and Dike 27.3 R. The hole was approximately 30 feet deeper in both models than the prototype.

Between Mile 26.6 and Mile 23.9, a bar formation occurred on the left descending bank in both models and the prototype. In the micro model, this bar was not continuous, and contained a break at Mile 24.8 (L). On the opposite side of the channel, both models exhibited a rather large scour hole, and this tendency was not observed in the prototype.

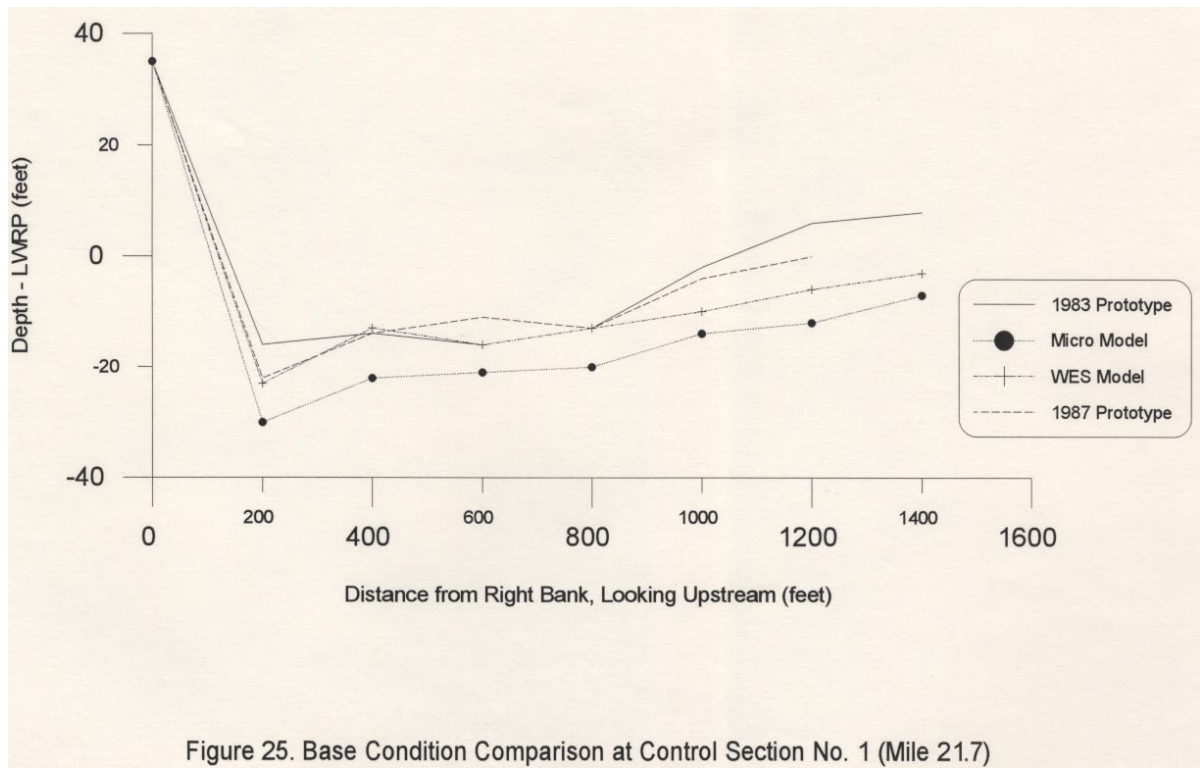
The navigation channel approach to Dogtooth Bend was different in the micro model as compared to the WES model and the prototype due to a model oversight. The channel was aligned too far north between mile 24.2 and mile 23.7. This may be attributed to the fact that 4 major dikes located on the right descending bank were not constructed in the micro model. These dikes could have forced the channel approach in the bend further toward the right descending bank.

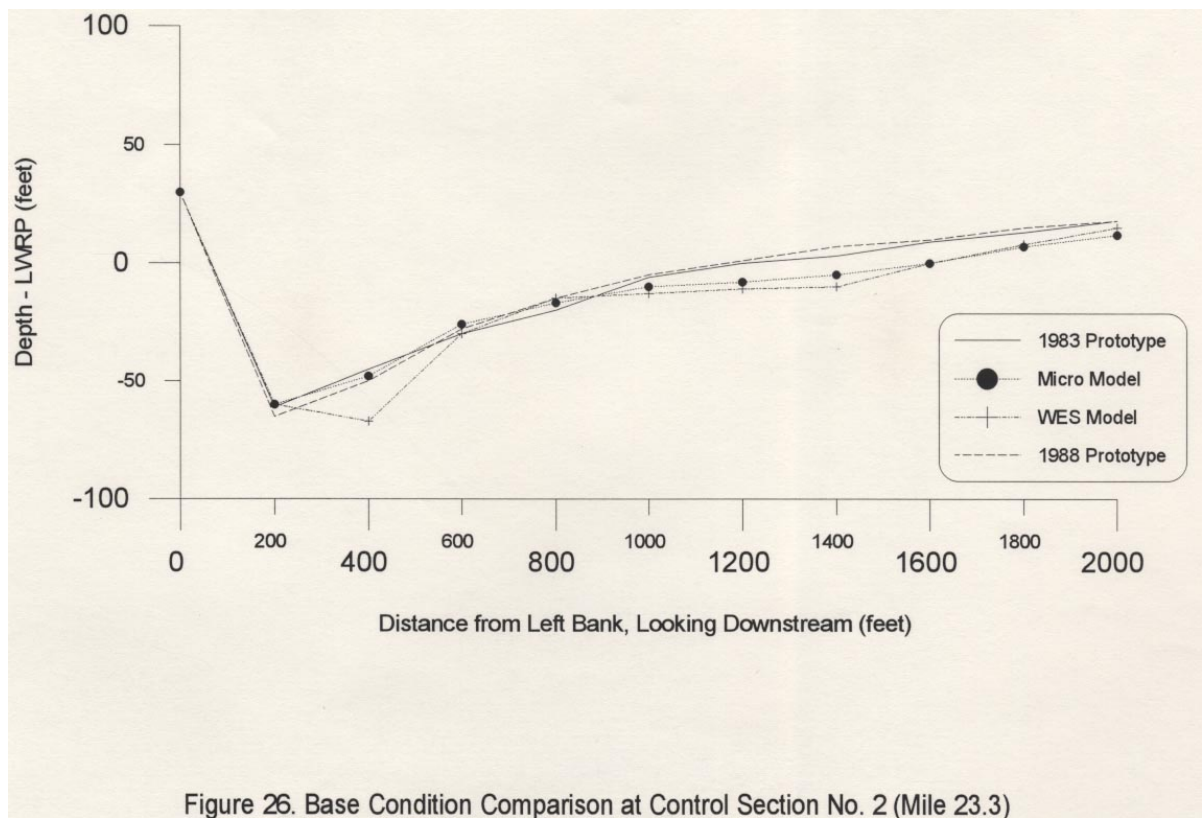
At Dogtooth Bend, Mile 24.2 to 22.1, both models exhibited a scour hole and point bar formation similar to the prototype. The micro model exhibited a side channel formation with bank caving tendencies similar to the

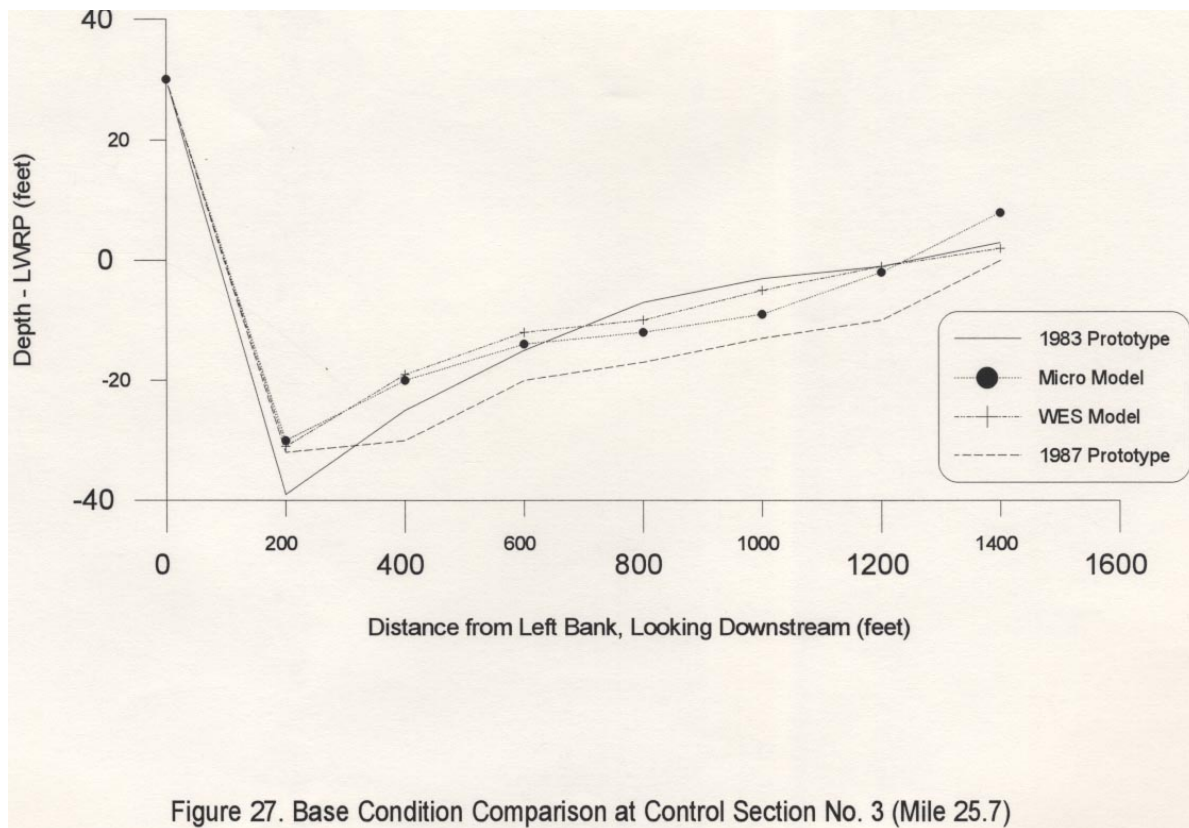
prototype on the right descending bank. This information was not contoured, since it was not considered an essential part of the study. In the WES model, the side channel was molded into the bed, but bank caving tendencies were not apparent during testing (33).

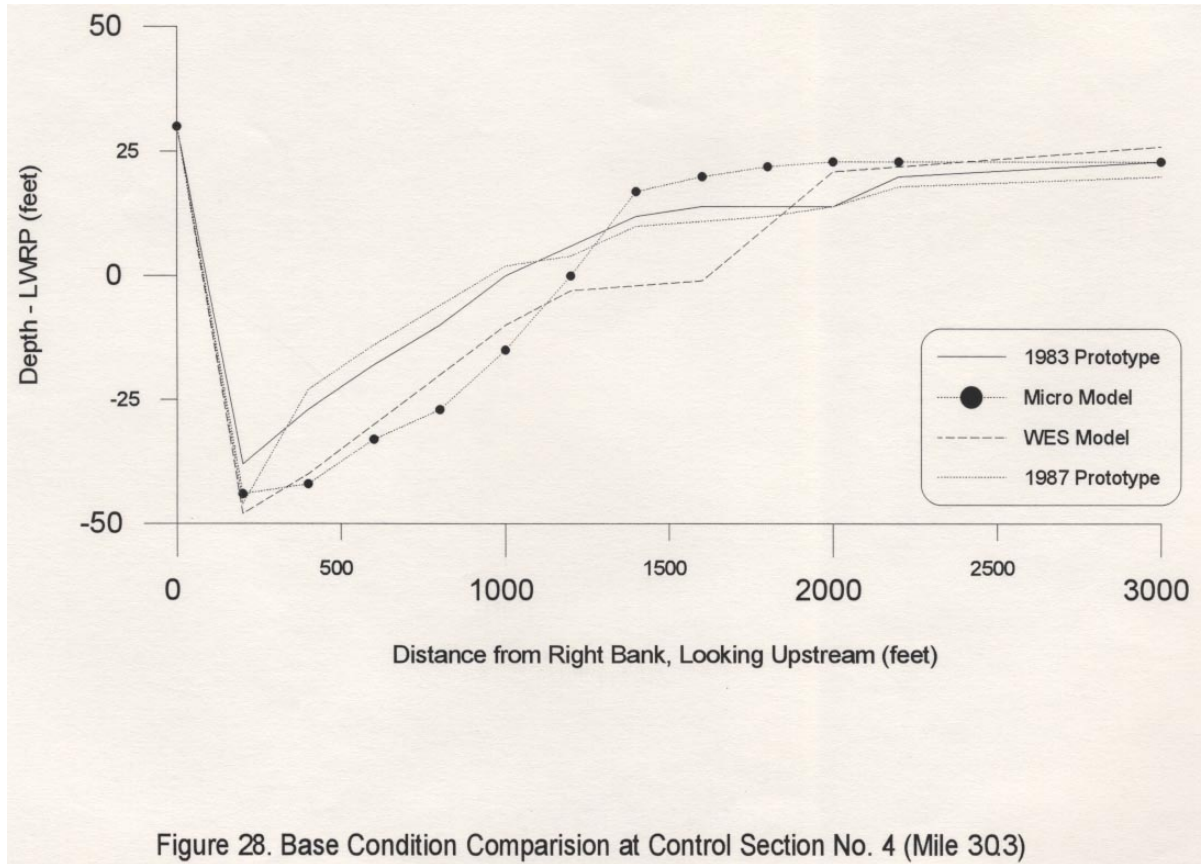
On the lower end of the study reach, between mile 22.1 and mile 18.9, a bar was observed on the right descending bank similar to the prototype, although the micro model bar was not continuous. Both models exhibited a deep channel off the left descending bank similar to the prototype.

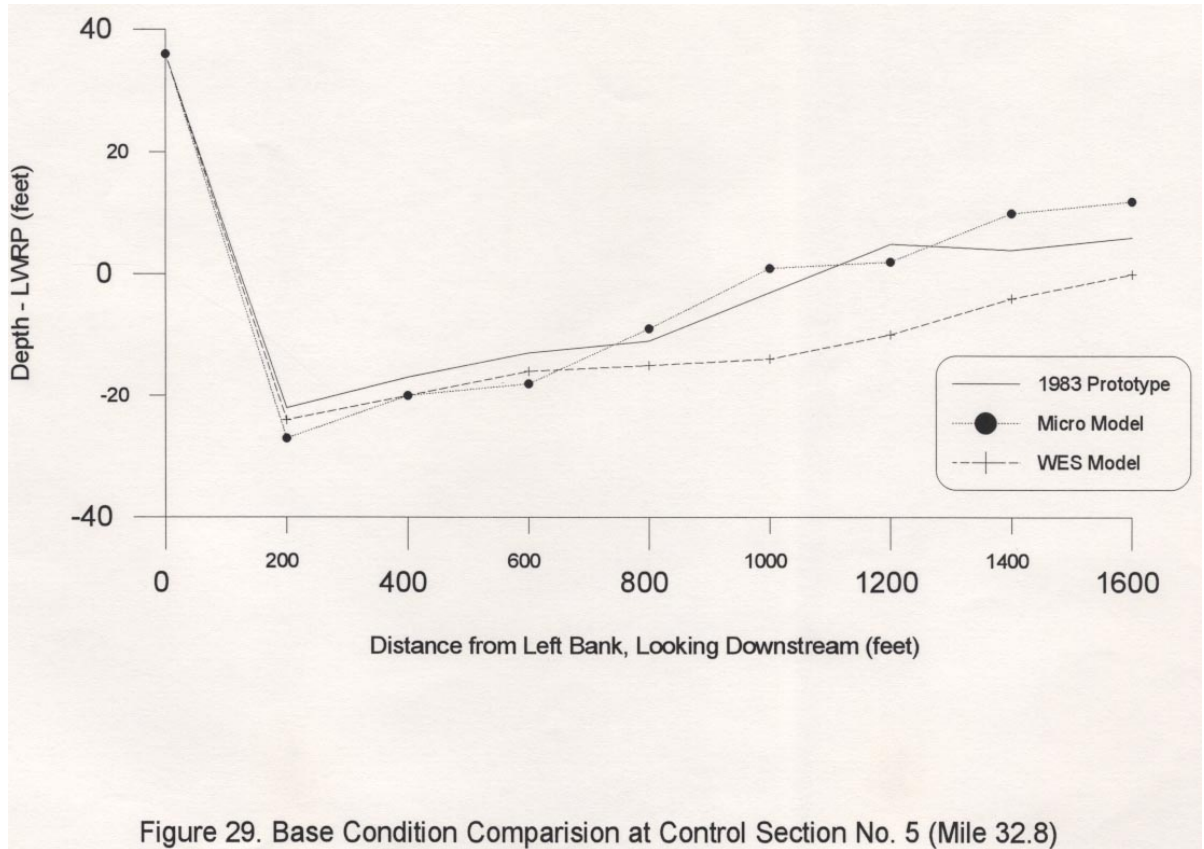
In summary, the micro model overall displayed similar bed configurations as compared to both the larger WES model and the Mississippi River hydrographic surveys. The only major difference was the absence of a scour hole formation in the prototype that was present in both models on the left descending bank between mile 24.5 and mile 25.5. This difference could possibly be attributed to a clay plug formation commonly found at the bottom of many channel areas in the Mississippi River. If this were the case, then the bottom of the river would essentially be armored, which would generate shallow depths in an area that would otherwise be relatively deep. Care then must be taken to investigate areas on the prototype that are suspect to clay plug formations. Geological exploration in the form of borings may be required for calibration/verification of the micro model.



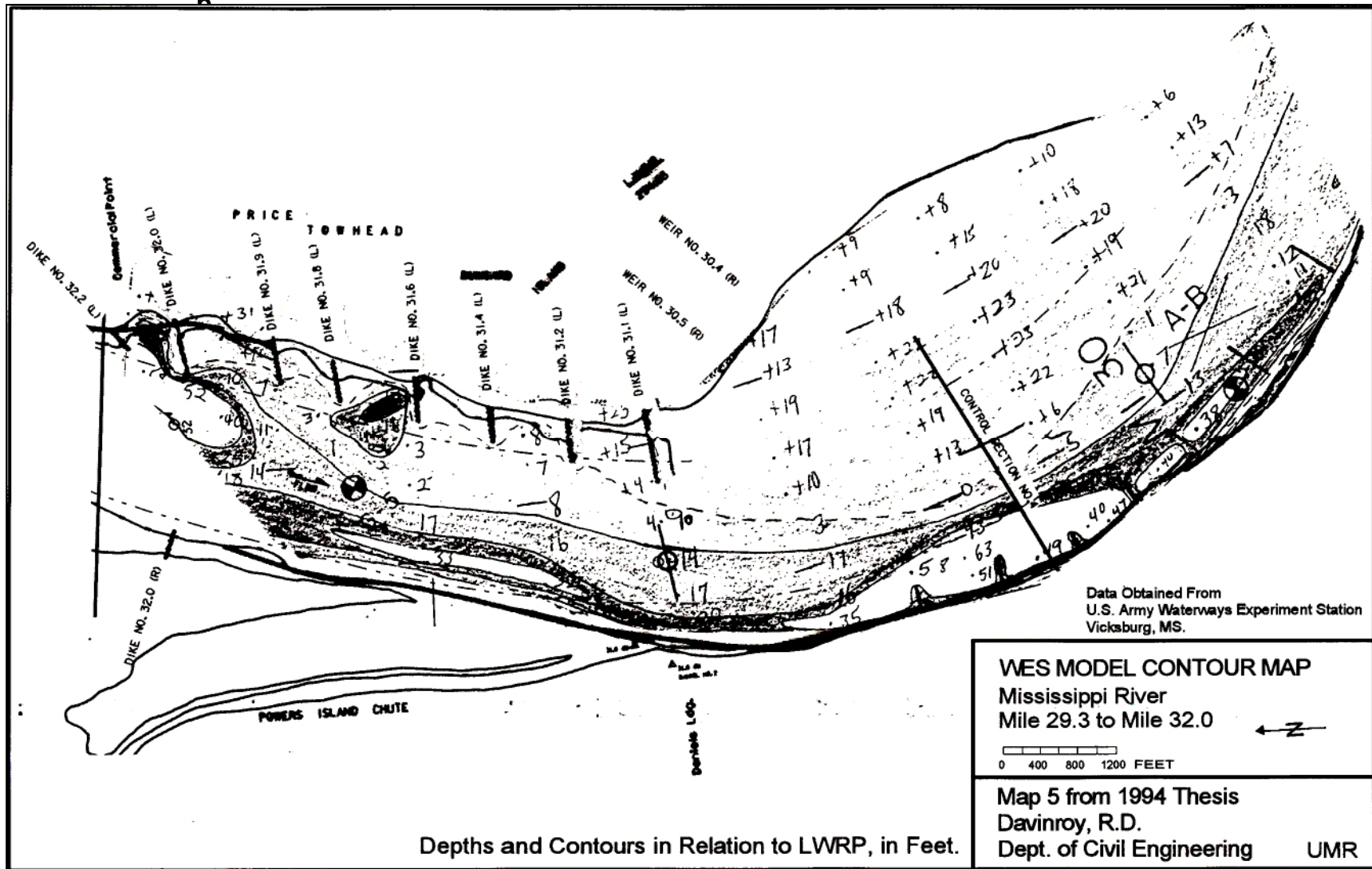




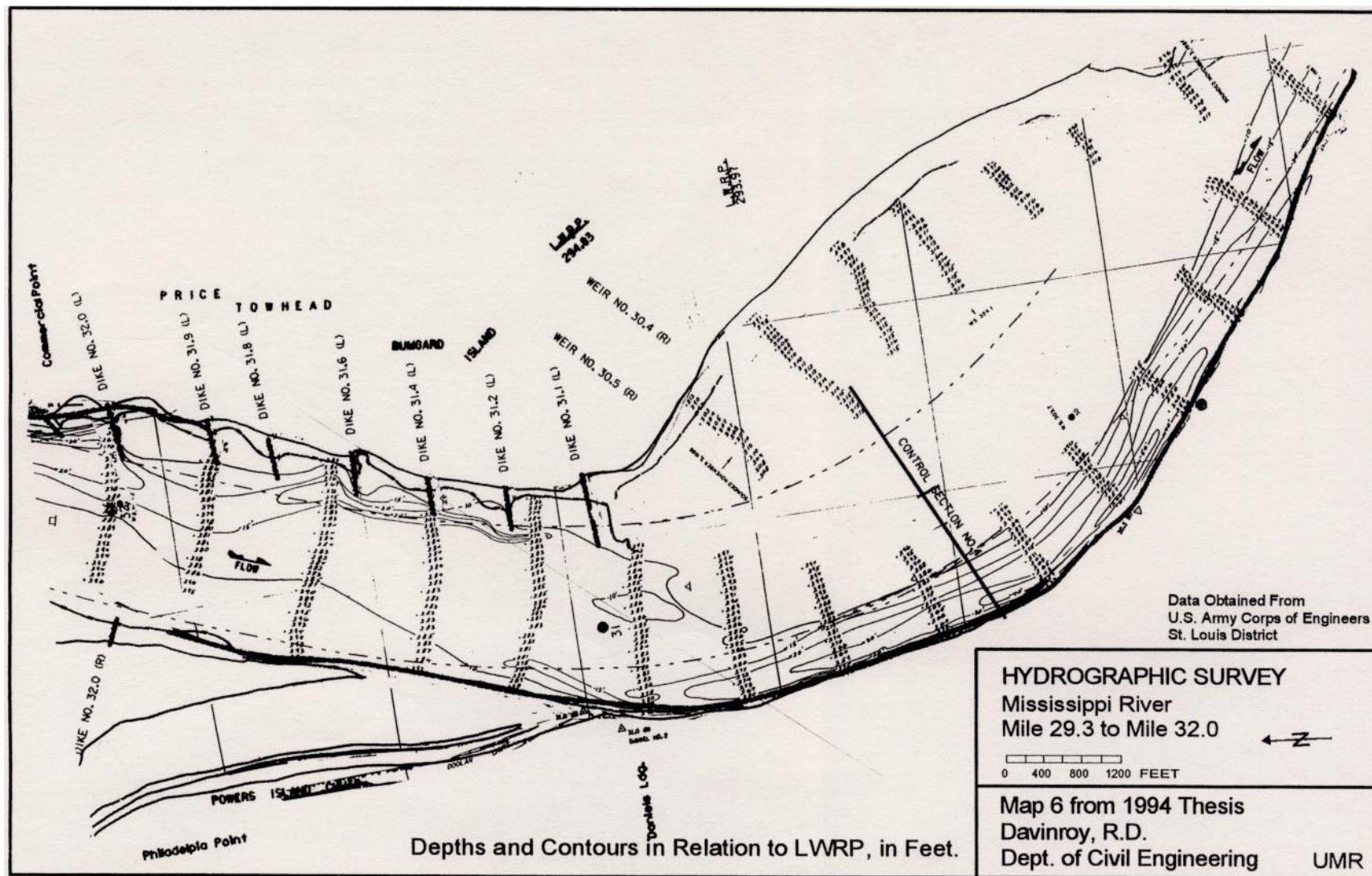




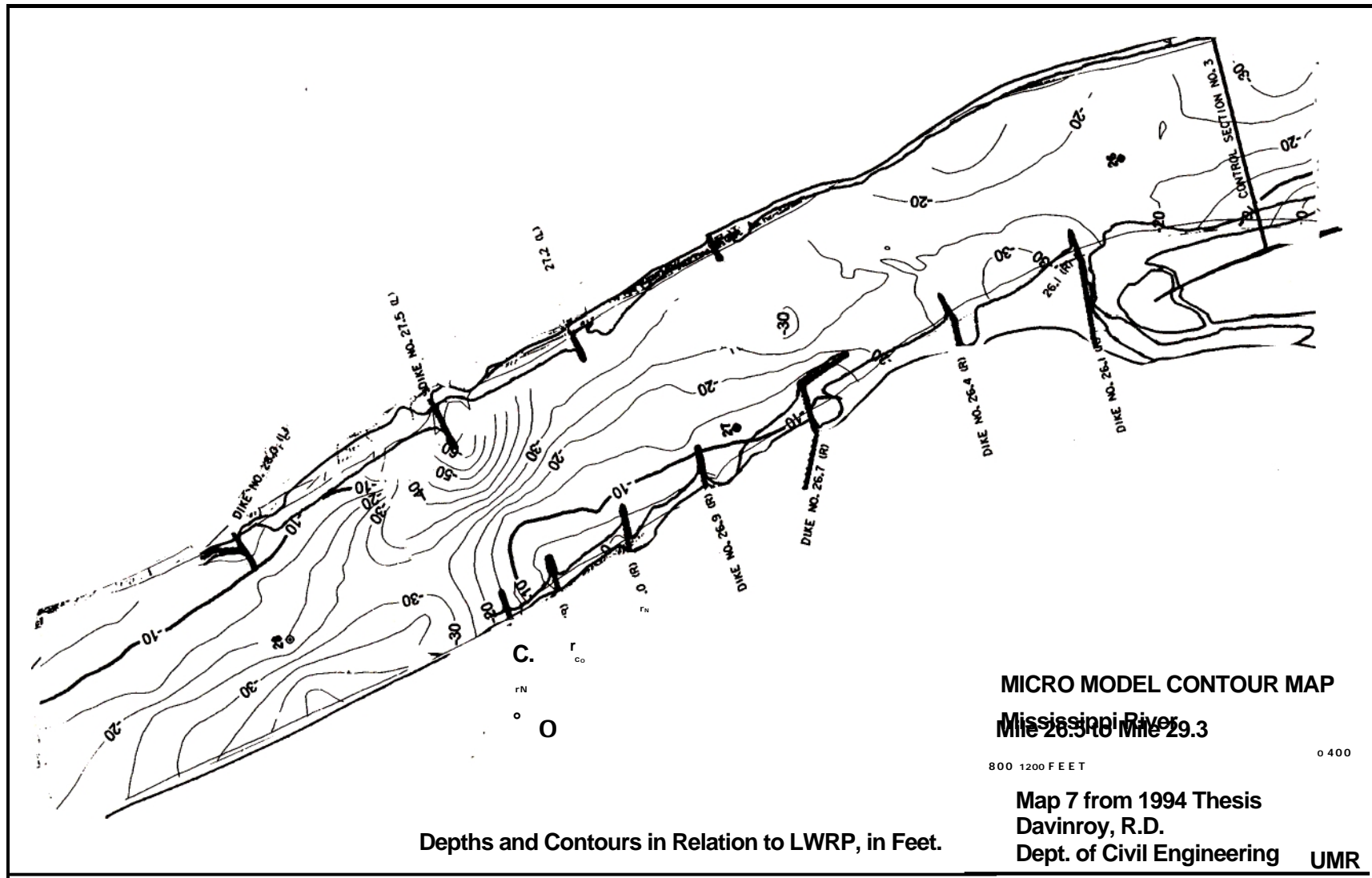
M
a
p



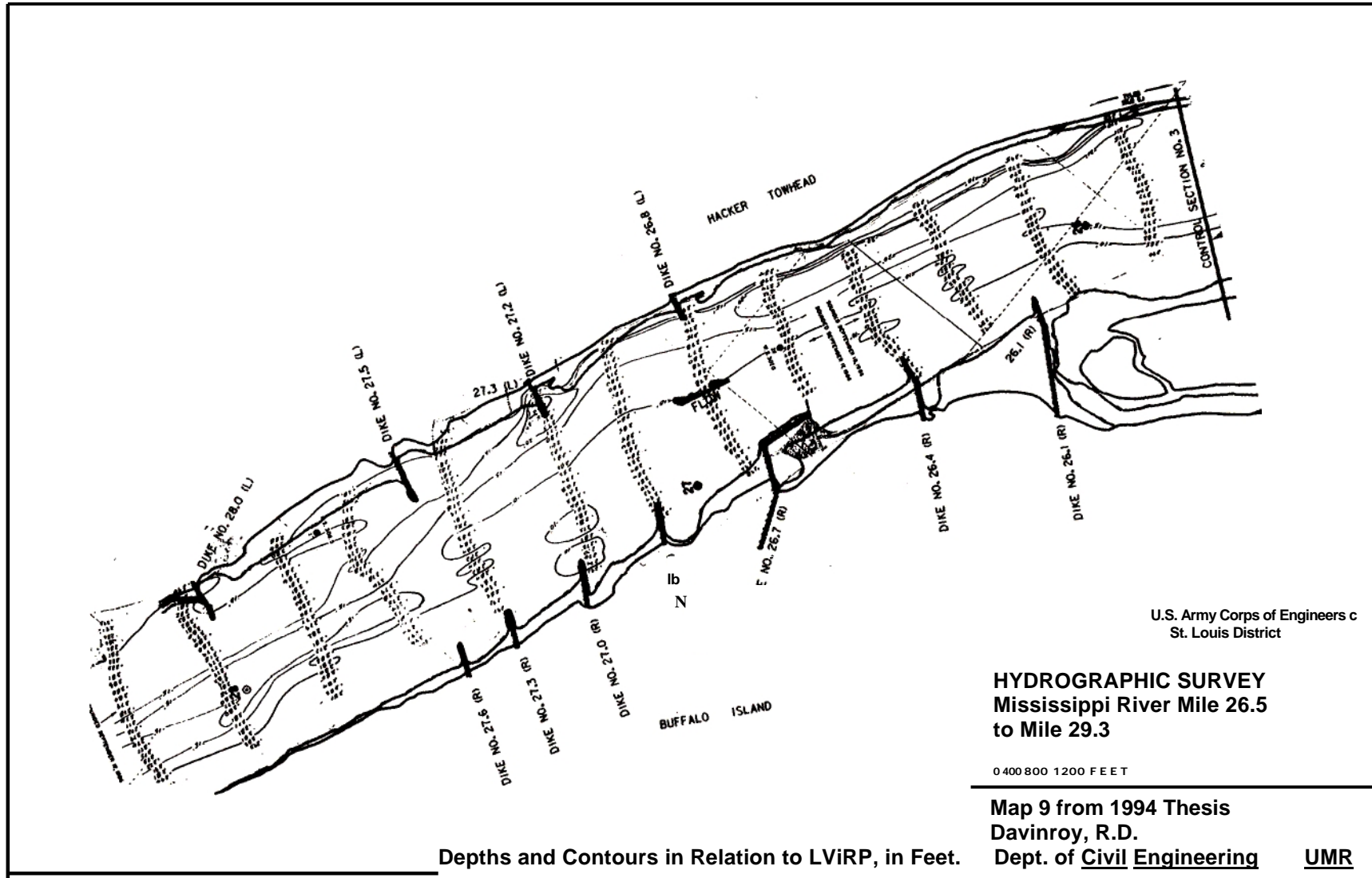
Map 5. WES Model Contour Map, Mile 29.3 to Mile 32.0



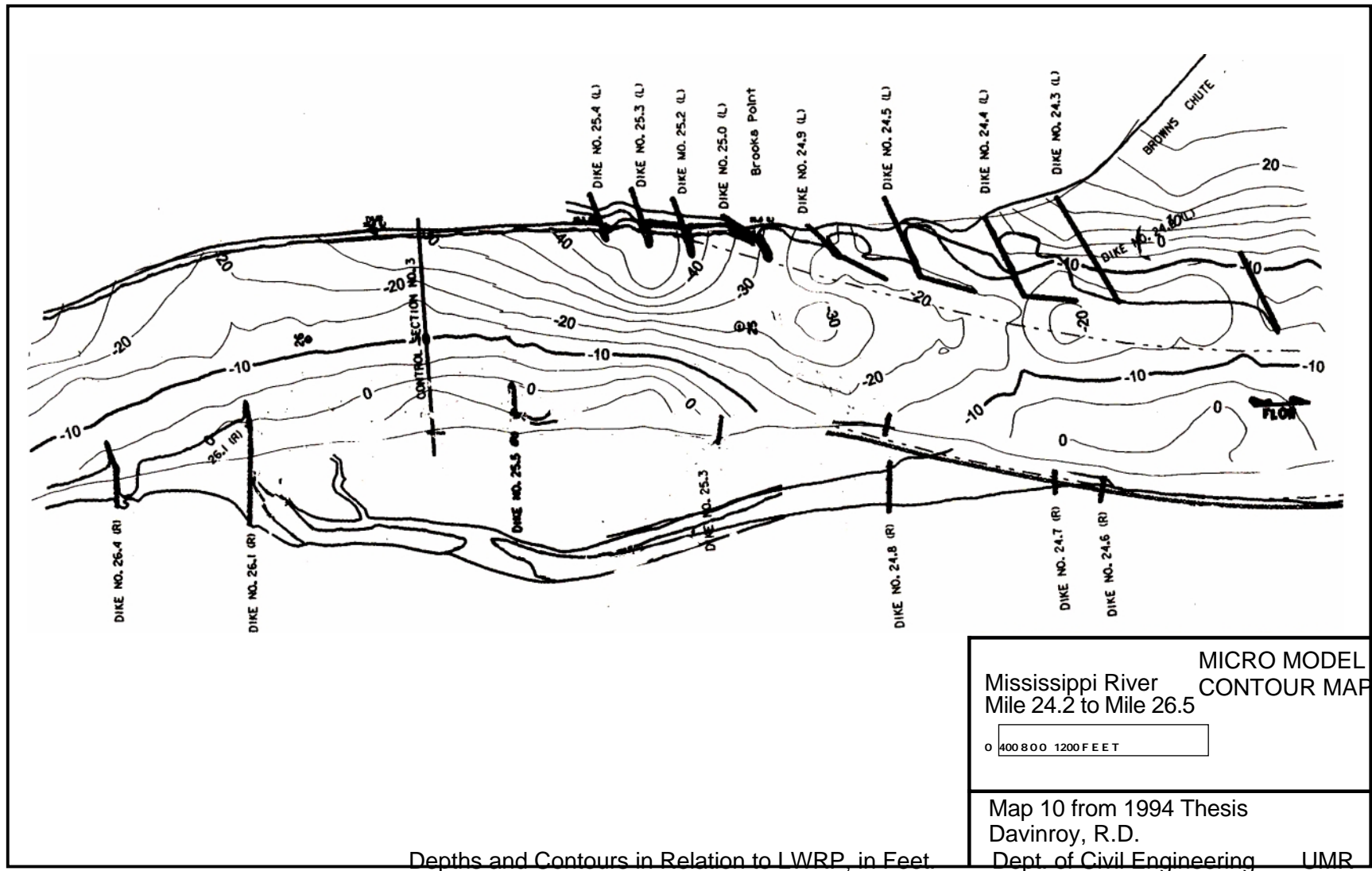
Map 6. Micro Model Contour Map, Mile 29.3 to Mile 32.0



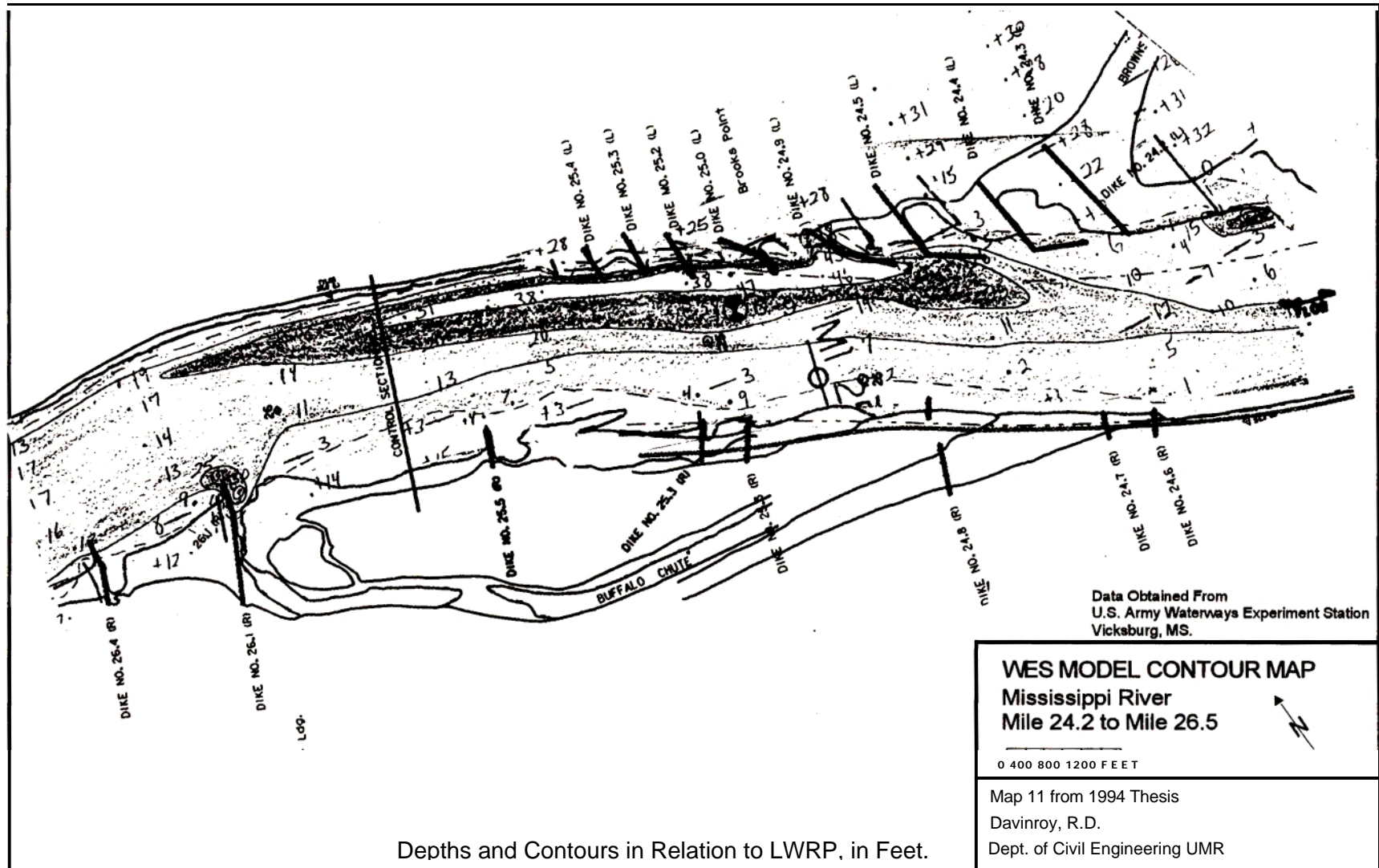
Map 7. Micro Model Contour Map, Mile 26.5 to Mile 29.3



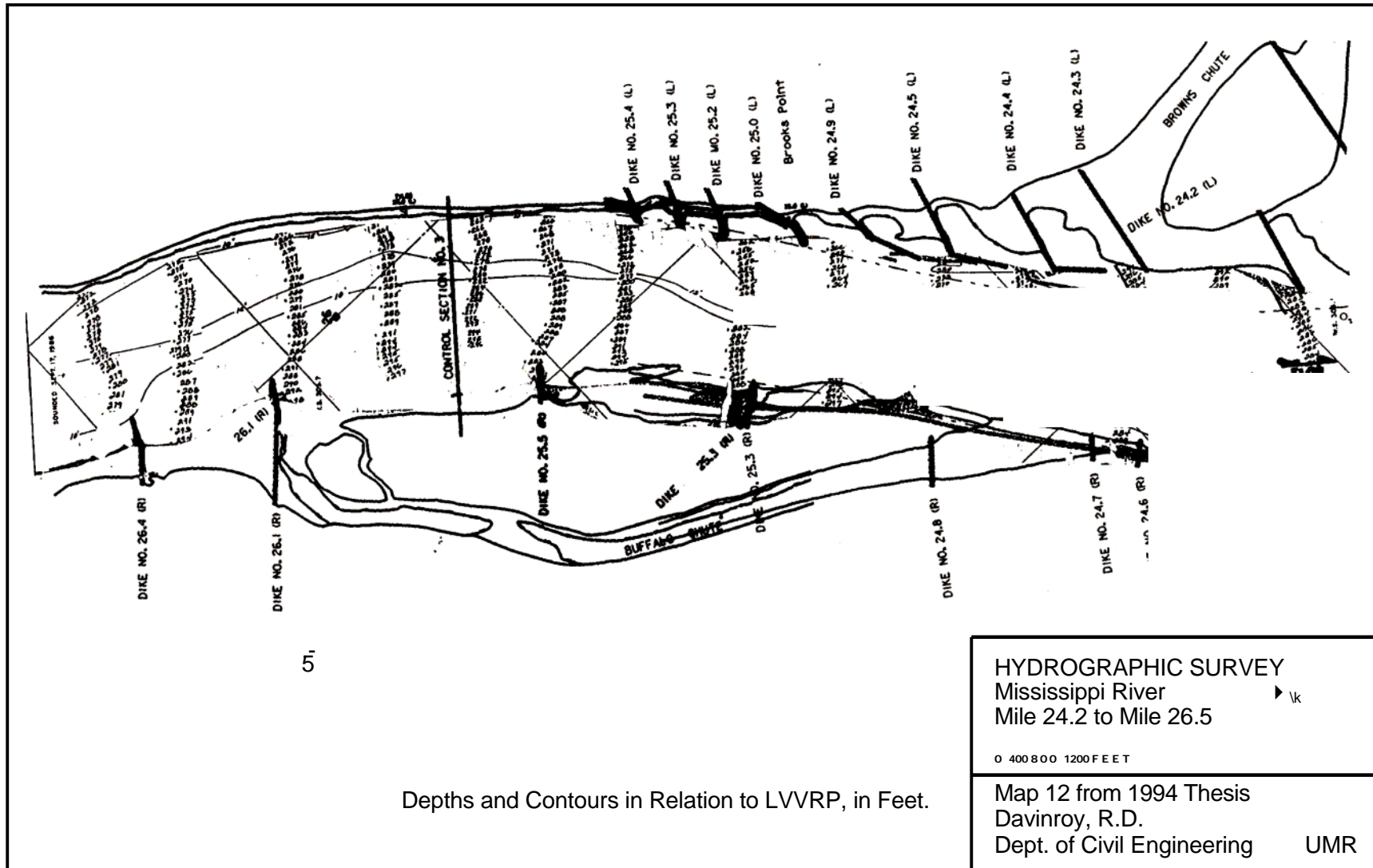
Map 9. Mississippi River Hydrographic Survey Map, Mile 26.5 to Mile 29.3



Map 10. Micro Model Contour Map, Mile 24.2 to Mile 26.5



Map 11. WES Model Contour Map, Mile 24.2 to Mile 26.5



Map 12. Mississippi River Hydrographic Survey Map, Mile 24.2 to Mile 26



Depths and Contours in Relation to LWRP, in Feet.

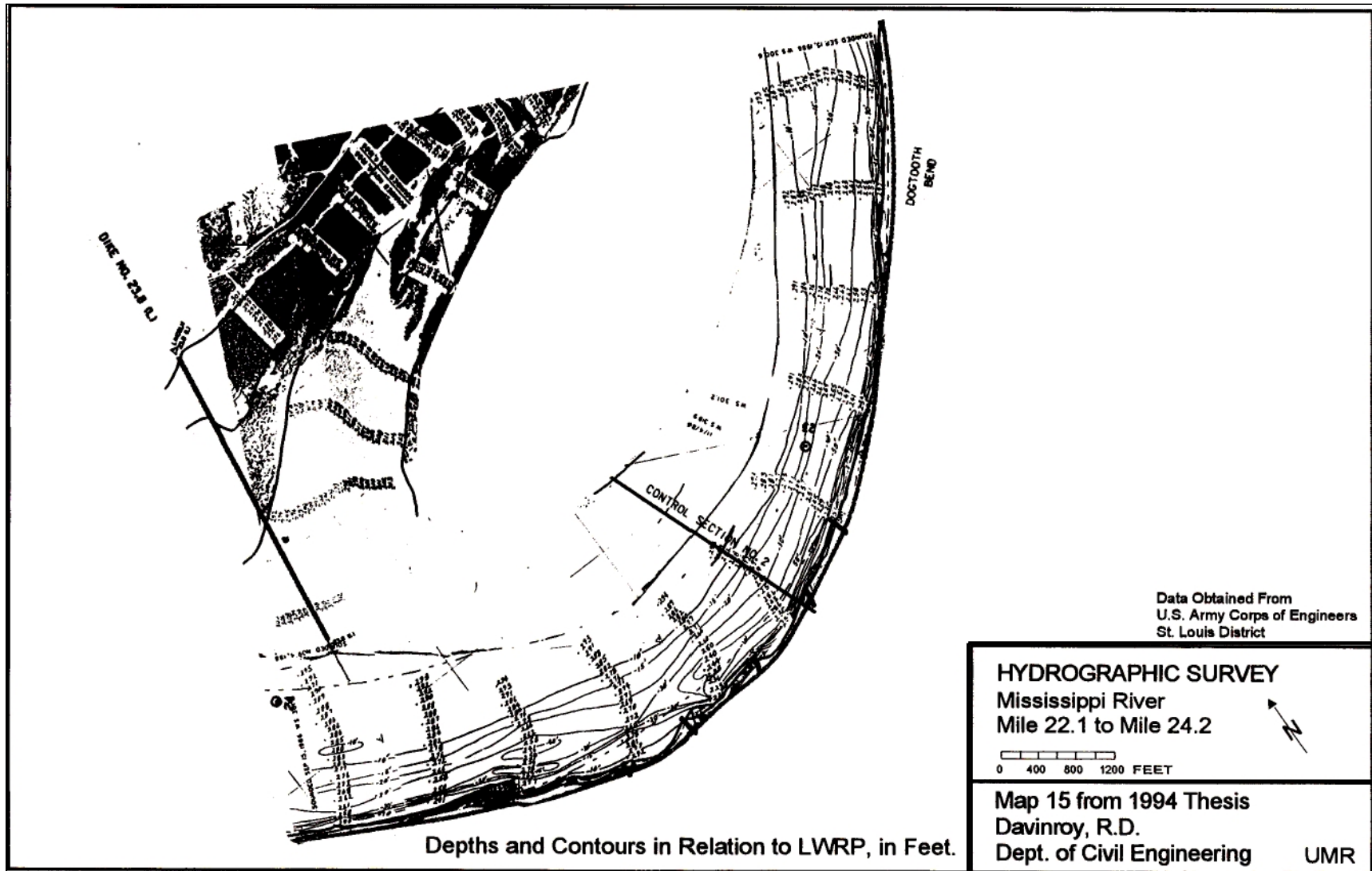
Data Obtained From
U.S. Army Waterways Experiment Station
Vicksburg, MS.

WES MODEL CONTOUR MAP
Mississippi River Mile 22.1 to
Mile 24.2

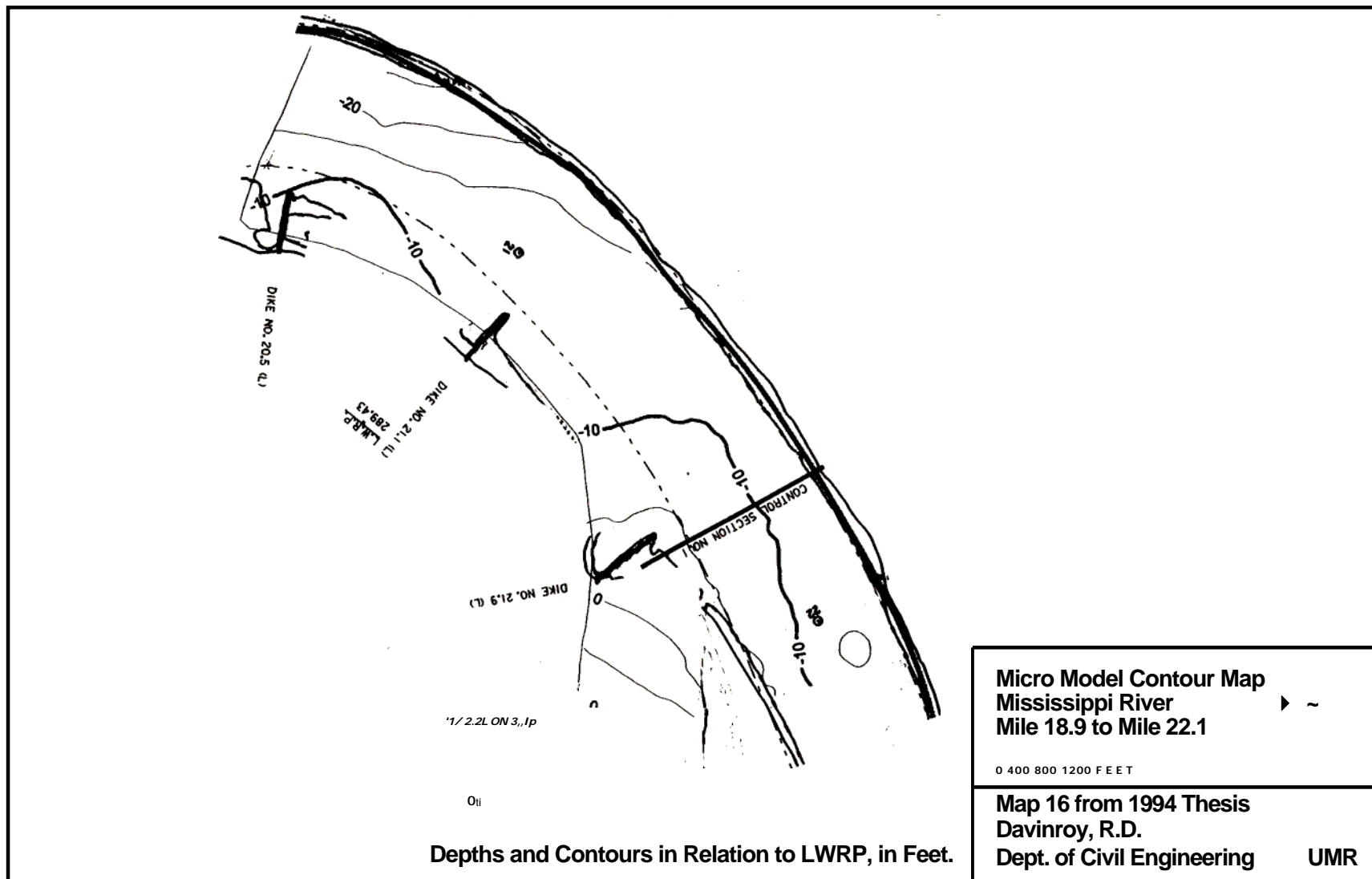
0 400 800 1200 FEET

Map 14 from 1994 Thesis
Davinroy, R.D.
Dept. of Civil Engineering UMR

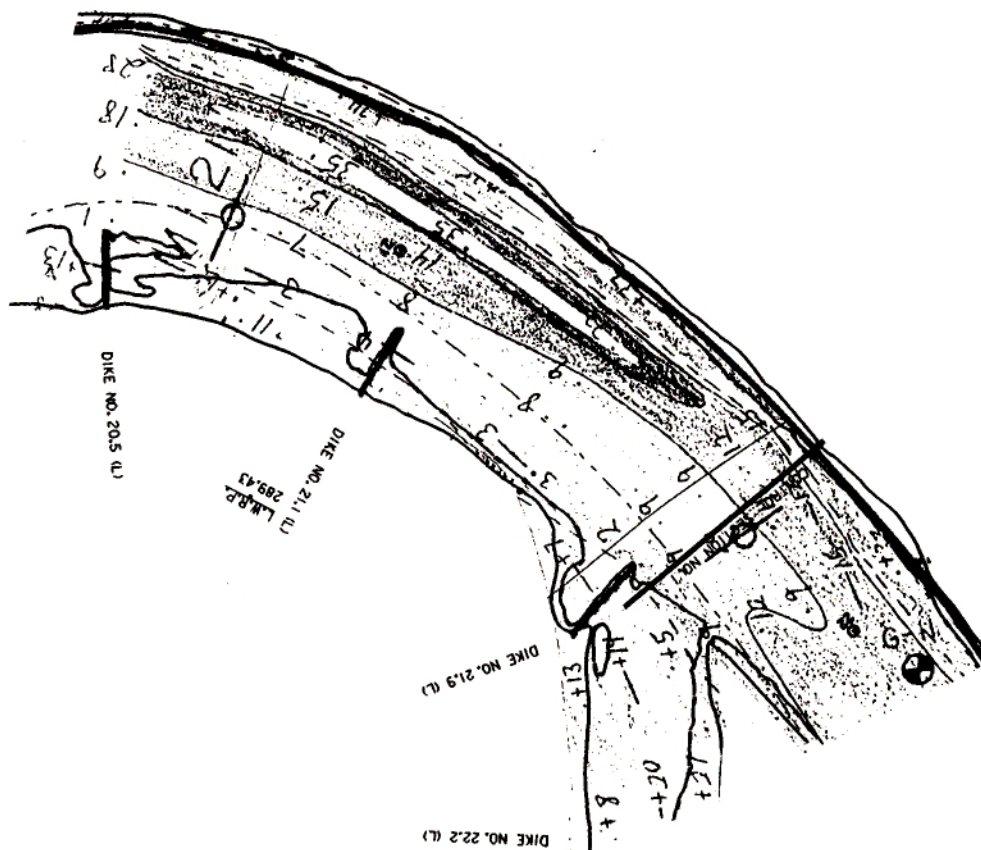
Map 14. WES Model Contour Map, Mile 22.1 to Mile 24.2



Map 15. Mississippi River Hydrographic Survey Map, Mile 22.1 to Mile 24.2



Map 16. Micro Model Contour Map, Mile 18.9 to 22.1



Data Obtained From
U.S. Army Watennays Experiment Station
Vicksburg, MS.

WES Model Contour Map
Mississippi River
Mile 18.9 to Mile 22.1

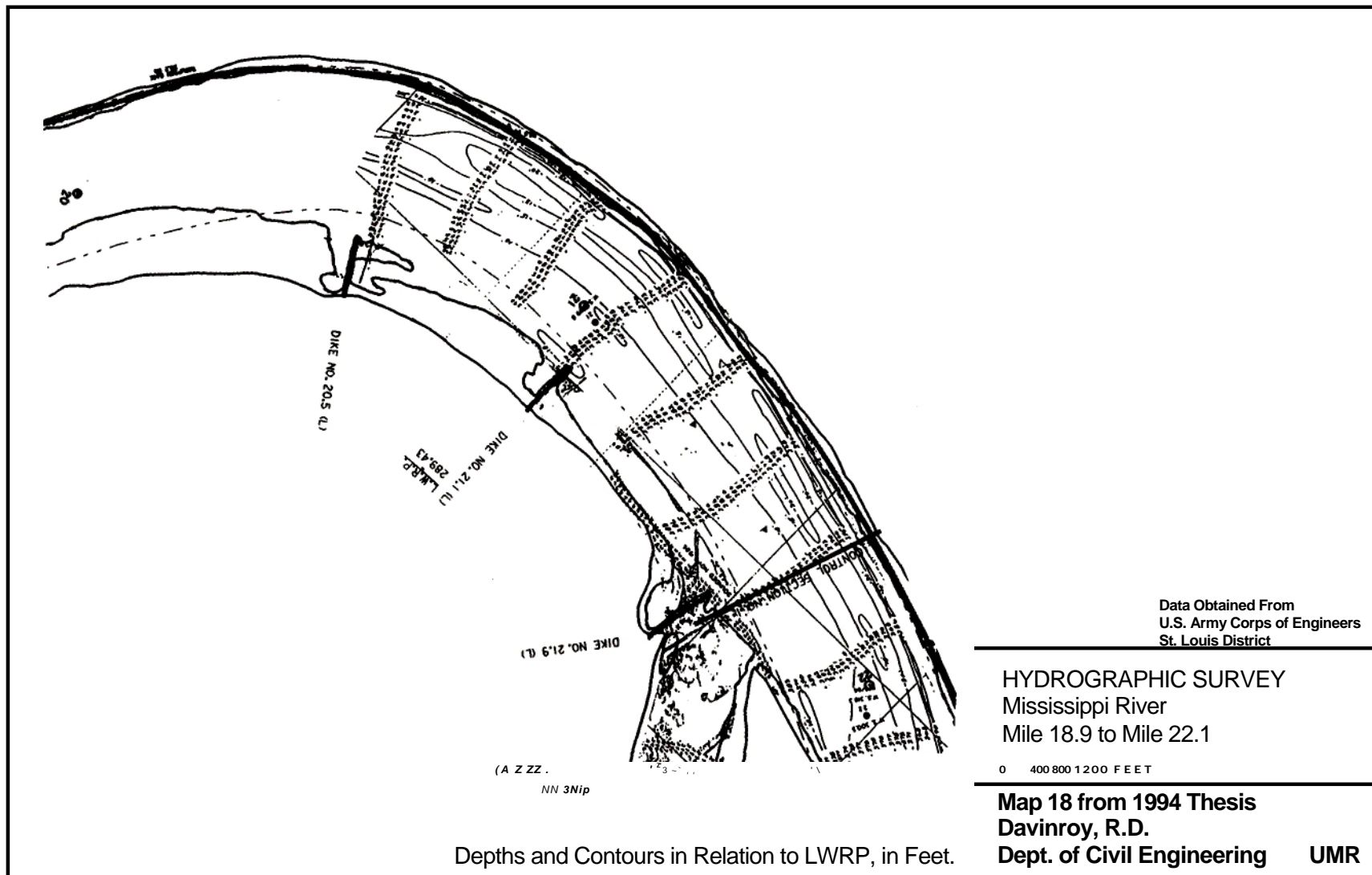
0 400 800 1200 FEET

Depths and Contours in Relation to LWRP, in Feet.

Map 17 from 1994 Thesis
Davinroy, R.D.
Dept. of Civil Engineering

UMR

Map 17. WES Model Contour Map, Mile 18.9 to 22.1



Map 18. Mississippi River Hydrographic Survey Map, Mile 18.9 to 22.1

B. BENDWAY WEIR DESIGN TEST COMPARISONS

A design test was simulated in the micro model to analyze the effects of bendway weirs. Bendway weirs are level crested, submerged rock structures located in the navigation channel. The structures are attached to the outer bendway bankline and directed upstream at an angle of 30 degrees to the perpendicular flowline at midbank stage. They are constructed to a crest height of -15 feet LWRP (Davinroy 1992). Two bendway weir fields were analyzed, one at Prices Bend (Mile 30) and the other at Dogtooth Bend (Mile 23).

The configuration of these structures tested in the Dogtooth Bend model at WES was the exact configuration tested in the micro model. The structures in the micro model were constructed out of thin sheet metal, while in the WES model, a cement-rock conglomerate was used. The following results and comparisons were observed;

Map 19 shows the resultant bed configuration of the micro model at Prices Bend after the installation of the bendway weirs. The navigation channel (the -10 ft. contour line) was approximately 400 feet wider at the apex of the bend. Some localized scour (10 to 20 feet) around the structures was observed in the bend as compared to the base condition. The navigation channel disappeared in the upstream approach to the bend, and had a tendency to become deeper and wider in the downstream section of the bend.

Map 20 shows the resultant bed configuration as observed in the WES Dogtooth Bend model. Approximately 250 feet of additional navigation channel width was observed at the apex of the bend. The navigation channel widened approximately 500 feet in the upstream bend approach.

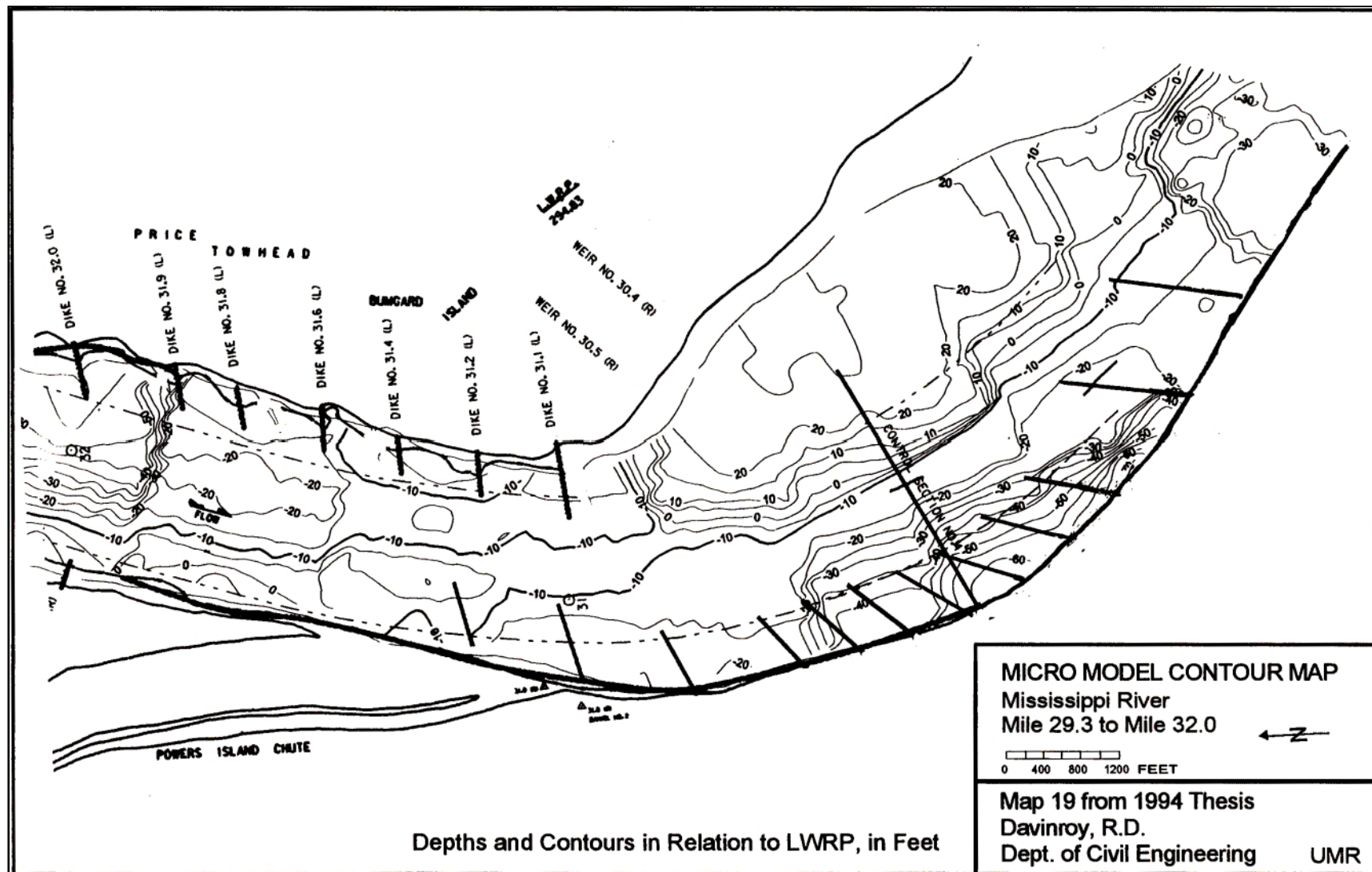
Map 21 shows the resultant bed configuration of the micro model after the installation of the bendway weirs at Dogtooth Bend. Results indicated that the sediment was more evenly distributed around the apex of the bend as compared to the base condition. The navigation channel was approximately 300 feet wider at the apex of the bend (mile 23.3) than the base condition. The upstream approach channel tended to narrow approximately 400 feet, and the bar formation in the upper end of the bend on the right descending bank migrated downstream approximately 1000 feet. Substantial channel widening (approximately 800 feet) occurred in the lower end of the bend. Approximately 10 feet of additional scour formed around a few of the structures as compared to the base condition. The two most upstream weirs became buried with sediment.

Map 22 shows the resultant bed configuration of the WES model. Approximately 250 feet of additional navigation channel width was developed at the apex of the bend as a result of the weirs. Most of the scour in the bend occurred at the third and fourth weir from the upstream end of the bend. Generally, more deposition tended to occur within the weirs on the right descending bank as compared to the base condition and the design test performed on the micro model. The upstream navigation channel

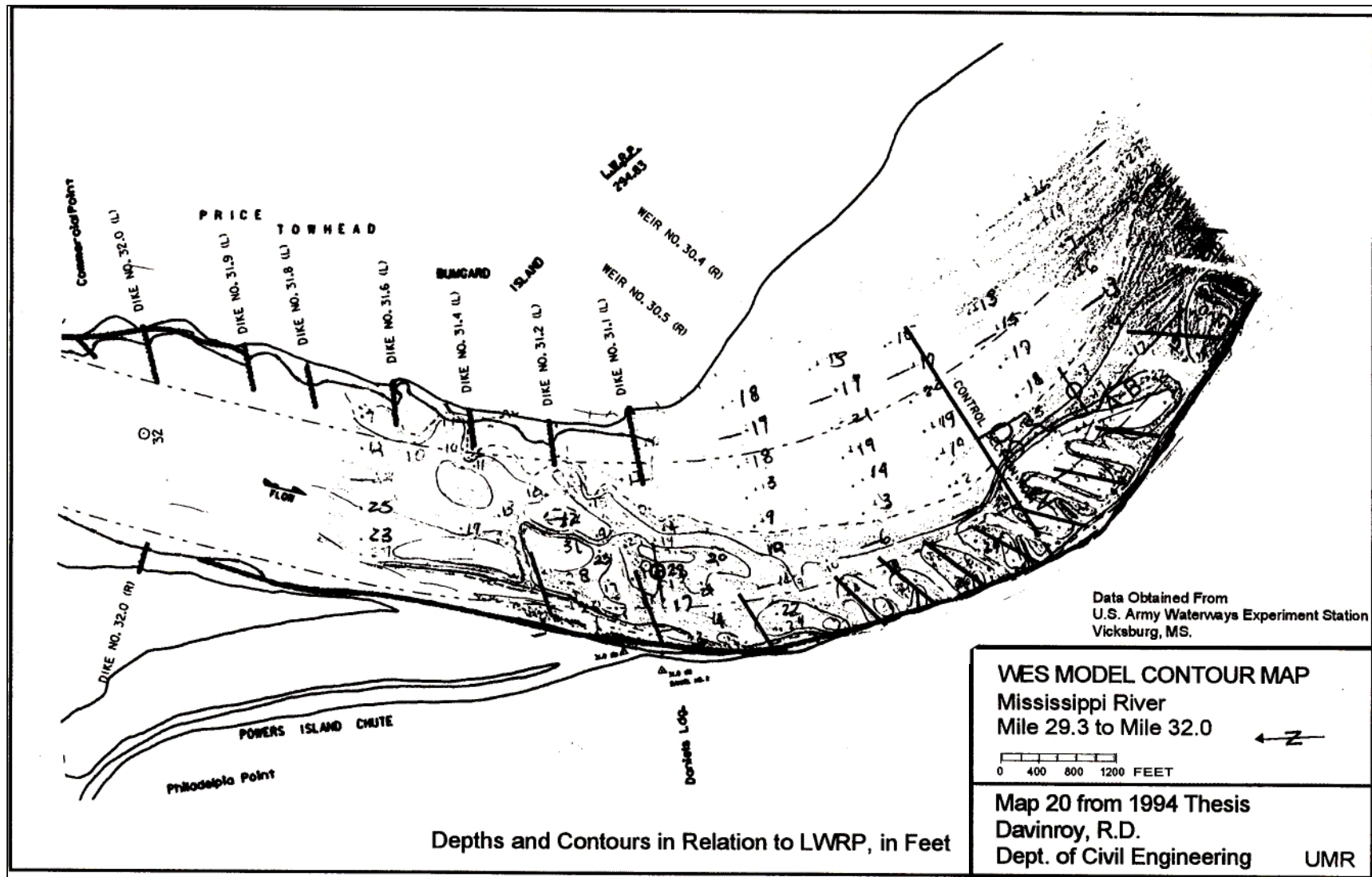
widened approximately 1000 feet. The downstream tendency for channel widening found in the micro model test was not apparent in this test.

The tendencies in the two models exhibited the same general redistribution of sediment in the bends as a result of the bendway weirs. The micro model test showed that the lower end of the bends became more dynamic, with increased scour and channel widening, while the WES test showed that the upstream to middle portion of the bend was more dynamic in this regard.

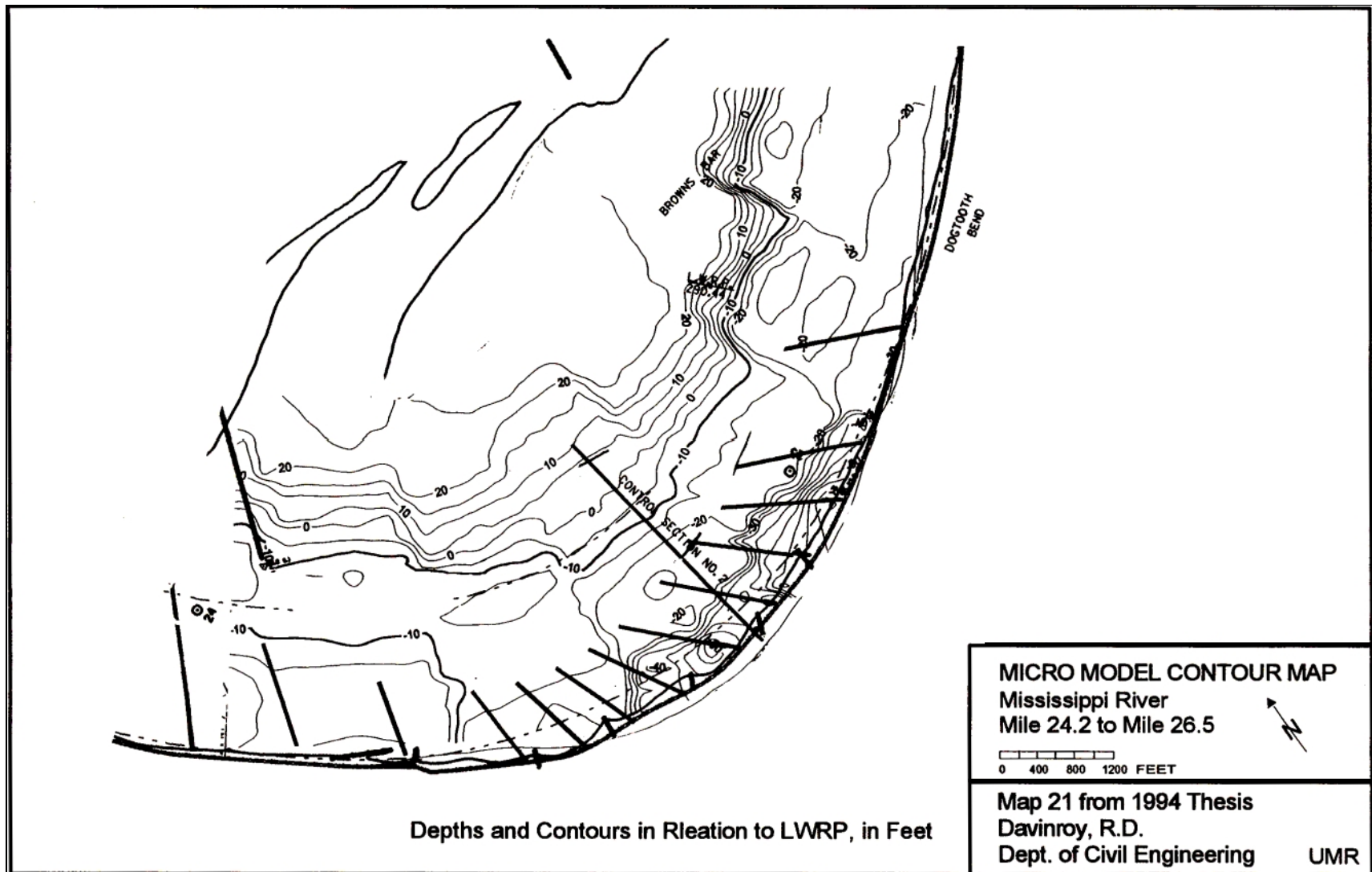
Bendway weirs have been installed in the actual prototype since 1992. Detailed hydrographic surveys were made available. However, it was felt that it would be improper to make a direct comparison of the two models to the prototype weirs. The structures placed in the prototype were of different lengths, which greatly effects the amount of the total redistribution of sediment (Davinroy 1992). Future tests of both models with the actual design plans constructed in the prototype would be the only fair way to evaluate the responsiveness of each model.



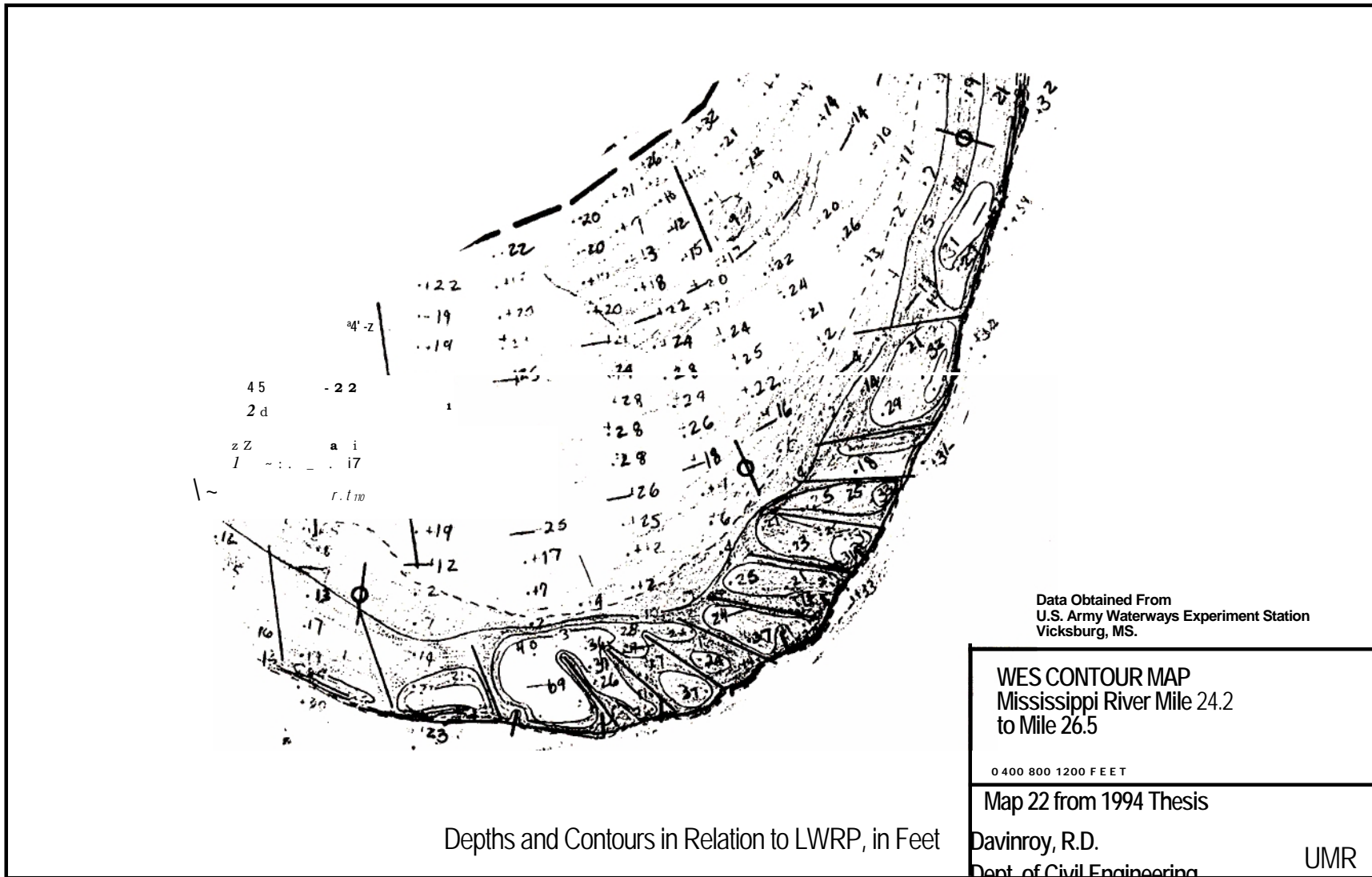
Map 19. Micro Model Contour Map, Bendway Weir Test, Mile 29.3 to Mile 32.0



Map 20. WES Model Contour Map, Bendway Weir Test, Mile 29.3 to Mile 32.0



Map 21. Micro Model Contour Map, Bendway Weir Test, Mile 24.2 to Mile 26.5



Map 22. WES Contour Map, Bendway Weir Test, Mile 24.2 to Mile 26.5

C. VELOCITY MEASUREMENTS

1. Velocity Distribution Comparison With the Prototype. Because the resultant bed configuration of the micro model was similar to the prototype, the velocity distribution that produced this configuration must be similar as well. To test this hypothesis, velocity measurements were conducted on the micro model and compared to Mississippi River prototype data.

Thermal anemetry was used to measure velocity in the model. This technology operates on the laws governing convective heat transfer. Thermal anemometers measure fluid velocity by sensing changes in heat transfer from a small, electrically heated hot-film sensor submersed in the fluid. A heated sensor or probe is held at a constant temperature using an electronic control circuit. The cooling effect provided by the fluid passing over the sensor is balanced by an increased current to the sensor, which maintains a constant temperature. The magnitude of this increase is available as an output voltage that is directly related to heat transfer and, thus, the flow velocity.

Figure 30 shows the setup of the anemometer system of the Civil Engineering Department, University of Missouri, Rolla. The devices used in this experiment were the CTA (Constant Temperature Anemometer), the A-D (analog to digital) Converter, and the Counter. For the purposes of this research, the hot-film probe was placed perpendicular to the flow, the corresponding analog voltage response was converted to a digital response

by the A-D Converter, and the digital response was then read on the screen of the Counter.

Since the voltage response from the CTA is continuous, an average value was computed and digitally output over a five second period by using an adjustment knob located on the Counter. This minimized large fluctuations in the readings due to flow turbulence.

The particular probe used for this research had to be small enough to accurately conduct measurements within the cross sections of the micro model, which were on the average only a few square inches in total area. The probe used was a model 1264, purchased by the University from TSI Incorporated. Figure 31 shows the specifications of the probe.

The probe was mounted on the sliding micrometer system (section III.6.3). Figure 32 is an illustration of the setup. The system was positioned perpendicular to the flow at the desired cross section. Both the probe and the micrometer were simultaneously placed in the water. The depth was recorded, and the micrometer was then raised out of the water to eliminate any adverse flow influence. The velocity output was recorded, and this procedure was then repeated at incremental points along the cross section.

An overheat ratio, whereby additional current can be supplied to the probe through the CTA, can be applied for increased sensitivity. In this case, the probe was made to collect average velocity readings for each point location. The probe had to be made sensitive enough to detect changes throughout the cross section, yet not made too sensitive so as to create

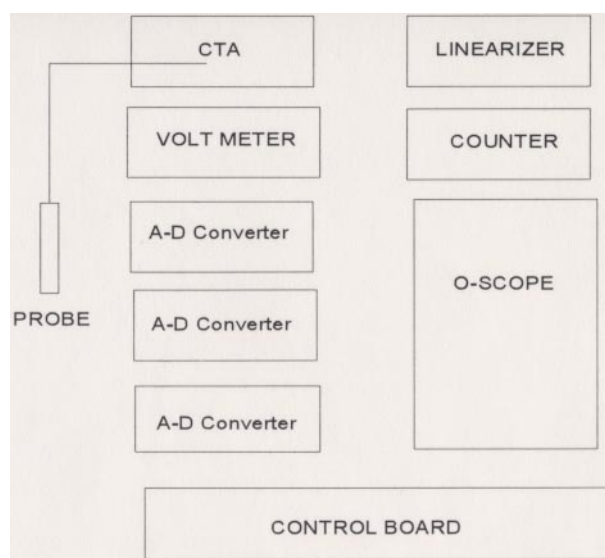
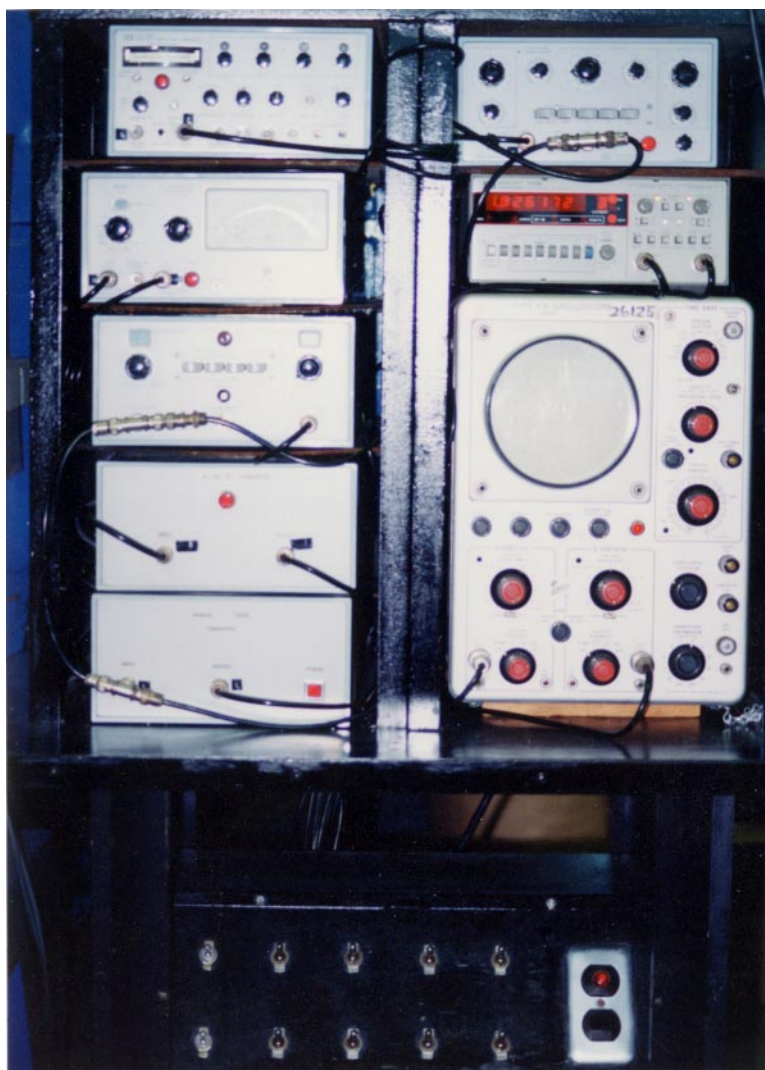


Figure 30. Anemometer System, Civil Engineering Department, UMR

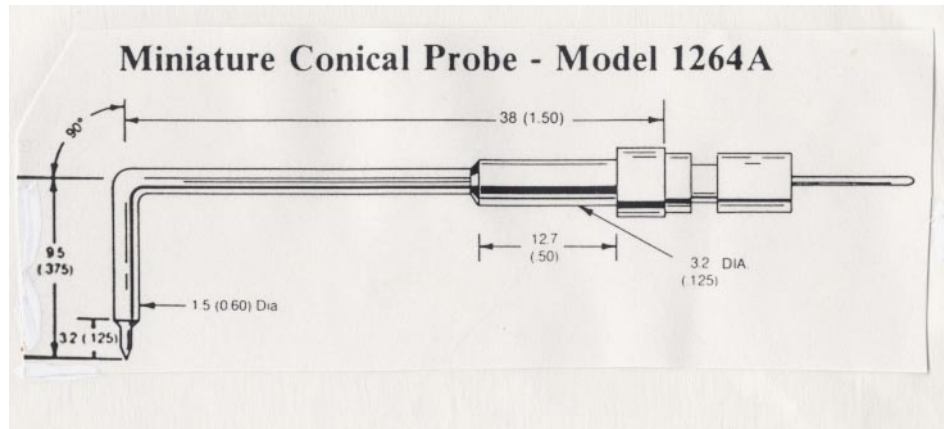


Figure 31. Specifications for Hot-Film Anemometer Probe

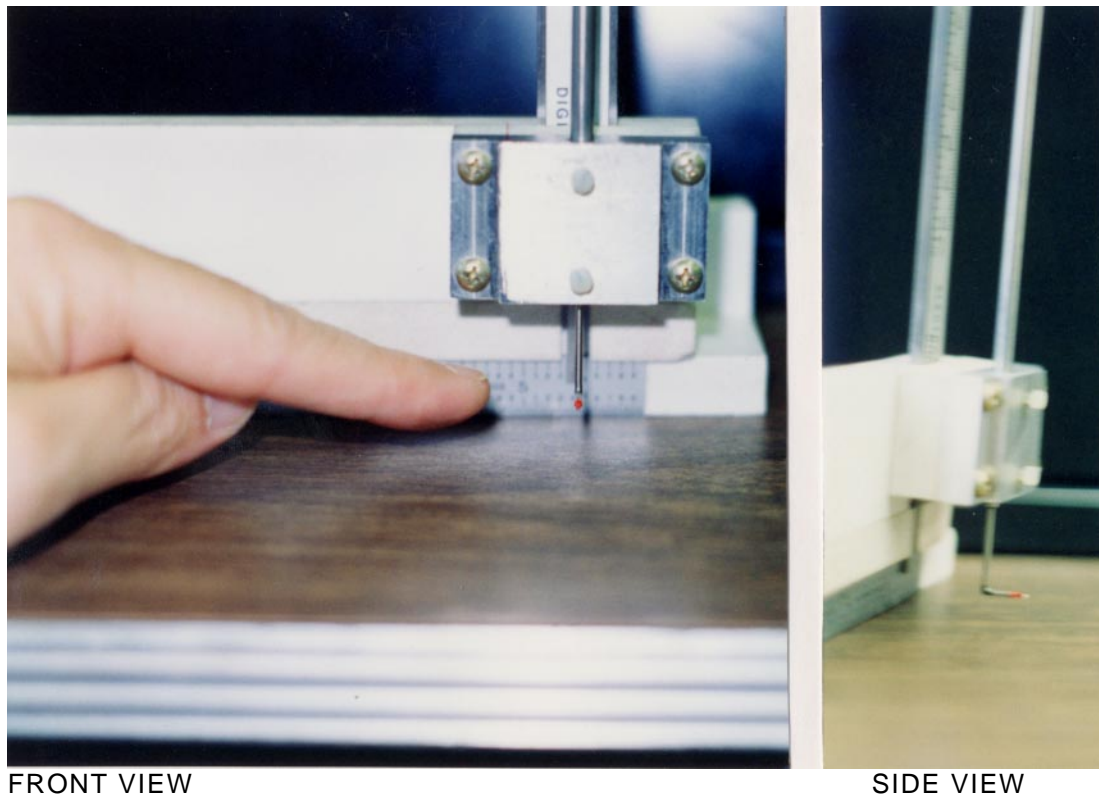


Figure 32. Anemometer Probe and Sliding Micrometer Setup

excessive fluctuations in the readings. During these tests, it was found that no overheat ratio was required, probably due to the smallness of the probe.

The application of this technology for this experiment probably varied somewhat from normal measurement procedures. Most measurements conducted with the anemometer are calibrated to known velocities measured in the laboratory (31). For fluid measurement, this is usually accomplished by use of the pitot tube. However, the actual magnitude of the velocity was not important in this experiment. Since the goal was to detect relative changes of velocity within a particular cross section, and then compare these changes to the prototype, the voltage was read directly during the measurements as a velocity index value.

To compare the velocity distribution of both model and prototype, a scheme was developed to plot cross sectional velocity isovels. Velocity data collected in the Mississippi River at Mile 34.3 (obtained from the St. Louis District Corps of Engineers), and velocity index data collected at the same relative location on the micro model were both formatted into x, y, and z data files (ISO.DAT). A computer program (ISOVEL2.BAS, Appendix B) was written to create a boundary or blanking file (ISO.BLN) which delineated the boundary points of the cross section. The two files were then input into SURFER for the plotting of the isovels.

The velocity data of the prototype was collected at somewhat even increments within the water column (approximately every 10 feet vertically

and every 200 feet horizontally). On the model, data was collected every one tenth of an inch vertically and every 0.2 tenths of an inch horizontally.

Figures 33 and 34 illustrate the comparison between the prototype and the micro model, respectively. Note the similarity in the isovels. There is a similar trend for higher velocity toward the right descending bank.

The velocity index values, as stated before, do not represent actual velocity magnitudes. However, it can be seen from this single comparison of data that a correlation factor could be developed between the model and the prototype. The limited amount of prototype data obtained (only one cross section) removed this possibility in this research. Future data collected from both the prototype and the micro model could make a direct velocity scale correlation factor possible.

Theoretically, the anemometer output values could be adjusted once a correlation factor or factors are developed so that readings on the micro model would represent actual readings in the prototype. This would further add to the application of the micro model beyond the scope of the research conducted in this thesis.

2. Plan View Isovels. Often times it is necessary to observe the relative velocity distribution in plan view in order to gain additional understanding of the flow regime. To demonstrate this, velocity measurements with the probe were conducted in the model through the two bends. Measurements were made with and without the installation of

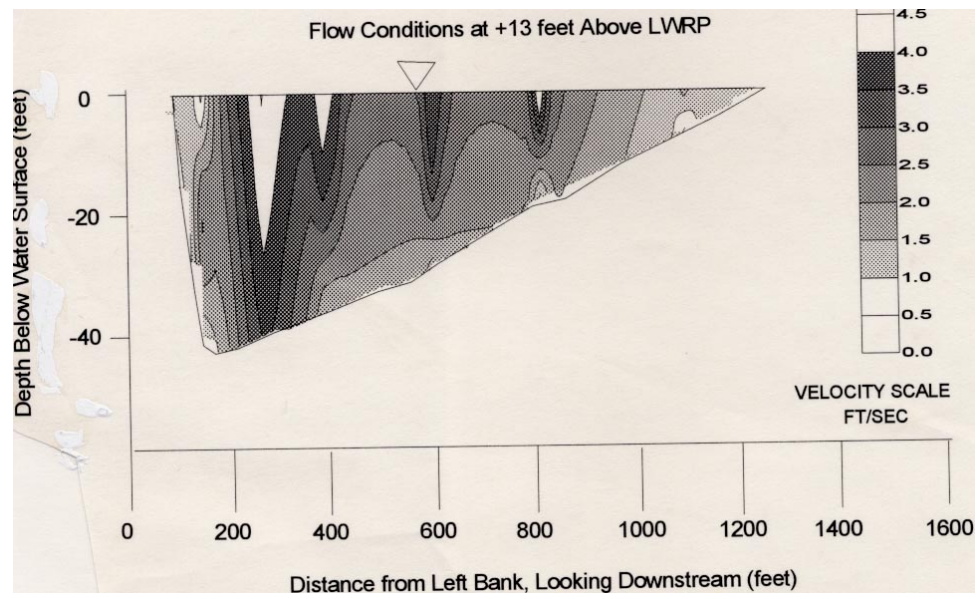


Figure 33. Cross Sectional Velocity Isovels at Mile 34.3, Prototype

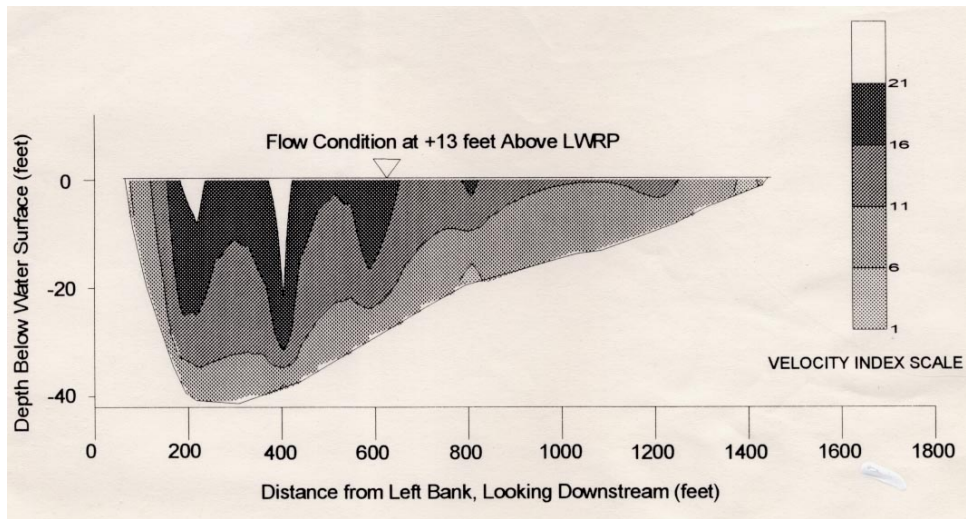


Figure 34. Cross Sectional Velocity Isovels at Mile 34.3, Micro Model

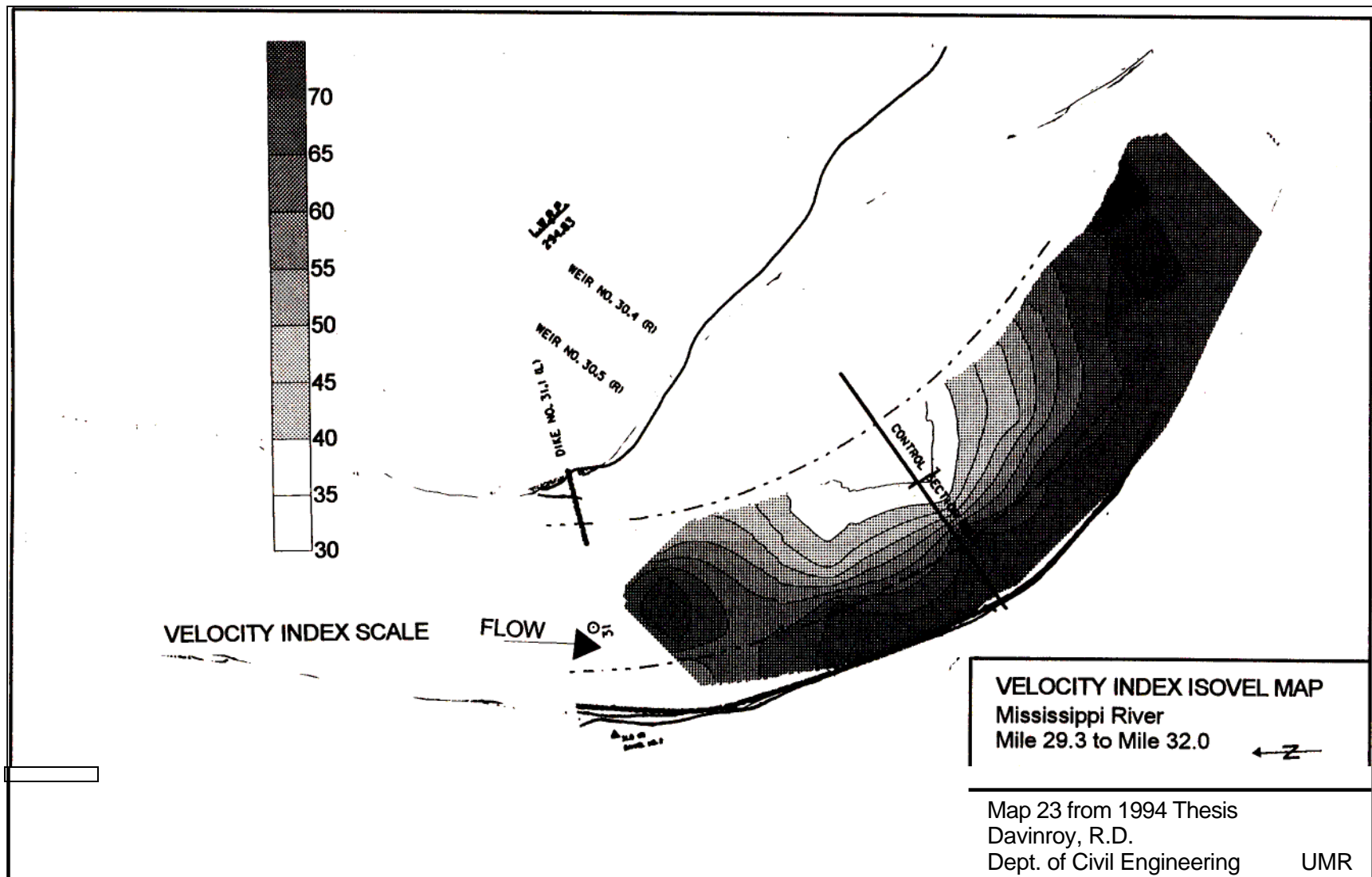
bendway weirs. Steady state flow conditions at 10 feet above LWRP were maintained throughout the tests.

Velocity index values were collected at even increments (0.2 inches) across several cross sections in each bend at a depth of -10 LWRP. This information was then input into SURFER, and plan view velocity index isovels were developed. Maps 23 and 24 show plan view isovels at Prices and Dogtooth Bends. The tendency for the faster velocity towards the right descending bank in both bends can be clearly seen. In Prices Bend, there appeared to be a tendency for faster, evenly distributed velocity in the most downstream portion of the bend. Maps 25 and 26 show isovels in the two bends with the installation of bendway weirs. Both plots show that the structures cause a more even distribution of velocity through the bends.

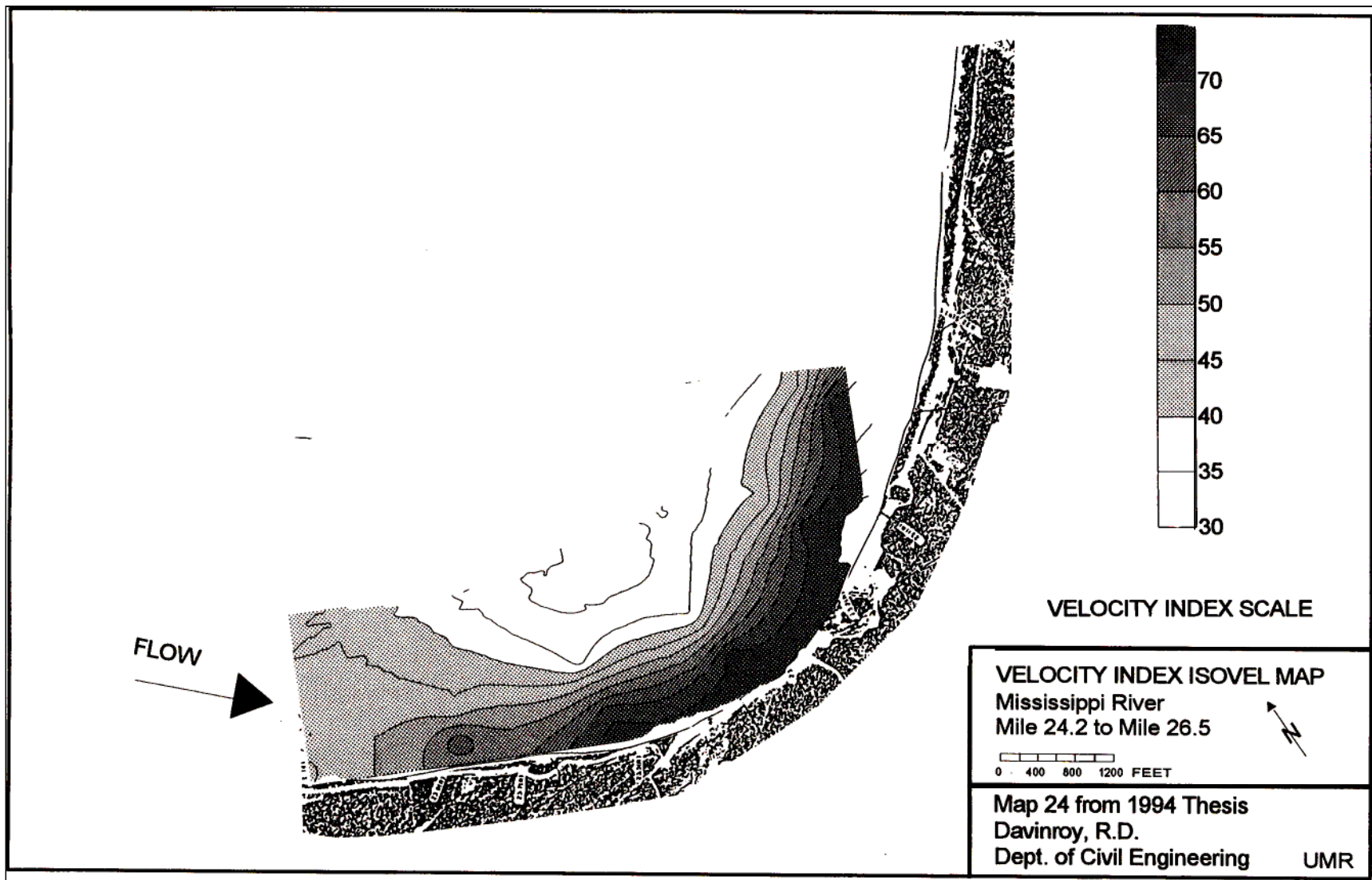
This kind of information, when supplemented by the flow visualization technique of time lapse photography (30), is important not only to the engineer, but also to the navigation industry, local landowners, and conservationists.

D. STATISTICAL VARIANCE STUDY

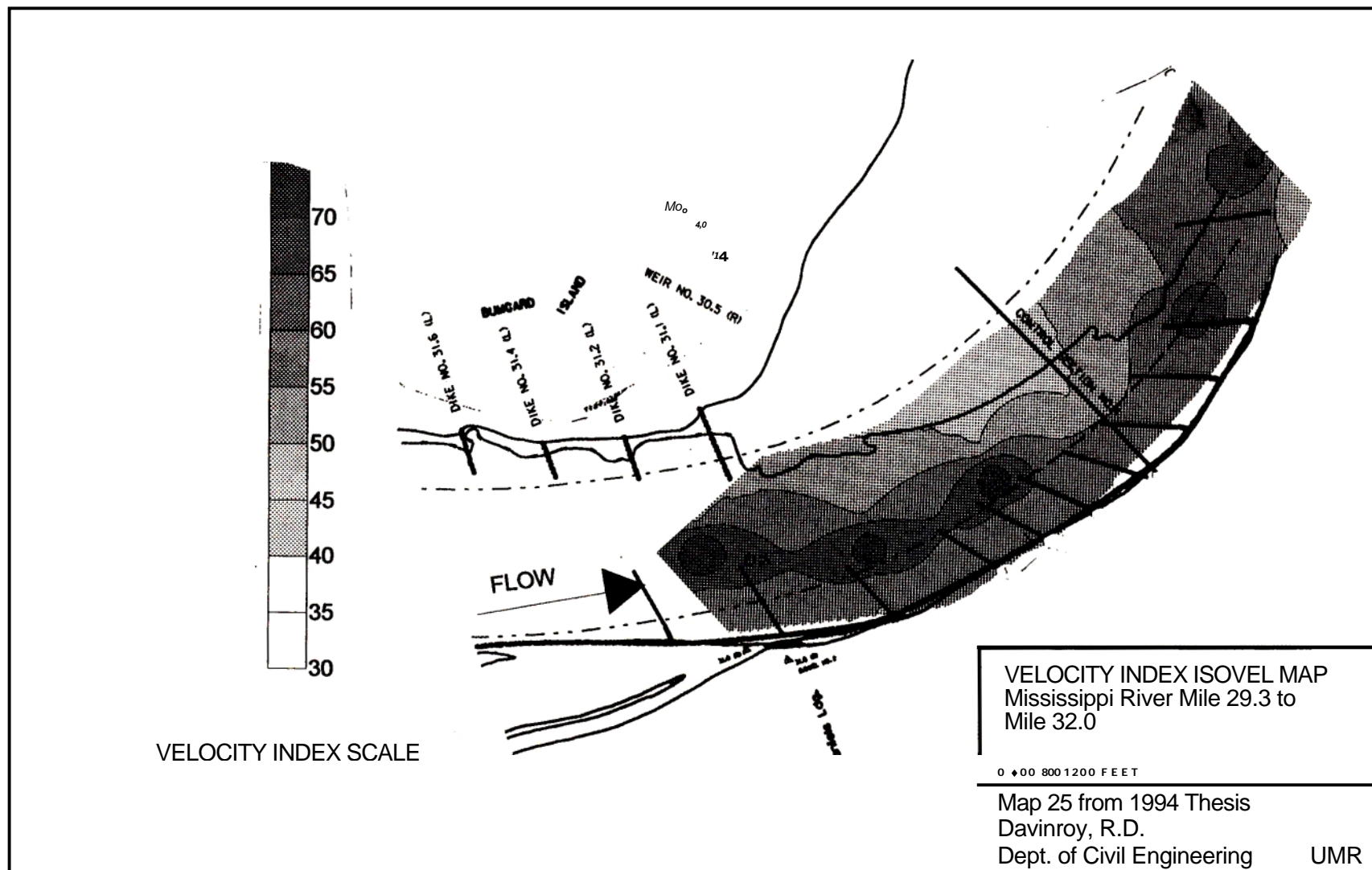
To measure the ability of the micro model to replicate the same resultant bed configuration between design hydrographs, or, in other words, to study the variability of the sediment response between identical experimental runs, a statistical study was conducted. Because the operational parameters of flow, stage, and sediment were manually controlled in the model, this study



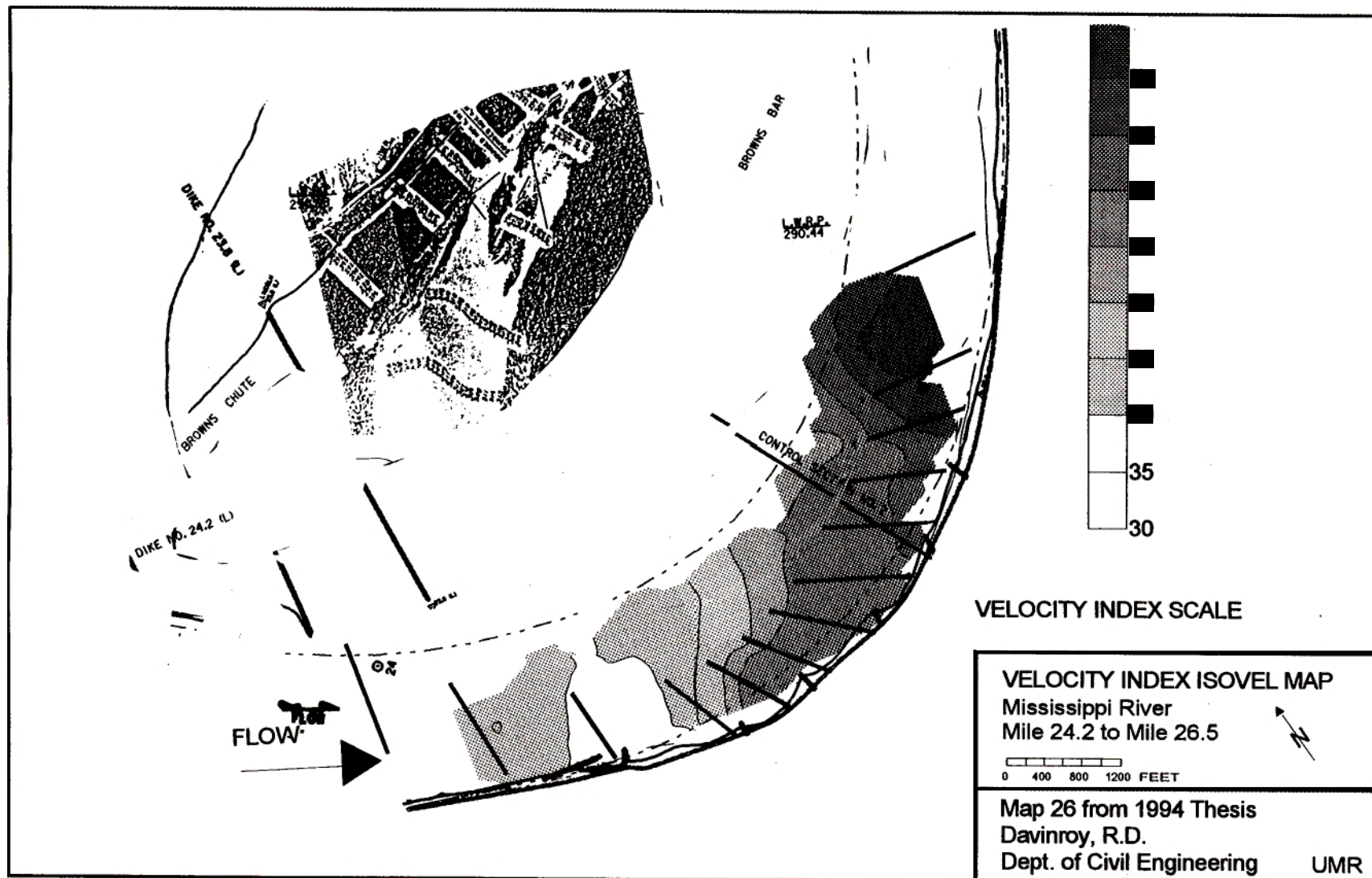
Map 23. Velocity Index Isovels, Base Condition, Mile 29.3 to Mile 32.0



Map 24. Velocity Index Isovels, Base Condition, Mile 22.1 to Mile 24.2



Map 25. Velocity Index Isovels, Bendway Weir Test, Mile 29.3 to Mile 32.0



Map 26. Velocity Index Isovels, Bendway Weir Test, Mile 22.1 to Mile 24.2

was conducted as a means to verify the reproductivity of tests. By studying the variance or deviation of data from one run to another, one could then make conclusions about the overall repeatability of tests.

The experimental data under study was the resultant bed configuration, considered the ultimate response indicator of the model. The bed configuration is a footprint of the sediment response of the model. To measure this response, the changes in the depth, or the z variable of the bed, were analyzed. Depth in this context represented elevation as referenced to a fixed sloping datum (LWRP).

Thus, the study measured the relative changes or variance in depth at particular points along a cross section between individual flow hydrographs. Depths were collected at the same incremental distances along the cross section for each of the 5 control sections on the model. This procedure was repeated after the testing of individual base condition runs, using the average annual hydrograph. Seven base condition tests were simulated, and the data points of each resultant bed configuration at the five cross sections were stored in a statistical data file.

Likewise, depths were collected at the same relative cross section locations from 7 individual base test runs of the Dogtooth Bend Model at WES. These data were also entered into a statistical data file.

The experiments from both models were similar in the following regards:

- 1). Each test was simulated using the annual design hydrograph.
- 2). Sediment input was the same for each test.

3). The calibration parameters of slope and discharge were held constant throughout all tests.

4). Each experiment or test in both cases was dependent upon the previous run. That is, the bed was not remolded on either model between runs. The experiments differed from each other as follows:

1). The micro model hydrograph was generated manually, using the discharge control valve and stopwatch. The WES model hydrograph was generated semi-automatically. Both the discharge control valve and the tailbay were controlled electronically, but required a person to operate the electronic controls during each incremental change in stage.

2). The hydrograph of the micro model was actually more sinusoidal in shape and continuous than the WES model due to the nature of operation. Both models employed the stair stepped average annual hydrograph (Figure 19). However, on the micro model, the manual opening and closing of the discharge control valve, combined with a 3 to 5 second lag between the discharge entrance point and the control gage at mile 23.3, allowed for a more continuous, sinusoidal response. On the WES model, flow was simulated at each desired stage, but then, instead of a transition to the next flow/stage increment, the flow was briefly halted, the tailbay was raised, the model was pooled or drained to the next desired stage, and the next flow increment was introduced. This made for a more stair-stepped, non-continuous hydrograph.

3). The tailbay was held constant during each hydrograph on the micro model, while the tailbay on the WES model was raised and lowered throughout the hydrograph.

4). Depths on the micro model were measured using a micrometer, measured to the nearest hundredth of an inch, while depths on the WES model were measured using a level and rod, measured to the nearest hundredth of a foot.

5). Water surface profiles were monitored visually by staff gages marked on the sides of the micro model channel, while on the WES model, the water surface was read from automatic recording gages.

6). Both the physical scale and the duration of the hydrograph were different, as discussed in section IC.

The procedure of the determination of the base condition was significantly different between the micro model and the WES model. On the micro model, a series of individual, dependent tests were run, with a survey conducted at the end of each hydrograph. The data was then averaged, representing the expected resultant bed configuration of the runs.

On the WES model, a series of dependent tests were run, with a survey also conducted at the end of each hydrograph. However, each test was also checked for stability, that is, at the end of each run, the total amount of sediment that exited the model was measured and compared to the constant amount of sediment that was introduced to the model. When the two parameters were approximately the same, the model was considered stable.

The resulting bed configuration survey for the run which produced the most stable condition (input equals output) was then chosen as the comparative survey for all future design tests, while the other surveys were ignored.

An additional assumption was made in the comparison of the two experiments. Although all tests in both models were dependent upon each other by experimental definition, it was assumed that the starting resultant bed configuration from the previous test did not influence the next configuration. This is a valid assumption if one realizes that once the design hydrograph is initiated, the bed instantaneously changes, and when the flow reaches bank full conditions, all influence of the previous bed configuration is absent. As the hydrograph falls, the channel alignment and the flow/sediment response is the only influence on the resultant bed configuration. Thus, for the purposes of this analysis, each design hydrograph test was considered independent.

The data for each of the two models was stored in a comma delimited statistical data file in the following format; model, base condition test run, cross section, depth 1, depth 2, depth 3,....depth n. The distances between each point were held constant throughout all runs on both models.

The depth data was analyzed using the computer program SASS. Appendix B is a listing of the input/output. In the input, the WES model represented model one, while the micro model represented model 2. The following output data was observed:

1) For the 5 cross sections, the variance of the WES model, model 1, ranged between the values of 3.17 and 12.5, while the variance for the micro model, model 2, ranged between 3.26 and 19.66.

2) The average total variance for each model was 8.34 and 10.46, respectively. The statistical tests on these variance values show that relative difference between models was statistically insignificant.

These numbers show that the variance of the vertical depth data was similar between the two models, and a general inference might be made that the two models behaved similarly even though the scale, operation, and materials were different. Also, the relatively low variance values indicated that there were not large differences in the depths of the bed during the experiments, indicating satisfactory repeatability from run to run.

V. CONCLUSIONS

From the results of this research, the use of a micro scale physical model to simulate and study the problems of sediment transport on the Mississippi River is possible. Comparisons made with both the prototype and a larger model show similar trends in the resultant bed configuration of the channel. The consistency with which the model reproduced itself is indicative of its reliability.

Many of the modeling procedures used today on typical movable bed models, such as building templates, adjusting slope railings, etc. are not required in the micro modeling procedures.

The advantages of modeling on this extremely small scale are numerous, including:

- 1). The model is inexpensive. The total construction costs of the model, including all appurtenances, was approximately \$4,000.00. This is tremendously cheaper than typical movable bed models, where costs can be in the hundreds of thousands of dollars.

- 2). The answers can be obtained quickly. The total time required for calibration and design testing took approximately one month. Typical movable bed model studies today can take anywhere from one to three years to complete.

- 3). The model is visual. The movement and pathways of sediment during the different stages of the hydrograph could be clearly seen during the tests. Because of the clarity of the water, the small scale, and the quick

time period, one can focus in on large segments of the model, such as complete bends, etc. and clearly see the formation of point bars, scour holes, etc. in a matter of a few seconds. This is not possible on typical models today because of the relative time scale used and the large physical size.

4). The model is portable. The model can be placed in the back of a pickup truck and transported wherever needed. This includes public meetings with local, state, and federal interests, court proceedings, classroom presentations, museums, etc.

5). By use of hot-film anemometry, relative velocity can be measured in the model to gain additional understanding of flow dynamics.

6). The model does not require a large amount of labor. The entire model required only one person to operate.

The use of this technology for application to other sedimentation related problems is unlimited. The same principles could be used in modeling other large rivers, streams, canals, oceans, estuaries, reservoirs, etc.

The low cost and the quick turnaround time make this tool affordable to most practicing engineers. It also means that more people, such as land owners, lawyers, etc., who might need to analyze a particular sedimentation problem, can more readily afford to call on the application of a physical model.

APPENDIX A

VELOCITY ISOVEL PROGRAM

ISOVEL2.BAS

```

1 REM      PROGRAM TO CREATE BLANKING FILE FOR CREATION
2 REM      OF CROSS SECTIONAL ISOVEL PLOT,
3 REM      MICRO SEDIMENT MODEL
4 REM      *****
5 REM      Rob Davinroy 4-18-94 @1994 Part of Master's Thesis
6 REM      University of Missouri-Rolla
7 REM
8 REM
9 REM
10 DIM x(100), y(100), z(100)
11 INPUT "Enter the cross section file (?.dat): "; dat$
13 OPEN "c:\surfer\files\dat$" FOR INPUT AS #1
30 OPEN "a:iso.bln" FOR OUTPUT AS #2
40 b = 0
50 i = 0
60 IF EOF(1) THEN 110
70 INPUT #1, x(i), y(i), z(i)
80 IF y(i) = 0 THEN 90 ELSE 60
90 i = i + 1
100 GOTO 60
110 CLOSE #1
120 OPEN "a:iso.dat" FOR INPUT AS #1
130 c = 0
140 IF EOF(1) THEN 190
150 INPUT #1, q(c), r(c), s(c)
160 IF r(c) <> 0 AND s(c) = 0 THEN 170 ELSE 140
170 c = c + 1
180 GOTO 140
190 e = c + i + 1
200 PRINT #2, e, b
210 FOR 1 = 0 TO i - 1 220 PRINT #2, x(1), y(1)
230 NEXT 1
231 FOR pass = 0 TO c - 1
232 FOR 1 = 0 TO c - 1
233 IF q(1) < q(1 + 1) THEN SWAP q(1), q(1 + 1) ELSE 235
234 SWAP r(1), r(1 + 1)
235 NEXT 1
237 NEXT pass
244 FOR 1 = 1 TO C
250 PRINT #2, q(1), r(1)
260 NEXT 1

```

ISOVEL2.BAS

```
270 PRINT #2, x(0), y(0)
280 CLOSE #1, #2
290 END
```

APPENDIX B

STATISTICAL VARIANCE INPUT AND OUTPUT USING

Licensed to UNIVERSITY OF MISSOURI AT ROLLA, Site 0001136002.

NOTE: Running on IBM Model 4381 Serial Number 013752.

SAS Release 6.06 is the production version of SAS at
UMR. 10/08/91 - SAS IML is now available (proc matrix
among others)

Please report any problems you encounter to Daniel
Uetrecht UETRECHT@UMRVMB.UMR.EDU

```
1      DATA A1 ;
2      INPUT MODEL POS RUN Y1-Y10;
3      REP=1; IF RUN > 4 THEN REP=2;
4      CARDS;
```

NOTE: The data set WORK.A1 has 7 observations and 14 variables.

```
12
13      PROC MEANS NOPRINT VAR ; BY REP;
14      VAR Y1-Y10;
15      OUTPUT OUT=V11 VAR=V1 V2 V3 V4 V5 V6 V7 V8 V9 V10;
```

NOTE: The data set WORK.V11 has 2 observations and 13 variables.

```
16      DATA A1B;
17      INPUT MODEL POS RUN Y1-Y9;
18      REP=1; IF RUN > 4 THEN REP=2;
19      CARDS;
```

NOTE: The data set WORK.A1B has 7 observations and 13 variables.

```
27
28      PROC MEANS NOPRINT VAR ; BY REP;
29      VAR Y1-Y9;
30      OUTPUT OUT=V21 VAR=V1 V2 V3 V4 V5 V6 V7 V8 V9;
```

NOTE: The data set WORK.V21 has 2 observations and 12 variables.

```
31      DATA B1;
32      INPUT MODEL POS RUN Y1-Y18;
33      REP=1; IF RUN > 4 THEN REP=2;
34      CARDS;
```

NOTE: The data set WORK.B1 has 7 observations and 22 variables.

```
42      ;
43
44      PROC MEANS NOPRINT VAR ; BY REP;
45      VAR Y1-Y18;
46      OUTPUT OUT=V12 VAR=V1 V2 V3 V4 V5 V6 V7 V8 V9 V10 V11 V12 V13 V14 V15 V16
      V17 V18;
```

2

47 v17 v18;

NOTE: The data set WORK.V12 has 1 observations and 20 variables.

```
48 DATA BIB;
49 INPUT MODEL POS RUN Y1-Y15;
50 REP=1; IF RUN > 4 THEN REP=2;
51 CARDS;
```

NOTE: The data set WORK.B1B has 7 observations and 19 variables.

```
59 ;
60 PROC MEANS NOPRINT VAR
61 VAR Y1-Y15;
62 OUTPUT OUT=V22 VAR=V1 V2 V3 V4 V5 V6 V7 V8 V9 V10 V11 V12 V13
```

NOTE: The data set WORK.V22 has 1 observations and 17 variables. V14 V15;

```
63 DATA CI ;
64 INPUT MODEL POS RUN Y1-Y7;
65 REP=1; IF RUN > 4 THEN REP=2;
66 CARDS;
```

NOTE: The data set WORK.C1 has 7 observations and 11 variables.

```
74 ;
75 PROC MEANS NOPRINT VAR
76 VAR Y1-Y7;
77 OUTPUT OUT=V13 VAR=V1 V2 V3 V4 V5 V6 V7;
```

NOTE: The data set WORK.V13 has 1 observations and 9 variables.

```
78 DATA C1B;
79 INPUT MODEL POS RUN Y1-Y9;
80 REP=1; IF RUN > 4 THEN REP=2;
81 CARDS;
```

NOTE: The data set WORK.C1B has 7 observations and 13 variables.

```
89 ;
90 PROC MEANS NOPRINT VAR
91 VAR Y1-Y9;
92 OUTPUT OUT=V23 VAR=V1 V2 V3 V4 V5 V6 V7 V8 V9;
```

NOTE: The data set WORK.V23 has 1 observations and 11 variables.

```
93 DATA DI ;
94 INPUT MODEL POS RUN Y1-Y13;
95 REP=1; IF RUN > 4, THEN REP=2;
96 CARDS;
```

NOTE: The data set WORK.D1 has 7 observations and 17 variables.

```
104 ;
105 PROC MEANS NOPRINT VAR
106 VAR Y1-Y13;
107 OUTPUT OUT=V14 VAR=V1 V2 V3 V4 V5 V6 V7 V8 V9 V10 V11 V12 V13;
```

NOTE: The data set WORK.V14 has 1 observations and 15 variables.

```
108 DATA D1B; 109 INPUT MODEL POS RUN Y1-Y12;
110 REP=1; IF RUN > 4 THEN REP=2;
111 CARDS;
```

NOTE: The data set WORK.D1B has 7 observations and 16 variables.

```
119 ;
120 PROC MEANS NOPRINT VAR
121 VAR Y1-Y12;
122 OUTPUT OUT=V24 VAR=V1 V2 V3 V4 V5 V6 V7 V8 V9 V10 V11 V12;
```

NOTE: The data set WORK.V24 has 1 observations and 14 variables.

```
123 DATA E1;
124 INPUT MODEL POS RUN Y1-Y10;
125 REP=1; IF RUN > 4 THEN REP=2;
126 CARDS;
```

NOTE: The data set WORK.E1 has 7 observations and 14 variables.

```
134 ;
135 PROC MEANS NOPRINT VAR
136 VAR Y1-Y10;
137 OUTPUT OUT=V15 VAR=V1 V2 V3 V4 V5 V6 V7 V8 V9 V10;
```

NOTE: The data set WORK.V15 has 1 observations and 12 variables.

```
138 DATA E1B;
139 INPUT MODEL POS RUN Y1-Y10;
140 REP=1; IF RUN > 4 THEN REP=2;
141 CARDS;
```

NOTE: The data set WORK.E1B has 7 observations and 14 variables.

```
149 ;
150 PROC MEANS NOPRINT VAR
151 VAR Y1-Y10;
152 OUTPUT OUT=V25 VAR=V1 V2 V3 V4 V5 V6 V7 V8 V9 V10;
```

NOTE: The data set WORK.V25 has 1 observations and 12 variables.

```
153 DATA V11;
154 SET V11;
155 MODEL=1; POS=1;
156 VAR=MEAN(V1, V2, V3, V4, V5, V6, V7, V8, V9, V10 );
```

NOTE: The data set WORK.V11 has 1 observations and 15 variables.

```
157 DATA V21;
158 SET V21;
159 MODEL=2; POS=1;
160 VAR=MEAN(V1, V2, V3, V4, V5, V6, V7, V8, V9 );
```

NOTE: The data set WORK.V21 has 1 observations and 14 variables.

4

The SAS System

```

161 DATA V12; SET V12;
162 MODEL=1; POS=2;
163 VAR=MEAN(V1, V2, V3, V4, V5, V6, V7, V8, V9, V10, V11, V12, V13, V14, V15, V16, V17, V18);

```

NOTE: The data set WORK.V12 has 1 observations and 23 variables.

```

164 DATA V22; SET V22;
165 MODEL=2; POS=2;
166 VAR=MEAN(V1, V2, V3, V4, V5, V6, V7, V8, V9, V10, V11, V12, V13, V14, V15 );

```

NOTE: The data set WORK.V22 has 1 observations and 20 variables.

```

167 DATA V13; SET V13;
168 MODEL=1; POS=3;
169 VAR=MEAN(V1, V2, V3, V4, V5, V6, V7 );

```

NOTE: The data set WORK.V13 has 1 observations and 12 variables.

```

170 DATA V23; SET V23;
171 MODEL=2; POS=3;
172 VAR=MEAN(V1, V2, V3, V4, V5, V6, V7, V8, V9 );

```

NOTE: The data set WORK.V23 has 1 observations and 14 variables.

```

173 DATA V14; SET V14;
174 MODEL=1; POS=4;
175 VAR=MEAN(V1, V2, V3, V4, V5, V6, V7, V8, V9, V10, V11, V12, V13, V14 );

```

NOTE: Variable V14 is uninitialized.

NOTE: The data set WORK.V14 has 1 observations and 19 variables.

```

176 DATA V24; SET V24;
177 MODEL=2; POS=4;
178 VAR=MEAN(V1, V2, V3, V4, V5, V6, V7, V8, V9, V10, V11, V12 );

```

NOTE: The data set WORK.V24 has 1 observations and 17 variables.

```

179 DATA V15; SET V15;
180 MODEL=1; POS=5;
181 VAR=MEAN(V1, V2, V3, V4, V5, V6, V7, V8, V9, V10 );

```

NOTE: The data set WORK.V15 has 1 observations and 15 variables.

```

182 DATA V25; SET V25;
183 MODEL=2; POS=5;
184 VAR =MEAN(V1, V2, V3, V4, V5, V6, V7, V8, V9, V10 );

```

NOTE: The data set WORK.V25 has 1 observations and 15 variables.

```

185 DATA ALL;
186 SET V11 V21 V12 V22 V13 V23 V14 V24 V15 V25;

```

NOTE: The data set WORK.ALL has 10 observations and 23 variables.

```

187 PROC GLM;
188 CLASSES MODEL POS;
189 MODEL VAR = MODEL POS ;
190 LSMEANS MODEL / PDIFF;

```

OBS	REP	_TYPE_	_FREQ_	V1	V2	V3	4	V5	V6	V7	V8	
1	1	0	4	0.33333	2.250	0.3333	0.33333	6.3333	1.5833	0.6667	4.9167	2.6667
2	2	0	3	1.00000	0.333	16.3333	2.33333	2.3333	1.0000	4.3333	9.0000	7.0000
3	1	0	4	0.00000	1.667	0.0000	0.25000	2.9167	18.9167	23.0000	69.6667	0.0000
4	2	0	3	0.00000	7.000	1.0000	2.33333	0.3333	31.0000	17.3333	16.0000	0.0000
5	1	0	4	1.00000	14.250	3.6667	0.25000	0.3333	0.2500	4.6667	0.2500	0.9167
6	2	0	3	5.33333	17.333	1.0000	0.33333	0.3333	1.3333	1.3333	0.0000	1.0000
7	1	0	4	0.00000	0.917	0.2500	3.00000	1.5833	2.0000	7.3333	10.2500	2.2500
8	2	0	3	0.00000	0.000	0.0000	0.00000	0.0000	0.0000	0.0000	0.0000	0.0000
9	1	0	4	4.25000	0.667	1.6667	2.25000	2.9167	1.6667	0.9167	.	.
10	2	0	3	0.00000	1.333	1.3333	7.00000	37.0000	2.3333	0.3333	.	.
11	1	0	4	0.00000	13.333	12.2500	5.33333	0.9167	3.6667	2.2500	14.9167	0.0000
12	2	0	3	0.00000	1.000	97.0000	4.00000	2.3333	2.3333	1.0000	1.0000	0.0000
13	1	0	4	2.91667	0.250	8.0000	1.00000	32.2500	0.2500	0.2500	0.0000	0.6667
14	2	0	3	0.33333	1.000	1.0000	1.00000	4.3333	4.3333	2.3333	0.3333	10.3333
15	1	0	4	0.00000	0.000	0.6667	1.00000	4.0000	25.6667	2.6667	14.2500	29.5833
16	2	0	3	0.00000	0.000	0.3333	0.33333	0.0000	19.0000	75.0000	2.3333	9.3333
17	1	0	4	1.66667	129.667	1.5833	1.58333	0.9167	0.3333	1.5833	0.6667	1.5833
18	2	0	3	7.00000	3.000	31.0000	1.33333	9.0000	19.0000	19.0000	3.0000	14.3333
19	1	0	4	0.00000	1.583	2.9167	7.00000	2.9167	1.0000	2.2500	0.9167	4.6667
20	2	0	3	0.00000	1.333	0.3333	3.00000	22.3333	10.3333	2.3333	0.0000	2.3333
OBS	V10	MODEL	POS	VAR	V11	V12	V13	V14	V15	V16	V17	V18
1	0.0000	1	1	1.9417
2	0.3333	1	1	4.4000
3	.	2	1	12.9352
4	.	2	1	8.3333
5	0.9167	1	2	6.6389	1.333	0.917	1.0000	18.2500	12.6667	52.9167	3	2.91667
6	0.3333	1	2	11.3519	7.000	9.333	7.0000	37.0000	26.3333	37.3333	48	4.00000
7	89.0000	2	2	29.5611	104.333	124.667	72.9167	24.9167	0.0000	.	.	.
8	6.3333	2	2	9.7556	5.333	28.000	97.3333	9.3333	0.0000	.	.	.
9	.	1	3	2.0476
10	.	1	3	7.0476
11	.	2	3	5.8519
12	.	2	3	12.0741
13	18.2500	1	4	14.8205	1.667	126.250	0.9167
14	3.0000	1	4	10.2308	14.333	86.333	4.3333
15	14.6667	2	4	8.9583	15.000	0.000
16	6.3333	2	4	10.5833	14.333	0.000
17	1.6667	1	5	14.1250
18	1.3333	1	5	10.8000
19	0.0000	2	5	2.3250
20	0.0000	2	5	4.2000

Class	Levels	Values
MODEL	2	1 2
POS	5	1 2 3 4 5

Number of observations in data set = 20

Dependent Variable: VAR

Source	DF	Sum of Squares	Mean Square	F Value	Pr > F
Model	9	452.82919358	50.31435484	1.85	0.1756
Error	10	271.84308230	27.18430823		
Corrected Total	19	724.67227588			

R-Square	C. V.	Root MSE	VAR Mean
0.624874	55.47197	5.21385733	9.39908527

Source	DF	Type III SS	Mean Square	F Value	Pr > F
MODEL	1	22.41659667	22.41659667	0.82	0.3852
POS	4	42.92586514	42.92586514		
MODEL*POS	4	64.67728409	64.67728409		

Source	DF	Type III SS	Mean Square	F Value	Pr > F
MODEL	1	22.41659667	22.41659667	0.82	0.3852
POS	4	42.92586514	42.92586514		
MODEL*POS	4	64.67728409	64.67728409		

MODEL	VAR LSMEAN	Pr > T H0: LSMEAN1=LSMEAN2
1	8.3403928	0.3852
2	10.4577778	

POS	VAR LSMEAN	Pr > T H0: LSMEAN(I)=LSMEAN(J) I/J	1	2	3	4	5
1	6.9025463	1	.	0.0717	0.9689	0.2763	0.7999
2	14.3268519	2	0.0717	.	0.0671	0.4088	0.1101
3	6.7552910	3	0.9689	0.0671	.	0.2609	0.7701
4	11.1482372	4	0.2763	0.4088	0.2609	.	0.3937
5	7.8625000	5	0.7999	0.1101	0.7701	0.3937	.

To ensure overall protection level, only probabilities associated with pre-planned comparisons should be used.

MODEL	POS	VAR LSMEAN	Pr > T H0: LSMEAN(I)=LSMEAN(J) I/J	1	2	3	4	5	6	7	8	9	10
1	1	3.1708333	1	.	0.2901	0.7971	0.1030	0.1051	0.1828	0.0101	0.2926	0.2343	0.9863
1	2	8.9953704	2	0.2901	.	0.4136	0.5137	0.5211	0.7597	0.0681	0.9952	0.8847	0.2973
1	3	4.5476190	3	0.7971	0.4136	.	0.1570	0.1600	0.2701	0.0159	0.4169	0.3401	0.8103
1	4	12.5256410	4	0.1030	0.5137	0.1570	.	0.9906	0.7243	0.2013	0.5099	0.6088	0.1060
1	5	12.4625000	5	0.1051	0.5211	0.1600	0.9906	.	0.7331	0.1976	0.5173	0.6169	0.1081
2	1	10.6342593	6	0.1828	0.7597	0.2701	0.7243	0.7331	.	0.1142	0.7552	0.8718	0.1878
2	2	19.6583333	7	0.0101	0.0681	0.0159	0.2013	0.1976	0.1142	.	0.0674	0.0871	0.0104
2	3	8.9629630	8	0.2926	0.9952	0.4169	0.5099	0.5173	0.7552	0.0674	.	0.8799	0.2999
2	4	9.7708333	9	0.2343	0.8847	0.3401	0.6088	0.6169	0.8718	0.0871	0.8799	.	0.2404
2	5	3.2625000	10	0.9863	0.2973	0.8103	0.1060	0.1081	0.1878	0.0104	0.2999	0.2404	.

To ensure overall protection level, only probabilities associated with pre-planned comparisons should be used.

BIBLIOGRAPHY

1. Lloyd William Taylor, Physics, The Pioneer Science, Houghton Mifflin Company, Boston Massachusetts, 1941.
2. J.M. Caldwell, National Bureau of Standards, Volume. 1, September 13, 1939
3. "History of Hydraulics", Dallas Times Herald, June 28, 1954
4. Reynolds, Osborne, "On Certain Laws Relating to the Regime of Rivers and Estuaries, and on the Possibility of Experiments on a Small Scale," Report of the British Association, Water Resource Center Archives, University of California, Berkely, 1887
5. Freeman, John R., Hydraulic Laboratory Practice, 1929, Comprising a Translation of DIE WASSERBAULABORATORIEN EUROPAS, Published in 1926 by Verein Deutscher Ingenieure, American Society of Mechanical Engineers, New York, 1929
6. Vogel, Herbert D., "Origin of the Waterways Experiment Station", The Military Engineer, March-April, 1951
7. Cotton, Gordon A., A History of the Waterways Experiment Station, 1929-1979, Vicksburg, Mississippi, 1979
8. Einstein, H.A., "The Bed Load Function for Sediment Transportation in Open Channel Flows," USDA Tech. Bull. 1026, 1950
9. Toffaleti, F.B., "Definite Computations of Sand Discharges in Rivers," Journal of Hydraulic Engineering, Volume 95, HY1, 1969
10. Raudkivi, A.J., Loose Boundary Hydraulics, Pergamon Press, Oxford, England, 1990
11. Ackers, P. and W.R. White, "Sediment Transport: New Approach and Analysis," Journal of Hydraulic Engineering, Volume 99, no. HY-11, 1973
12. Simons, Daryl B., "Practical Sediment Management Techniques Utilized in the United States", Proceedings of the Fifth Federal Interagency Sedimentation Conference, Federal Energy Regulatory Commission, 1991
13. Laursen, E.M., "Scour at Bridge Crossings", Transactions of the American Society of Civil Engineers, Volume 127, no. 3294, pgs. 166-209, 1962

14. Jarrett, Robert D. and Jeanne M. Boyle, "Pilot Study For Collection of Bridge Scour Data", Water Resources Investigations Report 86-4030, U.S. Department of the Interior, Denver, Colorado, 1986
15. Odgaard, A.J., "Flow and Bed Topography in Alluvial Channel Bends", Proc. ASCE, Vol. 110, HY-4, 1984
16. Davinroy, Robert D. "Bendway Weirs, A New Structural Solution to Navigation Problems on the Mississippi River", Bulletin 69, Permanent International Association of Navigation Congresses, Brussels, Belgium, 1992
17. HEC-6, Scour and Deposition in Rivers and Reservoirs, Hydrologic Engineering Center, Davis, California, 1977
18. Thomas, William A., and McAnally, William H., Jr., "TABS-2 User's Manual", Instruction Report HL-85-1, U.S. Army Engineer Waterways Experiment Station, Vicksburg, MS., 1985
19. Warnock, J.E. "Hydraulic Similitude", Engineering Hydraulics by Hunter Rouse, Proceedings of the Fourth Hydraulics Conference, Iowa Institute of Hydraulic Research, John Wiley and Sons, Inc. New York, New York, 1949
20. Pugh, Clifford A., "Design of Sediment Models", Proceedings of the Fifth Federal Interagency Sedimentation Conference, Federal Energy Regulatory Commission, 1991
21. Yalin, Selim M., Theory of Hydraulic Models, Macmillan Press LTD, London, 1971
22. Franco, John J., Guidelines for the Design, Adjustment, and Operation of Models for the Study of River Sedimentation Problems, Waterways Experiment Station, Vicksburg, Mississippi, 1978
23. Western Canada Hydraulic Laboratories LTD., Maple Ridge, British Columbia, Canada, 1992
24. Derrick, David, "Dogtooth Bend Model Study Report", unpublished report, U.S. Army Engineer Waterways Experiment Station, Vicksburg, Mississippi, 1992
25. Chow, Ven Te, Open Channel Hydraulics, McGraw-Hill Inc., New York, 1959
26. AUTOCAD, Autodesk, **Inc.** 1982-1990

27. Parker, Brian SHCROSS1, AutoLISP Computer Program For AUTOCAD, BLIPWARE, Rolla, Missouri, 1994
28. SURFER FOR WINDOWS, Golden Software, Inc., Golden Colorado, 1994
29. HEC-2, Water Surface Profile Computations Users Manual, U.S Army Corps of Engineers, Hydrologic Engineering Center, Davis California, 1990
30. Merzkirch, Wolfgang, Flow Visualization, Academic Press, Inc. London, 1974
31. Richards, Bryan E., Measurement of Unsteady Fluid Dynamic Phenomena, Hemisphere Publishing Corporation, London, 1977
32. Vardeman, Stephen B., Statistical Methodology in Engineering, PWS Publishing Company, Boston, Massachusetts, 1994
33. Derrick, David, Phone Conversations on the Dogtooth Bend Movable Bed Model, Waterways Experiment Station, Vicksburg, Mississippi, May, 1994

VITA

Robert Dale Davinroy, Jr., son of Robert and Jackie Davinroy, was born on July 3, 1958 in East St. Louis, Illinois. He attended primary school in Belleville, Illinois, where he also completed his secondary education at Althoff Catholic High School in 1976.

He received his college education from the University of Missouri-Rolla in Rolla, Missouri. He obtained his Bachelor of Science degree in Civil Engineering in May 1980.

That same month, he accepted a position with the U.S. Army Corps of Engineers, where he is still currently employed.

On September 29, 1989, he married Mimi Casa! of Kansas City, Missouri and formerly of Havana, Cuba.

He has one daughter, Danielle Olivia, born April 10, 1991.

He has been enrolled in the Graduate School of the University of Missouri-Rolla since August 1993.